

Syracuse University

SURFACE

Physics - Dissertations

College of Arts and Sciences

8-2012

Linear Sigma Models in QCD and S3 Symmetry for Neutrinos

Muhammad Naeem Shahid

Syracuse University

Follow this and additional works at: https://surface.syr.edu/phy_etd

 Part of the [Physics Commons](#)

Recommended Citation

Shahid, Muhammad Naeem, "Linear Sigma Models in QCD and S3 Symmetry for Neutrinos" (2012).

Physics - Dissertations. 126.

https://surface.syr.edu/phy_etd/126

This Dissertation is brought to you for free and open access by the College of Arts and Sciences at SURFACE. It has been accepted for inclusion in Physics - Dissertations by an authorized administrator of SURFACE. For more information, please contact surface@syr.edu.

ABSTRACT

LINEAR SIGMA MODELS IN QCD AND S_3 SYMMETRY FOR NEUTRINOS

Muhammad Naeem Shahid

Department of Physics

Doctor of Philosophy

This thesis has two parts with different topics in particle physics. In part I, we consider various linear sigma models and their applications to scalar mesons. It is shown that the tree amplitude for $\pi\pi$ scattering in the minimal linear sigma model has an exact expression which induces an infinite geometric series in which the pattern for both the $I = 0$ and $I = 2$ s -wave scattering lengths to orders p^2 , p^4 and p^6 seems to agree with chiral perturbation theory predictions. The model is then gauged to study the mass differences between the vector meson and the axial vector meson as a possibly useful “template” for the role of a light scalar in QCD as well as for (at a different scale) an effective Higgs sector for some recently proposed walking technicolor models. The model is applied to the s -wave pion-pion scattering in QCD. Both the near threshold region and (with an assumed unitarization) the “global” region up to about 800 MeV are considered. It is noted that there is a little tension

between the choice of “bare” sigma mass parameter for describing these two regions.

By including the parity reversed partner we study a simple two Higgs doublet model which reflects, in a phenomenological way, the idea of compositeness for the Higgs sector. It is relatively predictive. In one scenario, it allows for a “hidden” usual Higgs particle in the 100 GeV region and a possible dark matter candidate.

Poles in unitarized $\pi\pi$ scattering amplitude are studied in a generalized linear sigma model which contains two scalar nonets (one of quark-antiquark type and the other of diquark-antidiquark type) and two corresponding pseudoscalar nonets. It is shown that a reasonable agreement with experimental data is obtained up to about 1 GeV. Some comparison is made to the situation in the usual SU(3) linear sigma model with a single scalar nonet.

We show that the mixing of two “bare” nonets, one of which is of quark-antiquark type and the other of two quark- two antiquark type is, before chiral symmetry breaking terms are included, only possible for three flavors. Specifically, our criterion would lead one to believe that scalar and pseudoscalar states containing charm would not have “four quark” admixtures. We also discuss some aspects associated with the possibility of getting new experimental information about scalars from semileptonic decays of heavy charged mesons into an isosinglet scalar or pseudoscalar plus leptons.

In part II we explore a predictive model based on permutation symmetry S_3 for the masses and mixing matrix of three Majorana neutrinos. At zeroth order the model yielded degenerate neutrinos and a generalized “tribimaximal” mixing matrix. We first study the effects of the perturbation which violates S_3 but preserves the well known (23) interchange symmetry. This is done

in the presence of an arbitrary Majorana phase ψ which serves to insure the degeneracy of the three neutrinos at the unperturbed level. At this order the mass splitting was incorporated and the tribimaximal mixing matrix emerged with very small corrections but with a zero value for the parameter s_{13} . Next a different, assumed weaker, perturbation is included which gives a non zero value for s_{13} and further corrections to other quantities. These corrections are worked out and their consequences discussed under the simplifying assumption that the conventional CP violation phase vanishes. It is shown that the existing measurements of the parameter s_{23} provide strong bounds on s_{13} in this model.

LINEAR SIGMA MODELS IN QCD AND S_3 SYMMETRY FOR NEUTRINOS

by

Muhammad Naeem Shahid

M.Sc., Quaid-i-Azam University, Pakistan 2002

M.Phil., Quaid-i-Azam University, Pakistan 2005

DISSERTATION

Submitted in partial fulfillment of the requirements for the degree of
Doctor of Philosophy in Physics

Syracuse University
August 2012

Copyright © 2012 Muhammad Naeem Shahid

All Rights Reserved

ACKNOWLEDGMENTS

First and the foremost, I want to express my gratitude to my advisor Prof. Joseph Schechter for his invaluable guidance, support and encouragement throughout this research work. I greatly benefited from the knowledge of such an extraordinary person and physicist.

I am very happy to thank Prof. Amir Fariborz and Dr. Renata Jora for their suggestions and helpful discussions. I would like to thank Prof. A. P. Balachandran and Prof. Carl Rosenweig for their support during my graduate studies at Syracuse University.

My heartiest thanks to Heather Kirkpatrick and Diane Sanderson for being always very helpful and supportive.

Finally, I wish to record my deepest obligation to my parents and Sadia for their love and encouragements during my studies.

Contents

List of Figures	ix
List of Tables	xi
I Linear Sigma Models	1
1 Introduction to Linear Sigma Model	3
1.1 Linear Sigma Model as an Effective Theory of Mesons	3
1.2 Chiral Nonets	5
2 SU(2) Linear Sigma Models	9
2.1 $\pi\pi$ Scattering in SU(2) Linear Sigma Model	9
2.1.1 Numerical Comparison of Expanded Scattering Lengths	10
2.2 $\pi\pi$ Scattering in SU(2) Gauged Linear Sigma Model	13
2.2.1 The Model	14
2.2.2 $\pi\pi$ Scattering Near Threshold	19
2.2.3 Scattering Away from Threshold	21
2.2.4 Connections with Other Work	25
2.3 Two Higgs Doublet Model	31
2.3.1 Discussion	34
2.3.2 Higgs Potential Terms	36
2.3.3 First Model for a Hidden Higgs Scenario	39
2.3.4 Second Hidden Higgs Model	43
3 SU(3) Linear Sigma Models and Chiral Nonets	47
3.1 Brief Review of the Model	47
3.1.1 Chiral Nonet Mixing in $\pi\pi$ Scattering	51
3.1.2 Comparison with Experiment	53
3.2 More on Two Chiral Nonets – Three Flavors are Special	60
3.3 Semi-Leptonic Decay Modes of the D_s^+ (1968)	64
3.3.1 Chiral SU(3) Model – $K\ell 3$ Decay as a Simple Example	65
3.3.2 SU(3) MM' Model	67
3.3.3 Hybrid MM' Model with a Heavy Flavor	70

3.3.4	$D_s^+(1968) \rightarrow f_0(980)e^+\nu_e$	71
4	Conclusions for Linear Sigma Models	79
II	S_3 Symmetry for Neutrino Masses and Mixing	85
5	Introduction to S_3 Symmetry	87
5.1	S_3 Symmetry	87
5.2	Need for Perturbation	89
6	Perturbation Analysis	93
6.1	Effects of Different Perturbations	93
6.2	Zeroth Order Setup	96
6.3	Analysis of the First Perturbation	98
6.3.1	Neutrinoless Double Beta Decay	103
6.4	Adding the Second Perturbation and s_{13} Mixing Parameter	104
6.4.1	Elements of the Mixing Matrix	109
7	Conclusions for S_3 Symmetry for Neutrino Masses and Mixing	113
	Appendices	117
A	Part I Appendix	117
A.1	Lagrangian in Terms of Component Fields	117
A.2	Pion-pion Scattering Amplitude	118
A.3	Notation and Further Details	121
B	Part II Appendix	123
B.1	Alternative perturbation method	123
	Bibliography	127

List of Figures

2.1	The scattering length $m_\pi a_0^0$ as a function of the sigma mass in GeV.	22
2.2	The scattering length $m_\pi a_2^0$ as a function of the sigma mass in GeV.	23
2.3	Low energy data for real part of s -wave resonant amplitude.	24
2.4	Unitarized amplitudes plotted as a function of \sqrt{s} to 1 GeV.	25
2.5	Unitarized scattering amplitudes to 1.4 GeV with $m_\sigma = 0.85$ GeV	26
2.6	Unitarized scattering amplitudes with $m_0^2 = 0.27$	27
2.7	Predictions for the choice $m_\sigma = 0.85$ GeV in the region near threshold.	28
2.8	$g_{\rho\pi\pi}^{eff}$ vs g with the plus sign in Eq. (2.37).	30
2.9	$g_{\rho\pi\pi}^{eff}$ vs g with the minus sign in Eq. (2.37).	31
2.10	y vs. x	41
2.11	y' vs. x'	45
3.1	Real part of the unitarized $\pi\pi$ scattering amplitude	54
3.2	Real part of unitarized scattering amplitude for two values of A_3/A_1	55
3.3	The local minimum of function $\mathcal{F}(s_R, s_I)$	57
3.4	Predicted physical masses are compared with the “bare” masses	58
3.5	Predicted decay widths for two values of A_3/A_1	59
3.6	$K\ell 3$ decay hadronic current	66
3.7	D_s decay	72
3.8	Pseudoscalar partial widths for different values of A_3/A_1 and $m_\pi(1300)$	77
3.9	Scalar partial widths for different values of A_3/A_1 and $m_\pi(1300)$	78
6.1	Isosceles triangle with the equal length 2-vectors α and $\alpha + 3\beta$	97
6.2	Sketch of perturbative region	103

List of Tables

2.1	Comparison of scattering length increments	12
2.2	$g, v, w, b, B, m_0^2 + Cv^2/2$ as functions of the axial vector meson mass.	19
2.3	Values of $m_\eta, g_{\sigma\eta\eta}$ and Higgs potential parameters	41
2.4	Widths of the \mathbf{a} bosons	43
2.5	Values of $m_a, g_{\sigma a^0 a^0}$	45
3.1	The physical mass and decay width of the isosinglet scalar states	56
3.2	Pseudoscalars.	74
3.3	Scalars	75
6.1	Stable mixing matrices for each S_2 invariant perturbation	96

Part I

Linear Sigma Models

Chapter 1

Introduction to Linear Sigma Model

1.1 Linear Sigma Model as an Effective Theory of Mesons

The theory of quarks and gluons, Quantum Chromodynamics (QCD), is the accepted theory of strong interactions. In order to satisfy Pauli exclusion principle for the observed hadrons, quarks must come with three colors, a new quantum number. In 1973 Politzer, Gross and Wilczek [1] found that QCD can have negative β -function i.e. the charge decreases with the distance or increases with energy, a phenomenon confirmed by experiments and known as asymptotic freedom. It can be found that the to lowest order the β -function is,

$$\beta = -\frac{g^2}{48\pi^2}(11N_c - 2N_f), \quad (1.1)$$

for $SU(N)$. Note that g is decreasing with energy until $N_f < 5.5N$ indicating six flavors of the quarks. From here the running coupling constant can be found as,

$$\alpha = \frac{g^2}{4\pi} = \frac{12\pi}{(11N_c - 2N_f)\ln(Q^2/\Lambda_{QCD}^2)}, \quad (1.2)$$

where Q corresponds to the energy at which the theory is applied and Λ is of the order of 200 MeV, scale of QCD.

It is clear from Eq. (1.2) that at the energies much above Λ_{QCD} (several GeV), QCD is perturbative. On the other side when $Q^2 \sim \Lambda_{QCD}^2$, perturbation is not possible. In order to discuss this low energy region of QCD, one way is to work with effective Lagrangian with light meson fields. This is a reasonable approach as mesons are strongly bound states of quarks and thus interact weakly and so can be treated perturbatively. But one has to respect the symmetries of QCD for these Lagrangians.

As an example, imposing the Wigners isotopic spin symmetry $SU(2)_V$, proton and neutron can be represented as a spinor and pions as a vector.

$$N = \begin{pmatrix} p \\ n \end{pmatrix}, \quad \phi = \frac{1}{\sqrt{2}}\boldsymbol{\pi} \cdot \boldsymbol{\tau}. \quad (1.3)$$

Then the Yukawas theory [2] implies an effective Lagrangian with the $SU(2)_V$ invariant interaction terms,

$$ig_Y \bar{N}\phi\gamma_5 N + \lambda[Tr(\phi^2)]^2, \quad (1.4)$$

where g_Y is Yukawa coupling constant and λ_{QCD} is the coupling constant for $\pi\pi$ scattering.

It is evident from the first term of Eq. (1.4) that the πN scattering at the tree level is propotional to g_Y^2 which happened to be an order of magnitude larger than the experimental value near the threshold. The problem was solved by the use of linear sigma model (LSM) [3] which is chiral $(SU(2)_L \times SU(2)_R)$ symmetric, for massless

case. The chiral partner of the pion called sigma has the same coupling to nucleon as pion and the diagram due to sigma exchange cancels the contribution due to the nucleon exchange. The result agrees with the experiment within 15%.

The linear sigma model also helped to clarify the role of chiral symmetry and its spontaneous breakdown [4] in strong interaction physics. The partial conservation of the axial currents together with their algebraic structure resulted in calculations for low energy pion physics which gave, for the first time, reasonable agreements with experiment. While the original calculations [5] were roundabout, it was found that they could be greatly simplified by straightforward perturbative calculations in the non-linear version of the model obtained by assuming the sigma field to be very heavy. Experimental evidence at that time did not clearly demand a light sigma meson. Remarkably, the original linear version also turned out to be useful at a higher energy scale as the Higgs potential [6] of the electroweak standard model, with the sigma identified as the Higgs field.

1.2 Chiral Nonets

It has been realized for a long time that the nonet structure of mesons with respect to SU(3) flavor transformations should, at a more fundamental level, be expanded to SU(3) chiral symmetry transformations; this amounts to an SU(3) for massless left-handed quarks and another SU(3) for massless right-handed quarks. This chiral symmetry is that of the fundamental QCD Lagrangian itself, with neglect of quark mass terms. The spontaneous breaking of this symmetry, which gives zero mass pseudoscalars, is a basic part of the present understanding of low energy QCD. The light quark mass terms play a relatively small role and are treated as perturbations. It thus appears that chiral (rather than just the vector) symmetry should be considered

the first approximation for an understanding of the structure of hadrons.

Available evidence indicates that the predicted states arising from the addition of the charm and beauty quarks would fit in with corresponding SU(4) and SU(5) extensions (having respectively 16 and 25 members) of the SU(3) nonets. Of course a possible extension to states made with top quarks is of less interest, owing to the rapid weak decay of the top quark. Naturally the much heavier masses of the c and b quarks make the SU(4) and SU(5) symmetries not as good as SU(3). Nevertheless the observed particles still fit into the extended multiplets.

Although the exact nature of the low lying scalar mesons has been a topic of intense debate, the fact that these states play important roles in our understanding of low-energy QCD seems to be shared by all. Various models have been put forward for the properties of the scalar mesons. A general discussion of the experimental situation on light scalars is given in [7]. However, in the last few years there has been a growing recognition that the lightest nine scalar states do not seem to fit well into the above classification [8]. The scalars below 1GeV appear to fit into a nonet as:

$$\begin{aligned}
I = 0 & : m[f_0(600)] \approx 500\text{MeV} & s\bar{s} \\
I = 1/2 & : m[\kappa] \approx 800\text{MeV} & n\bar{s} \\
I = 0 & : m[f_0(980)] \approx 980\text{MeV} & n\bar{n} \\
I = 1 & : m[a_0(980)] \approx 980\text{MeV} & n\bar{n},
\end{aligned} \tag{1.5}$$

and for the vector meson nonet,

$$\begin{aligned}
I = 1 & : m[\rho(776)] \approx 776\text{MeV} & n\bar{n} \\
I = 0 & : m[\omega(783)] \approx 783\text{MeV} & n\bar{n} \\
I = 1/2 & : m[K^*(892)] \approx 892\text{MeV} & n\bar{s} \\
I = 0 & : m[\phi(1020)] \approx 1020\text{MeV} & s\bar{s}.
\end{aligned} \tag{1.6}$$

It can be seen from above that there are two unexpected features. First the masses of these states are significantly lower than the other “constituent quark model” p -wave states (i.e. tensors and two axial vectors with different C properties). Secondly, the order, with increasing mass - isosinglet, isodoublet and roughly degenerate isosinglet with isotriplet - seems to be reversed compared to that of the “standard” vector meson nonet.

Clearly such a light and reversed order nonet requires some rethinking of the standard picture of the scalar mesons. Actually, a long time ago, it was observed [9] that the reversed order could be explained if the light scalar nonet were actually composed of two quarks and two antiquarks. In that case the number of strange quarks (which determines the direction of increasing masses) rises with the reversed order given. For example the lowest mass “isolated” isosinglet scalar $\sigma(600)$ would look like $(u\bar{u} + d\bar{d})^2$ while, for comparison, the highest mass isolated vector isosinglet $\phi(1020)$ looks like $s\bar{s}$. At that time the existence of a light σ and a light κ was considered dubious. More recent work has now pretty much confirmed the existence of such states as well as the plausibility that they fit into a three flavor nonet.

It has also been pointed out¹ [10], [11], [12], [13], [14], [15] - [20], that four quark components alone are not sufficient for understanding the physical parameters of these states which seems to require a scenario based on an underlying mixing between quark-antiquark nonets and nonets containing two quarks as well as two anti quarks. In [10] it is proposed that the mixing between a $qq\bar{q}\bar{q}$ scalar nonet together with a usual p -wave $q\bar{q}$ nonet could produce this effect due to the “level repulsion” expected in quantum mechanics perturbation theory. A simple picture for scalar states below 2 GeV then seems to emerge. Amusingly, this mixing [20] automatically leads to light scalars that are dominantly of two quark- two antiquark nature and light conventional

¹Related models for thermodynamic properties of QCD are discussed in [14]

pseudoscalars that are, as expected from established phenomenology, dominantly of quark-antiquark nature.

In the next two chapters we will explain our work on the different versions of linear sigma model in detail. The second chapter has the applications of SU(2) linear sigma model to $\pi\pi$ scattering at various energies [21], [22]. We will also discuss the role of linear sigma model in the Higgs sector of the standard model [23]. In the third chapter we will concentrate on the SU(3) version and its mixing with another four quark nonet [24]. We will also extend to higher flavor cases in order to explore some interesting features regarding semileptonic decays of the heavy mesons [25], [26].

Chapter 2

SU(2) Linear Sigma Models

2.1 $\pi\pi$ Scattering in SU(2) Linear Sigma Model

The chiral perturbation theory (χ PT) [27] - [29]) approach provides a systematic method for improving the "current algebra" or tree level "non-linear chiral Lagrangian" results for low energy QCD in powers of a characteristic squared momentum, p^2 (or number of derivatives). Intuitive understanding of the resulting physics in some cases has been obtained by computing the amplitudes of interest based on pole-dominance. For example vector meson dominance [30] is known to be good at low energies; a typical well known immediate prediction gives the squared charge radius of the pion simply as $r_\pi^2 = 6/m_\rho^2$. This kind of approach may be theoretically justified to some extent by invoking the $1/N$ expansion of QCD [31], [32] which yields tree level dominance.

In the case of the pion s-wave scattering lengths, the long controversial, but now apparently accepted, sigma particle would appear to play the role of the rho meson. However, a simple sigma dominance approximation is not viable because it would not guarantee the nearly spontaneous breakdown of chiral symmetry mechanism which

is crucial for QCD. Such a mechanism is guaranteed by the use of a linear sigma model of some type. Here, we will just point out that the minimal $SU(2)$ linear sigma model¹ [3] provides a useful approximation to the lightest sigma of a model which may contain a number of them. A crucial effect is that the linear sigma model has an important contact term. The actual low energy scattering is known to result from an enormous cancellation between the sigma pole and the contact contributions. This unpleasant feature is mitigated in the non-linear sigma model (which forms the basis of the chiral perturbation scheme. Another way to mitigate this feature is at the amplitude level. Then the amplitude is expanded² [16], [18] in a Taylor series about $s = m_\pi^2$ and the cancellation may be explicitly made. The result is proportional to a simple geometric series in the variable $(s - m_\pi^2)/(m_B^2 - m_\pi^2)$. Then in order to compare it with something, it is natural to compare it with another power series in squared momentum - χ PT.

2.1.1 Numerical Comparison of Expanded Scattering Lengths

With the Mandelstam notation, the invariant pion scattering amplitude computed at tree level in the minimal $SU(2)$ linear sigma model reads:

$$A(s, t, u) = \frac{2(m_B^2 - m_\pi^2)}{F_\pi^2} \left[\left(1 - \frac{s - m_\pi^2}{m_B^2 - m_\pi^2}\right)^{-1} - 1 \right], \quad (2.1)$$

where $F_\pi = 131$ MeV and m_B denotes the “bare” sigma mass which appears in the Lagrangian.

This equation is seen to contain a contact term as well as a pole term which has been rewritten for convenience. In this form it is apparent that there is a geometric series expansion in powers of $(s - m_\pi^2)/(m_B^2 - m_\pi^2)$, which should be rapidly convergent for s close to the pion- pion threshold:

¹By the minimal model we mean just the meson terms.

² In this model there are four different scalars.

$$A(s, t, u) = \frac{2(s - m_\pi^2)}{F_\pi^2} \left[1 + \frac{s - m_\pi^2}{m_B^2 - m_\pi^2} + \frac{(s - m_\pi^2)^2}{(m_B^2 - m_\pi^2)^2} + \frac{(s - m_\pi^2)^3}{(m_B^2 - m_\pi^2)^3} + \dots \right]. \quad (2.2)$$

Actually, a similar expansion may be derived when a number of different scalar mesons are present [?]. In that instance the lowest lying scalar meson is expected to dominate near threshold.

The isospin 0 scattering length is proportional to $3A(s, t, u) + A(t, s, u) + A(u, t, s)$ evaluated at $s = 4m_\pi^2, t = u = 0$ while the isospin 2 scattering length is obtained by evaluating $A(t, s, u) + A(u, t, s)$ instead. Then we find for the “dimensionless” s -wave scattering lengths:

$$m_\pi a_0^0 = \frac{m_\pi^2}{16\pi F_\pi^2} \left[7 + 29 \frac{m_\pi^2}{m_B^2 - m_\pi^2} + 79 \frac{m_\pi^4}{(m_B^2 - m_\pi^2)^2} + 245 \frac{m_\pi^6}{(m_B^2 - m_\pi^2)^3} + \dots \right], \quad (2.3)$$

and,

$$m_\pi a_0^2 = -\frac{m_\pi^2}{8\pi F_\pi^2} \left[1 - \frac{m_\pi^2}{m_B^2 - m_\pi^2} + \frac{m_\pi^4}{(m_B^2 - m_\pi^2)^2} - \frac{m_\pi^6}{(m_B^2 - m_\pi^2)^3} + \dots \right]. \quad (2.4)$$

Evidently, these terms may be consecutively interpreted as p^2 , p^4 , p^6 , and p^8 etc. contributions.

The χ PT results to the first three orders³ [33], [34], [35] as well as the comparison with experiment may be conveniently read from Fig. 10 of [36]. We have subtracted the values presented there to get the incremental corrections for comparison with Eqs. (2.3) and (2.4). The order p^2 entries [33] in Table 6.1 are of course the same and we made the choice $m_\pi = 140$ MeV to enforce this feature. The only unfixed parameter in the linear sigma model is the bare sigma mass, m_B which we chose to be 550 MeV to give a p^4 contribution to the resonant partial wave scattering length which approximately agrees with χ PT at that order. (Alternatively, a similar value

³The order p^4 and p^6 calculation are from [34] and [35] respectively.

can be found on an a priori basis by fitting the near threshold $I = 0$, s -wave scattering data).

Order:	p^2	p^4	p^6	p^8
$m_\pi a_0^0$ in χ PT:	0.16	0.04	0.02 ± 0.005	–
$m_\pi a_0^0$ in LSM:	0.159	0.046	0.009	0.0019
$m_\pi a_0^2$ in χ PT:	– 0.046	0.004	$- 0.002 \pm 0.001$	–
$m_\pi a_0^2$ in LSM:	– 0.0454	0.0031	– 0.0002	0.000015

Table 2.1 Comparison of scattering length increments

We notice that the increments to $m_\pi a_0^2$ are predicted to alternate in sign with increasing order. This pattern manifestly agrees with what was found in the first three orders of chiral perturbation theory.

If the p^4 increment of $m_\pi a_0^0$ is taken as approximately a common input, the magnitude of the p^4 increment to $m_\pi a_0^2$ is predicted to be about 75% of the χ PT one. Also the magnitude of the p^6 increment to $m_\pi a_0^0$ is predicted to be about 50% of the χ PT one. Finally, the magnitude of the p^6 increment to $m_\pi a_0^0$ could be about 20% of the χ PT one (which contains a large uncertainty however). Thus it seems fair to say that the tree level linear sigma model result exactly reproduces the signs of the chiral perturbation amplitudes and tracks well the magnitudes. It will be interesting to compare the predicted p^8 increments given above when the χ PT calculation is carried to that order.

Differences between the chiral perturbation results for the s -wave scattering lengths and the present ones may be evidently interpreted physically as due to contributions from effects other than the existence of the sigma meson. It is likely that the next most important effects should arise from including the rho meson and a higher mass

scalar meson like the $f_0(980)$ in the formulation of the chiral invariant linear sigma model. Work in this direction is under way.

2.2 $\pi\pi$ Scattering in $SU(2)$ Gauged Linear Sigma Model

Our initial motivation of this work is the further understanding of the properties of light scalar mesons. This is essentially connected with the s -wave $\pi\pi$ scattering problem. It seems instructive to formulate this in a chiral invariant way using a generalized $SU(3)$ linear sigma model. Now in these generalized sigma models there are more than one scalar and the s -wave scattering is more complicated. At least qualitatively, the s channel is dominated by these scalars. In the region near threshold, the lowest mass sigma is most important. Thus, as a start to studying the effects of the vector mesons in such models, it seems natural to go back to the original linear sigma model and add the vector meson, ρ with its chiral partner. A review of older work in this context is given in [37] and recent papers include those in [38].

Even though the plain linear sigma model is quite simple to deal with, the addition of spin 1 fields increases the overall complexity by an order of magnitude. We will add the vector and axial vector fields as (initially) Yang Mills gauge fields. The local gauge symmetry is then manifestly broken by the addition of the three simplest chiral invariant spin 1 field mass terms. The determination of all Lagrangian parameters is carried out analytically with respect to the experimental inputs. The s -wave pion scattering is studied both for the threshold region and for the region away from threshold which is expected to be influenced by the presence of the lightest sigma. The scattering is explicitly compared with that of the plain linear sigma model as well as with experiment.

2.2.1 The Model

As mentioned in the introduction the basic fields are the scalar, σ and pion, $\boldsymbol{\pi}$, which are contained in $M = (\sigma + i\boldsymbol{\pi} \cdot \boldsymbol{\tau})/\sqrt{2}$ and its Hermitian conjugate. The starting piece is the kinetic term for M , which is invariant under the chiral transformation, $M' = U_L M U_R^{-1}$. One can naturally introduce the left (l_μ) and the right (r_μ) vector fields by gauging the chiral symmetry. The resulting gauge invariant Lagrangian density is then,

$$\mathcal{L} = -\frac{1}{2}\text{Tr}(F_{\mu\nu}^r F_{\mu\nu}^r + F_{\mu\nu}^l F_{\mu\nu}^l) - \frac{1}{2}\text{Tr}(D_\mu M^\dagger D_\mu M), \quad (2.5)$$

where the covariant derivatives of M and M^\dagger are,

$$\begin{aligned} D_\mu M &= \partial_\mu M - igl_\mu M + igMr_\mu, \\ D_\mu M^\dagger &= \partial_\mu M^\dagger - igr_\mu M^\dagger + igM^\dagger l_\mu, \end{aligned} \quad (2.6)$$

and the field strength tensors take the form,

$$\begin{aligned} F_{\mu\nu}^l &= \partial_\mu l_\nu - \partial_\nu l_\mu - ig[l_\mu, l_\nu], \\ F_{\mu\nu}^r &= \partial_\mu r_\nu - \partial_\nu r_\mu - ig[r_\mu, r_\nu]. \end{aligned} \quad (2.7)$$

The vector and axial vector mesons are defined as

$$\begin{aligned} V_\mu &= l_\mu + r_\mu = \frac{1}{\sqrt{2}}\mathbf{V}_\mu \cdot \boldsymbol{\tau}, \\ A_\mu &= l_\mu - r_\mu = \frac{1}{\sqrt{2}}\mathbf{A}_\mu \cdot \boldsymbol{\tau}. \end{aligned} \quad (2.8)$$

The terms which contribute to particle masses are:

$$\begin{aligned}
& - m_0^2 \text{Tr}(l_\mu l_\mu + r_\mu r_\mu) + B \text{Tr}(M r_\mu M^\dagger l_\mu) - C \text{Tr}(l_\mu^2 M M^\dagger + r_\mu^2 M^\dagger M) \\
& - V_0(M, M^\dagger) - V_{SB}.
\end{aligned} \tag{2.9}$$

The first, m_0^2 term, which breaks the gauge invariance (and also the formal scale symmetry), gives the same mass to the vector and the axial vector mesons. The C term also gives the same mass to both spin 1 mesons, but maintains the scale symmetry. The B term breaks the mass degeneracy of the two spin 1 mesons. This is important since, experimentally, the lightest isovector, axial vector meson with negative G -parity (the $a_1(1260)$ is heavier than the ρ meson. Another contribution to this mass splitting arises from spontaneous chiral symmetry breaking in the model, but his effect by itself will be seen to be insufficient. The last two terms are the scalar potential terms which respectively yield the spontaneous chiral symmetry breaking and the explicit symmetry breaking due to the small quark mass; explicitly,

$$V_0(M, M^\dagger) = a_1(\sigma^2 + \boldsymbol{\pi} \cdot \boldsymbol{\pi}) + a_3(\sigma^2 + \boldsymbol{\pi} \cdot \boldsymbol{\pi})^2, \quad V_{SB} = -2\sqrt{2}A\sigma. \tag{2.10}$$

Here, a_3 is positive while a_1 is chosen to be negative so that spontaneous chiral symmetry breaking will give a nontrivial vacuum expectation value v for σ . The explicit symmetry breaking term V_{SB} mocks up the light quark mass terms. The coefficients in this potential can be determined by the minimum condition in terms of the sigma and pion mass parameters, with the definition $V \equiv V_0 + V_{SB}$, as follows:

$$\begin{aligned}
\left\langle \frac{\partial V}{\partial \sigma} \right\rangle &= 0 = 2a_1 v + 4a_3 v^3 - 2\sqrt{2}A, \\
\left\langle \frac{\partial^2 V_0}{\partial \sigma^2} \right\rangle &= m_\sigma^2 = 2a_1 + 12a_3 v^2, \\
\left\langle \frac{\partial^2 V_0}{\partial \pi^2} \right\rangle &= m_\pi^2 = 2a_1 + 4a_3 v^2.
\end{aligned} \tag{2.11}$$

From this, one can easily derive the coefficients,

$$\begin{aligned}
m_\pi^2 &= \frac{2\sqrt{2}A}{v}, \\
a_1 &= \frac{1}{2}(m_\sigma^2 - \frac{3}{2}(m_\sigma^2 - m_\pi^2)), \\
a_3 &= \frac{m_\sigma^2 - m_\pi^2}{8v^2}.
\end{aligned} \tag{2.12}$$

The potential terms can be expressed in terms of the fields as:

$$\begin{aligned}
V_0(M, M^\dagger) &= \frac{1}{2}m_\pi^2 \boldsymbol{\pi} \cdot \boldsymbol{\pi} + \frac{1}{2}m_\sigma^2 \sigma^2 + \frac{1}{2}g_{\sigma\pi\pi} \sigma \boldsymbol{\pi} \cdot \boldsymbol{\pi} + \frac{1}{4}g_4 (\boldsymbol{\pi} \cdot \boldsymbol{\pi})^2 + \dots, \\
g_{\sigma\pi\pi} &= \frac{m_\sigma^2 - m_\pi^2}{v}, \quad g_4 = \frac{2g_{\sigma\pi\pi}}{v}.
\end{aligned} \tag{2.13}$$

Here, quadrilinear terms involving σ have not been written. Also note that the quantities m_π , $g_{\sigma\pi\pi}$ and g_4 are not the physical ones, which will be defined later. It is understood that $\sigma = v + \tilde{\sigma}$ where $\tilde{\sigma}$ is the physical σ field. The rest of the Lagrangian in terms of the component fields is given in Appendix (A.1).

In this model, we have the five parameters g , v , m_0^2 , B and C to be determined from experiment. g and v are intrinsic parameters of the model while m_0^2 , B and C represent different ways to introduce vector and axial vector masses. Specifically the vector and axial vector masses are given by:

$$\begin{aligned}
m_V^2 &= m_0^2 - \frac{Bv^2}{4} + C\frac{v^2}{2}, \\
m_A^2 &= m_0^2 + \frac{Bv^2}{4} + C\frac{v^2}{2} + \frac{g^2v^2}{2} \equiv m_0'^2 + \frac{g^2v^2}{2}.
\end{aligned} \tag{2.14}$$

The Lagrangian yields a pion-axial vector meson mixing term proportional to $v\vec{A}_\mu \cdot \partial_\mu \vec{\pi}$. The Lagrangian can be diagonalized by introducing the physical (tilde) quantities as

$$\begin{aligned}\vec{A}_\mu &= \vec{\tilde{A}}_\mu + b\partial_\mu\vec{\tilde{\pi}}, \\ \vec{\pi} &= w\vec{\tilde{\pi}}.\end{aligned}\tag{2.15}$$

b is determined from the condition of zero mixing between the physical pion and the physical axial vector meson, while w is determined from the condition of correct normalization of the pion kinetic term. We find

$$\begin{aligned}b &= \frac{gv}{\sqrt{2}wm_0^2}, \\ w &= \sqrt{1 + \frac{g^2v^2}{2m_0^2}}.\end{aligned}\tag{2.16}$$

The following alternate forms also are useful:

$$\begin{aligned}b &= \frac{gvw}{\sqrt{2}m_A^2} \\ w^2 &= \frac{m_A^2}{m_0^2} = \frac{1}{1 - \frac{g^2v^2}{2m_A^2}}\end{aligned}\tag{2.17}$$

Note that m_0^2 was defined in Eq. (2.14) above. The physical pion decay constant, \tilde{F}_π is obtained from the Noether's theorem calculation of the single particle contributions to the axial current in our Lagrangian:

$$\begin{aligned}(J_\mu^A)_1^2 &= -\sqrt{2}v\left(\frac{\partial L}{\partial(\partial_\mu\pi)}\right)_1^2 = \partial_\mu\left(\frac{\vec{\tau}\cdot\vec{\pi}}{\sqrt{2}}\right)_1^2 - \frac{gv}{\sqrt{2}}\left(\frac{\vec{\tau}\cdot\vec{A}_\mu}{\sqrt{2}}\right)_1^2 \\ &= \frac{\sqrt{2}v}{w}\partial_\mu\tilde{\pi}^+ - gv^2\tilde{A}_\mu^+, \end{aligned}\tag{2.18}$$

where we used Eq. (2.15) and, for example, $\tilde{\pi}^+$ is the physical positive pion field.

The coefficient in front of $\partial_\mu\tilde{\pi}^+$ is identified as the physical pion decay constant:

$$\tilde{F}_\pi = \frac{\sqrt{2}v}{w}.\tag{2.19}$$

The effective $\rho\pi\pi$ coupling constant for on-shell rho as:

$$g_{\rho\pi\pi}^{eff} = g\left(1 - \frac{Bv^2}{2m_0^2} - \frac{b^2}{2}m_\rho^2\right).\tag{2.20}$$

The coupling constant $g_{\rho\pi\pi}^{eff}$ is related to the ρ meson width by

$$\Gamma(\rho) = (g_{\rho\pi\pi}^{eff})^2 |q_\pi|^3 / (12\pi m_\rho^2). \quad (2.21)$$

For $\Gamma(\rho) = 149.4$ MeV, one finds $|g_{\rho\pi\pi}^{eff}| \approx 8.66$.

Now we will solve for the vacuum value, v by the following procedure. First replace w in the second of Eqs. (2.16) by, from Eq. (2.19), the quantity $\sqrt{2}v/\tilde{F}_\pi$. Then replace $2m_0'^2$ by, using Eqs. (2.14), $2m_A^2 - g^2v^2$. Squaring both sides gives the quadratic equation for v^2 :

$$v^4 - \frac{2m_A^2}{g^2}v^2 + \frac{2m_A^2\tilde{F}_\pi^2}{2g^2} = 0. \quad (2.22)$$

This can be solved easily in terms of g^2v^2 to get:

$$g^2v^2 = m_A^2 \left(1 \pm \sqrt{1 - \frac{g^2\tilde{F}_\pi^2}{m_A^2}} \right). \quad (2.23)$$

This is an equation which determines the product gv in terms of g and experimentally known quantities. We can find another relation between g and v by substituting $Bv^2/2 = m_A^2 - m_\rho^2 - g^2v^2/2$ and $b = gvw/(\sqrt{2}m_A^2)$ into Eq. (2.20):

$$g_{\rho\pi\pi}^{eff} = g \left(1 - \frac{1}{2m_A^2 - g^2v^2} \left(2(m_A^2 - m_\rho^2) - g^2v^2 \left(1 - \frac{m_\rho^2}{2m_A^2} \right) \right) \right) \quad (2.24)$$

Substituting Eq. (2.23) into Eq. (2.24) gives an equation for the Yang-Mills coupling constant, g by itself. Knowing this we can substitute back into Eq. (2.23) to determine v . Then we can determine B from:

$$B = \frac{2}{v^2} (m_A^2 - m_\rho^2) - g^2. \quad (2.25)$$

Finally, we may determine the linear combination, $m_0^2 + Cv^2/2$ from:

$$m_0^2 + Cv^2/2 = (m_\rho^2 + m_A^2)/2 - g^2v^2/4. \quad (2.26)$$

From the given inputs it is only possible to obtain the given linear combination of m_0^2 and C . Later we will consider two different “models” corresponding to either $m_0 =$

0 or $m_0 \neq 0$. Table 2.2 shows the results based on the best fit value of m_A as well as its maximum and minimum values. Note also that the solution requires the sign in Eq. (2.23) to be positive. The solutions with zero value for the square root and with the minus sign will be discussed in a later section.

m_A in GeV	g	v in GeV	w	b in GeV^{-1}	B	$m_0^2 + Cv^2/2$ in GeV^2
1.270	7.83	0.2	2.2	1.55	-12.9	0.456
1.230	7.78	0.197	2.13	1.53	-13.73	0.467
1.190	7.72	0.19	2.06	1.51	-14.65	0.468

Table 2.2 $g, v, w, b, B, m_0^2 + Cv^2/2$ as functions of the axial vector meson mass. We used $\tilde{F}_\pi = 0.131$ GeV, $m_\rho = 0.775$ GeV, $g_{\rho\pi\pi}^{eff} = 8.56$ as inputs. Note that g, w and B are dimensionless.

It can be seen that the predicted parameters are not much affected by the uncertainty in the mass of the $a_1(1260)$ meson. Thus we will use the central value in what follows.

2.2.2 $\pi\pi$ Scattering Near Threshold

Using the well known experimental results for the ρ mass and width as well as the $a_1(1260)$ mass, we specified in Table 2.2 the Lagrangian parameters g, v, w, b, B and the linear combination $m_0^2 + Cv^2/2$. The only remaining “unknowns” are the “bare” mass of the sigma, m_σ and the relative sizes of m_0^2 and C . For definiteness we will initially consider the case, $m_0 = 0$; soon we will see that the case, $m_0 \neq 0$, gives a poorer fit in the region away from threshold. Then the near threshold scattering will depend just on the value, m_σ . Of course one first considers the s -wave scattering lengths (See Appendix (A.2)).

The scattering length $m_\pi a_0^0$ is plotted in Fig. 2.1 as a function of m_σ . Also shown

are the predictions in the case of the “pure” linear sigma model, in which the vector and axial vector mesons are absent. It is seen that any given value of $m_\pi a_0^0$ (above the “current algebra” value of about 0.16 [33]) may be obtained for some m_σ . However, for a given value of the scattering length, m_σ is seen to be substantially lower when the vector and axial vector mesons are present. The experimental value of about 0.22 is obtained for $m_\sigma \approx 550$ MeV in the plain linear sigma model but for $m_\sigma \approx 360$ MeV in the model containing the spin 1 mesons. Fig. 2.2 similarly shows the dependence of the non-resonant scattering length, $m_\pi a_0^2$ on m_σ .

Here we denote the angular momentum l partial wave elastic scattering amplitude for isospin I as T_l^I . Note also that, for example,

$$\tilde{m}_\pi a_0^0 = \frac{T_0^0}{\rho}, \quad \rho = \sqrt{1 - 4\tilde{m}_\pi^2/s}, \quad (2.27)$$

wherein T_0^0/ρ is evaluated at threshold, remembering to first cancel the overall factor of ρ in T_0^0 . The amplitude is purely real in the present tree approximation. It is clearly convenient to compare with the real part of the partial wave amplitude. The experimental real part, R_0^0 is related to the experimental phase shift, δ_0^0 as

$$R_0^0 = \frac{1}{2} \sin(2\delta_0^0). \quad (2.28)$$

In Fig.2.3, for orientation, some values of R_0^0 near threshold obtained from the phase shifts found by the Na48/2 experiment [39] are shown. It can be seen that these data points near threshold may be reasonably explained by a value of $m_\sigma \approx 0.42$ GeV in the present model including spin 1 mesons but with the larger value $m_\sigma \approx 0.62$ GeV in the model without spin 1 mesons. It is hard to distinguish the two fits at the lower energies but above $\sqrt{s} \approx 0.35$ MeV the two model curves begin to diverge from each other and also to approach the unitarity bound, $R_0^0 = 1/2$. Clearly, the accuracy of the model must be improved to obtain a “global” description of the physics which does not violate the unitarity bound.

An easy way to cure this theoretical problem in the present model is to use the well known K -matrix unitarization. As applied to $l = 0, I = 0$ amplitude, we identify the “Born” term T_0^0 with K and write for the unitarized partial wave amplitude, $(T_0^0)_U$:

$$(T_0^0)_U = \frac{T_0^0}{1 - iT_0^0}. \quad (2.29)$$

Clearly, near threshold, where T_0^0 is small, the unitarized amplitude is essentially the same as the non-unitarized one. This unitarization is actually familiar in ordinary scattering since it converts a generic simple pole into a Breit Wigner form. Diagrammatically, it has the structure of a “bubble sum”. It is easy to verify⁴ [16] that the scattering length is unchanged from the value obtained at tree level with this type of unitarization. Although the amplitude is now exactly unitary, it is important to recognize that this K -matrix procedure is, after all, a model.

2.2.3 Scattering Away from Threshold

Fig. 2.4 shows the unitarized amplitudes, just defined, calculated up to 1 GeV. Both the linear model with $m_\sigma = 0.62$ GeV and the present model with additional spin 1 fields and $m_\sigma = 0.42$ GeV are again seen to start the same way. However afterwards, the spin 1 model amplitude rises more sharply and has its first zero, as required [since $R_0^0 \equiv T_0^0/(1 + (T_0^0)^2)$ goes to zero when T_0^0 goes to infinity] at 0.42 GeV while the plain linear model amplitude has its first zero at 0.62 GeV. The shapes of these two curves do not fit the experimental data beyond the threshold region very well. A more realistic fit would correspond, for example, to a plain linear sigma model which has its first zero in the 0.85 GeV region; see Fig. 8 and Table II in the [11]. (It is also seen there that the addition of the scalar $f_0(980)$ in that $SU(3)$ linear sigma model framework allows one to fit the peculiar looking amplitude from about 0.8 GeV to

⁴See the discussion around Eq. (47).

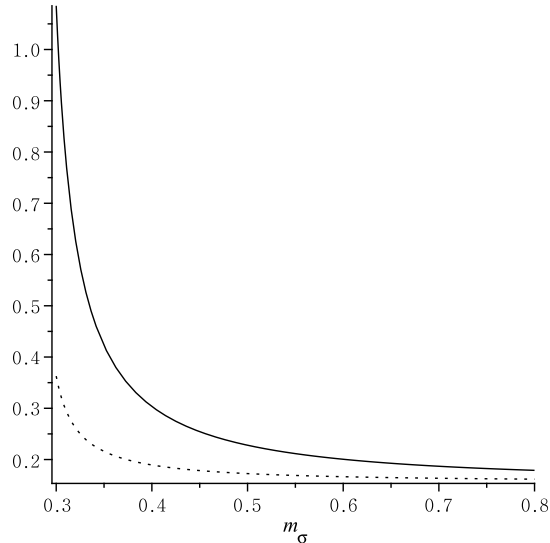


Figure 2.1 The scattering length $m_\pi a_0^0$ as a function of the sigma mass in GeV. The solid line: pure linear sigma model. The dotted line: the present model including spin 1 mesons.

about 1.2 GeV.) As a check of the validity of this “global” fit up to about 0.8 GeV we note that the sigma pole position came out to be in decent agreement with the one recently obtained by a detailed analysis [40] of the experimental data. The sigma pole position in the complex s plane is found by separating the tree amplitude into pole and non-pole pieces as:

$$T_0^0 = \alpha(s) + \frac{\beta(s)}{m_\sigma^2 - s}. \quad (2.30)$$

Then the pole position, z in the complex s plane for the K -matrix unitarized amplitude, $(T_0^0)_U$ is the solution to the equation,

$$(m_\sigma^2 - z)(1 - i\alpha(z)) - i\beta(z) = 0. \quad (2.31)$$

We find the numerical result in the simple K -matrix unitarized linear sigma model without spin 1 particles, $z^{1/2} = 0.51 - 0.23i$. This may be compared with the recent

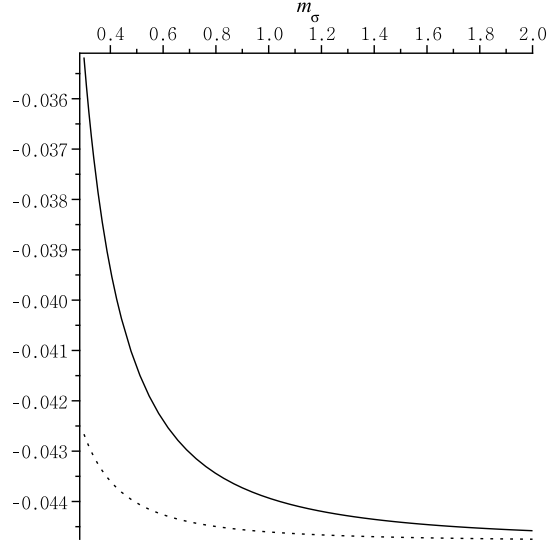


Figure 2.2 The scattering length $m_\pi a_2^0$ as a function of the sigma mass in GeV. The solid line: pure linear sigma model. The dotted line: present model including spin 1 mesons.

value, $z^{1/2} = 0.461 - 0.255i$, with an uncertainty of about .015 in each term. In Fig. 2.5 the model amplitudes for both the plain linear sigma model and the one with spin 1 particles are plotted up to 1.4 GeV using $m_\sigma = 0.85$ GeV just mentioned. The case including spin 1 particles was calculated with the choice $m_0^2 = 0$ so that $C \neq 0$. (Remember that only the combination $m_0^2 + Cv^2/2$ is known from our inputs.) While, as we just mentioned, the curve for the plain linear sigma model essentially fits the data, the curve representing the model with spin 1 particles is a rather rough approximation to it. This can be verified by noting that the pole position comes out to be, $z^{1/2} = 0.38 - 0.52i$. The fit is not improved by lowering the value of m_σ .

It is also of some interest to look at the dependence of the predicted amplitude on the parameter m_0^2 . for the case with spin 1 particles. The results for the non-zero choice, $m_0^2 = 0.27 \text{ GeV}^2$ are shown in Fig. 2.6. In this case the predictions for the

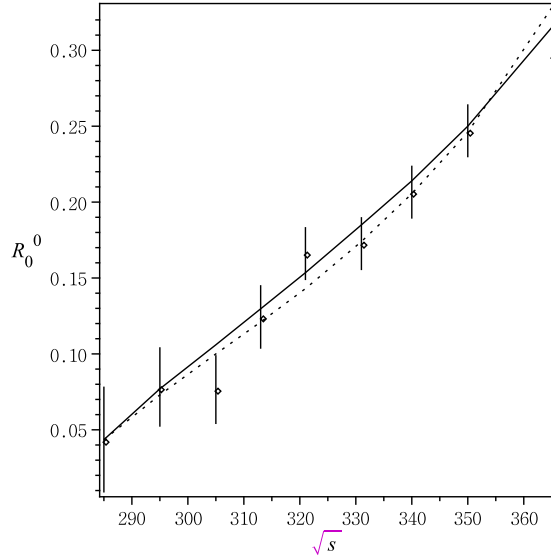


Figure 2.3 Low energy data for real part of s -wave resonant amplitude plotted against \sqrt{s} in MeV. The dotted curve is a fit to the present model with $m_\sigma = 0.42$ GeV while the solid curve is a fit to the plain linear sigma model with $m_\sigma = 0.62$ GeV

$m_0^2 \neq 0$ case seem to be further distorted, showing that $m_0^2 = 0$ provides a better fit.

How much does the $m_\sigma = 0.85$ GeV choice, which was used for the region up to about 0.8 GeV change the fit to the data close to threshold obtained with smaller values of m_σ ? This is shown in Fig. 2.7. Clearly, both plots lie below the low energy data. Thus there is some tension between a reasonable fit close to threshold (which requires a low value of m_σ) and a fit over a larger range (which requires a larger value of m_σ).

It is clear that the direct channel $f_0(980)$ MeV state must be also included to adequately treat the scalar $I = 0$ amplitude in the region from 800 to about 1200 MeV. We consider this region to be beyond the range of applicability of the model with a single sigma state.

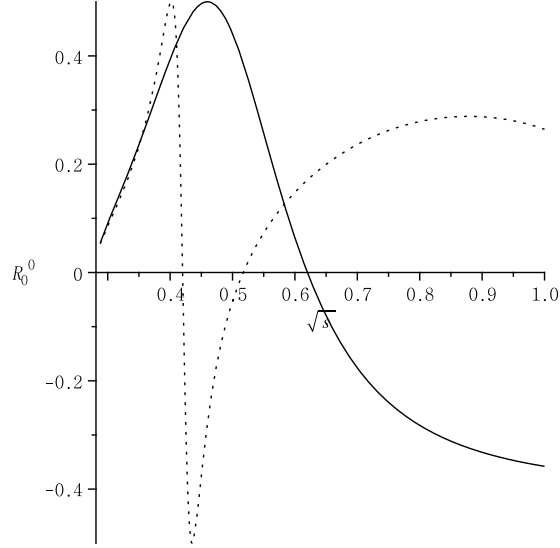


Figure 2.4 Unitarized amplitudes plotted as a function of \sqrt{s} to 1 GeV. The dashed curve corresponds to the present model with $m_\sigma = 0.42$ GeV while the solid curve corresponds to the plain linear sigma model with $m_\sigma = 0.62$ GeV.

2.2.4 Connections with Other Work

In the historical treatment of chiral models containing vector and axial vector mesons as well as the pion, two plausible relations among their parameters - the KSRF [41] and Weinberg [42] formulas have been widely discussed. Eventually, it was accepted that they are not forced to hold by chiral symmetry but in some limit can be correlated with each other. These formulas are, respectively,

$$\begin{aligned} (g_{\rho\pi\pi}^{eff})^2 &= 2m_\rho^2/\tilde{F}_\pi^2, \\ m_A^2 &= 2m_\rho^2. \end{aligned} \tag{2.32}$$

Numerically, the first relation holds to about 4% while the second only holds to about 26%.

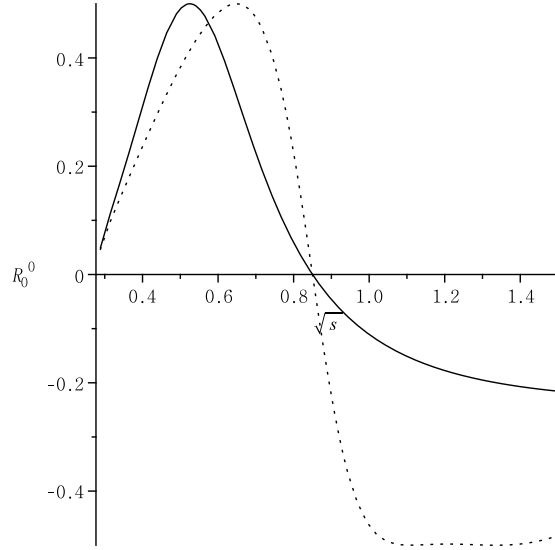


Figure 2.5 Unitarized scattering amplitudes to 1.4 GeV with m_σ chosen to be 0.85 GeV for both the plain (solid curve) and spin 1 meson (dashed curve) sigma models. Here $m_0^2 = 0$ was assumed.

In the present work it was not necessary to use either of these formulas. Nevertheless, it may be interesting to first briefly discuss the limit of our model which correlates the two formulas. This limit corresponds to, first, approximating $g_{\rho\pi\pi}^{eff}$ by g and, second, setting $B = 0$. We will show that the Weinberg relation then implies the KSRF relation. From both of Eqs. (2.14) we then note that w^2 in Eq. (2.17) becomes simply,

$$w^2 = \frac{m_A^2}{m_\rho^2} = 2. \quad (2.33)$$

Eq. (2.19) then reads $v^2 = \tilde{F}_\pi^2$ so that,

$$m_A^2 - m_\rho^2 = m_\rho^2 = g^2 v^2 / 2 = g^2 \tilde{F}_\pi^2 / 2, \quad (2.34)$$

which is the KSRF relation. Note that approximating $g_{\rho\pi\pi}^{eff}$ by g amounts physically to neglecting the B term in the Lagrangian as well as the induced three derivative

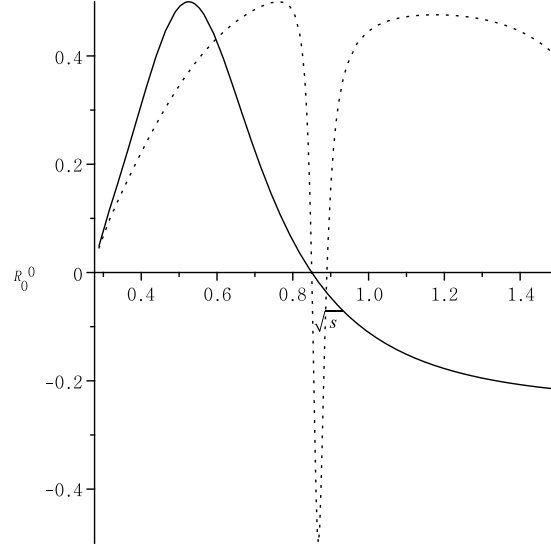


Figure 2.6 Same as Fig. 2.5 but assuming $m_0^2 = 0.27 \text{ GeV}^2$ instead

$\rho\pi\pi$ interaction term. It is also seen that the two equations in Eq. (2.32) hold at the special point where the square root in Eq. (2.23) vanishes (with $B = 0$).

An interesting different possible application of the present chiral model containing vector and axial vector mesons is to the effective Higgs sector of the minimal walking technicolor theory [43]. That theory may provide the mechanism for constructing a technicolor model which gives consistent values of the electroweak “oblique” parameters. A characteristic feature is the situation where the vector boson is heavier than the axial vector boson. To investigate this possibility we now search for more general parameter solutions, including those with the negative sign in Eq. (2.23).

It is convenient to define

$$\chi = \frac{g^2 v^2}{2m_A^2}. \quad (2.35)$$

Then the pion wave function renormalization is given by,

$$w^2 = \frac{1}{1 - \chi}. \quad (2.36)$$

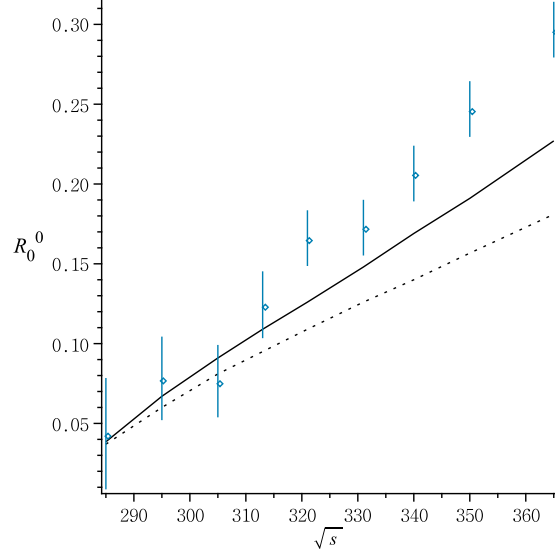


Figure 2.7 Predictions for the choice $m_\sigma = 0.85$ GeV in the region near threshold. Same conventions as in Fig. 2.3

Eq. (2.23) then reads:

$$\chi = \frac{1}{2} \left(1 \pm \sqrt{1 - \frac{g^2 \tilde{F}_\pi^2}{m_A^2}} \right), \quad (2.37)$$

Notice that to have a consistent solution for the parameters we must require:

$$g^2 \leq m_A^2 / \tilde{F}_\pi^2. \quad (2.38)$$

Finally, Eq. (2.24) can be rewritten as,

$$g_{\rho\pi\pi}^{eff} = \frac{g\tau}{2} \left(\frac{2 - \chi}{1 - \chi} \right), \quad (2.39)$$

where we defined, for convenience,

$$\tau = \frac{m_\rho^2}{m_A^2}. \quad (2.40)$$

Note especially that when Eq. (2.37) is inserted into Eq. (2.39), we can use it to find $g_{\rho\pi\pi}^{eff}$ as a function of g for given values of the physical quantities, \tilde{F}_π and m_A . This determines g and then v etc.

In Fig. 2.8, in which the plus sign in Eq. (2.37) has been chosen, the lower curve displays $g_{\rho\pi\pi}^{eff}$ as a function of g for the physical choice,

$$\tau_{QCD} = \left(\frac{m_\rho}{m_A}\right)^2 \approx 0.4. \quad (2.41)$$

We see that the physical value, $g_{\rho\pi\pi}^{eff} \approx 8.56$ corresponds to the value $g = 7.78$, which is safely below the bound at,

$$\frac{m_A}{\tilde{F}_\pi} = 9.46. \quad (2.42)$$

The upper curve in Fig. 2.8 corresponds, for illustration of the $m_\rho > m_A$ case, to a choice, $\tau = 1.2$. In this case we have no experimentally a priori way of specifying the physical parameters and the bound. Nevertheless, we observe that $g_{\rho\pi\pi}^{eff}$ would be exceptionally large for a reasonable solution.

In Fig. 2.9, which corresponds to the choice of the minus sign in Eq. (2.37), it is seen that the QCD case (lower curve) has no consistent parameter solution since $g_{\rho\pi\pi}^{eff} = 8.56$ can not be achieved for $g < 9.46$. On the other hand, the upper curve, which corresponds again to $\tau = 1.2$, gives reasonable values of $g_{\rho\pi\pi}^{eff}$.

To summarize: the QCD case corresponds to the plus sign choice in Eq. (2.37) while a possible consistent parameter solution in a non-QCD setting with $m_\rho > m_A$ is likely to correspond to the minus sign choice.

It is amusing to observe that the relation between the vacuum value v and \tilde{F}_π differs for the two sign choices:

$$\begin{aligned} \tilde{F}_\pi &< v && (+sign), \\ \tilde{F}_\pi &> v && (-sign). \end{aligned} \quad (2.43)$$

To see this note that for the plus sign case, Eq. (2.37) gives $1/2 < \chi < 1$ which, using Eq. (2.36) translates to $w > \sqrt{2}$ and the desired result when Eq. (2.19) is noted. The minus sign case is obtained similarly after first noting $1 < w < \sqrt{2}$ in that situation.

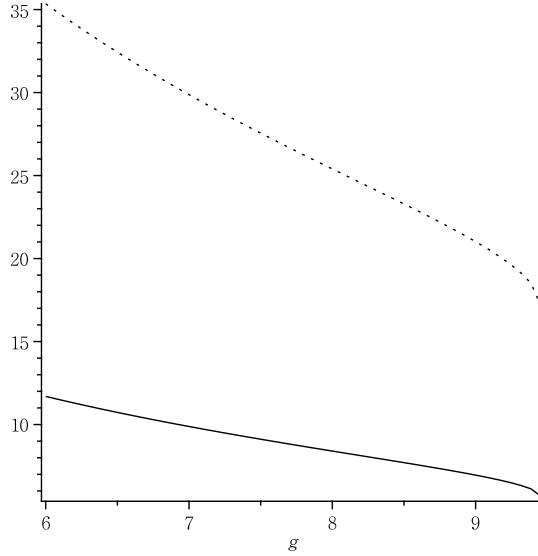


Figure 2.8 $g_{\rho\pi\pi}^{eff}$ vs g with the plus sign in Eq. (2.37). The lower curve is the QCD case while the upper curve corresponds to a hypothetical “walking technicolor” case with $m_\rho > m_A$.

We have seen that the choice of sign in Eq. (2.37) distinguishes the two cases where m_ρ is less than or greater than m_A . This choice occurs in fitting the parameters to experiment. It may be of some interest to ask how this distinction is related to the parameters of the effective Lagrangian directly. To investigate this, we just subtract the second of Eqs. (2.14) from the first:

$$m_\rho^2 - m_A^2 = -\frac{v^2}{2}(B + g^2). \quad (2.44)$$

In the QCD case, Table 2.2 shows that B is negative and that the right hand side above is negative because $g^2 > |B|$. In the case which should correspond to a walking technicolor theory we evidently must require, if B is also negative, the opposite condition $g^2 < |B|$. That condition seems intuitively plausible. Since B is the coefficient of a scale invariant term in the effective Lagrangian, we might expect it not to change sign in going from one theory to the other. Furthermore, we would expect the

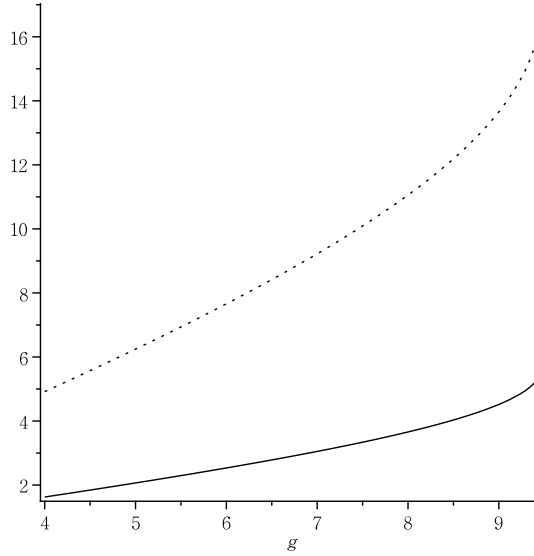


Figure 2.9 $g_{\rho\pi\pi}^{eff}$ vs g with the minus sign in Eq. (2.37). The lower curve is the QCD case while the upper curve corresponds to a hypothetical “walking technicolor” case with $m_\rho > m_A$.

phenomenological coupling constant g to behave something like the underlying gauge theory coupling constant and hence to decrease in strength for a “walking” theory ⁵

2.3 Two Higgs Doublet Model

It is well known that the ordinary Higgs potential is formally identical to the Gell-Mann Levy $SU(2)$ linear sigma model [3] potential:

$$V = \alpha_1 I_1 + \alpha_3 (I_1)^2, \quad (2.45)$$

where the $SU(2)_L \times SU(2)_R$ invariant I_1 is simply expressed in terms of the scalar singlet σ and the pseudoscalar triplet $\boldsymbol{\pi}$ as $I_1 = \sigma^2 + \boldsymbol{\pi}^2$. The sigma is identified with the Higgs and the $\boldsymbol{\pi}$ with the particles eaten by the W and Z bosons. The

⁵See for example Fig. 5 in the second to the last paper in [43] above.

analogues of these two particles are the lowest lying ones in ordinary QCD. Clearly a technicolor model which is a straightforward copy of ordinary QCD would be expected to give such a potential as a first approximation. However, it is not easy to rigorously explore the low lying spectrum of an arbitrary strongly interacting gauge theory [44]. Furthermore it is now known that a so-called “walking” technicolor model [43] may be a more reasonable candidate than straightforwardly extended QCD. Thus we will not insist that a technicolor induced Higgs potential be identical to the above and shall not try to estimate the particle masses. Rather we will just ask the effective Higgs potential to satisfy the general properties:

1. $SU(2)_L \times SU(2)_R$ flavor invariance.
2. Parity invariance and charge conjugation invariance.

These are clearly very reasonable for a strong interaction gauge theory with two massless flavors.

In the present note we introduce a second Higgs doublet based on the fact that the fundamental representation of $SU(2)$ is equivalent to its complex conjugate. This has the consequence that the $(\boldsymbol{\pi}, \sigma)$ multiplet used above is irreducible under the chiral $SU(2)_L \times SU(2)_R$ group without including the parity reversed partners, denoted as (\mathbf{a}, η) . It seems natural to investigate what happens when these parity reversed partners are included in a second Higgs doublet. Then, the three basic invariants are,

$$\begin{aligned}
 I_1 &= \sigma^2 + \boldsymbol{\pi}^2, \\
 I_2 &= \eta^2 + \mathbf{a}^2, \\
 I_3 &= \sigma\eta - \boldsymbol{\pi} \cdot \mathbf{a}.
 \end{aligned}
 \tag{2.46}$$

These forms are readily understandable since the two quartet fields may be regarded as 4-vectors in the $O(4) \sim SU(2)_L \times SU(2)_R$ space [45] and these are the three basic

invariants which can be made from them. Then the Higgs potential becomes,

$$V = \alpha_1 I_1 + \alpha_2 I_2 + \alpha_3 I_1^2 + \alpha_4 I_2^2 + \alpha_5 I_3^2 + \alpha_6 I_1 I_2 \quad (2.47)$$

The lack of terms linear in I_3 is due to the assumption of parity invariance. This implies that the fields \mathbf{a} and η each only occur in the potential paired off with either itself or the other. This feature may be expressed as the invariance of the potential under the transformation:

$$\eta \rightarrow -\eta, \quad \mathbf{a} \rightarrow -\mathbf{a}, \quad (2.48)$$

while the fields in the multiplet, $(\boldsymbol{\pi}, \sigma)$ are unchanged. Altogether there are six real constants. The present potential is supposed to be an effective one, arising from some underlying renormalizable gauge theory.

Interactions violating the invariances in 1. and 2. above are introduced as perturbations in the model when the chiral fields are coupled to the $SU(2) \times U(1)$ gauge fields in the usual way. The two quartets of the chiral group are conveniently written for this purpose as two spinors,

$$\Phi = \begin{bmatrix} i\pi^+ \\ \frac{\sigma - i\pi^0}{\sqrt{2}} \end{bmatrix}, \quad \Psi = \begin{bmatrix} -ia^+ \\ \frac{\eta + ia^0}{\sqrt{2}} \end{bmatrix}, \quad (2.49)$$

and their conjugates. Furthermore,

$$\pi^+ = \frac{\pi_1 - i\pi_2}{\sqrt{2}} \quad a^+ = \frac{a_1 - ia_2}{\sqrt{2}}. \quad (2.50)$$

The gauged kinetic terms for these fields give the usual Lagrangian contribution:

$$\mathcal{L} = -D_\mu \Phi^\dagger D_\mu \Phi - D_\mu \Psi^\dagger D_\mu \Psi \quad (2.51)$$

where

$$\begin{aligned} D_\mu \Phi &= \partial_\mu \Phi - igW_\mu \Phi + \frac{ig'}{2} B_\mu \Phi, \\ D_\mu \Phi^\dagger &= \partial_\mu \Phi^\dagger + ig\Phi^\dagger W_\mu - \frac{ig'}{2} B_\mu \Phi^\dagger, \end{aligned} \quad (2.52)$$

with similar forms containing Ψ . Here B_μ is the U(1) gauge boson and the SU(2) gauge bosons are expanded as:

$$W_\mu = \frac{1}{2} \boldsymbol{\tau}^a \cdot \mathbf{W}_\mu^a = \frac{1}{2} \begin{bmatrix} W_\mu^0 & \sqrt{2}W_\mu^+ \\ \sqrt{2}W_\mu^- & -W_\mu^0 \end{bmatrix}$$

The presence of the pure SU(2) \times U(1) gauge field kinetic terms in \mathcal{L} is to be understood. Finally consider the Yukawa terms containing the coupling of the quarks and leptons to the Higgs field. For this purpose, it seems natural to demand the symmetry in Eq. (2.48), which can be rewritten as,

$$\Phi \rightarrow \Phi, \quad \Psi \rightarrow -\Psi. \quad (2.53)$$

We also assume here that the quarks and leptons do not change under this symmetry transformation. Then only the original Higgs multiplet Φ can couple to the fermions and the Yukawa couplings are just the usual ones.

2.3.1 Discussion

There has been a very extensive discussion of various two Higgs doublet models in the literature. Recent related work includes that of Randall [46], who considers a model with a heavy extra doublet in which the mixing between singlet states is very small (i.e., large $\tan\beta$), Ma⁶ [47] who stresses the connection with the dark matter problem, Gerard and Herquet [48] who consider connections with the custodial symmetry and Lopez Honorez, Nezri, Oliver and Tytgat [49] who discuss the dark matter application extensively.

In the present work we emphasize that the idea of compositeness for the Higgs bosons motivates both the SU(2)_L \times SU(2)_R as well as the P and C invariance of the

⁶In this paper, a model similar to the present one is mentioned as a special case of a more general two Higgs scheme.

Higgs potential. This contains the usual custodial $SU(2)_V$ symmetry together with a discrete Z_2 symmetry. If it is true that the model arises from some underlying technicolor theory, it is reasonable to think that the Higgs potential is an approximation to the underlying theory describing the interactions of its lowest lying scalar states. From this point of view the electroweak interactions represent a perturbation to this “strong” interaction. Then it seems natural to classify the symmetries of the Higgs potential according to the larger “strong” interaction symmetry. This stands in contrast to discussing the symmetry from the point of view of the spinors Φ and Ψ in Eq. (2.49). In that language, our invariant I_1 is identified as $2\Phi^\dagger\Phi$ while I_2 is identified as $2\Psi^\dagger\Psi$. Also our I_3 corresponds to the combination $[\Phi^\dagger\Psi + \Psi^\dagger\Phi]$. On the other hand, the combination $i[\Phi^\dagger\Psi - \Psi^\dagger\Phi]$ is easily seen to violate the proposed $SU(2)_L \times SU(2)_R$ invariance and will not be included. This gives an additional simplification of the potential.

It is interesting to remark that the “minimal walking technicolor theory” automatically respects the symmetries 1. and 2. which we are advocating. That theory contains the Higgs bosons we are studying but also contains other effective fields associated with the technicolor interactions.

2.3.2 Higgs Potential Terms

Recent discussions of general two Higgs doublet potentials are given in⁷ [50]. The present case, in which the field variables comprise two $O(4)$ vectors, is simpler than the general case. First, we note the constraints which follow from the requirement that the Higgs potential be positive for large field configurations. This implies that the quartic terms of the potential,

$$V = \dots + \alpha_3(I_1)^2 + \alpha_4(I_2)^2 + [\alpha_5 \cos^2 \theta + \alpha_6]I_1I_2, \quad (2.54)$$

where we used the $O(4)$ property that $I_3^2 = I_1I_2 \cos^2 \theta$ for some angle θ , be positive for large field configurations. Then taking either I_1 or I_2 to be dominant for large fields we get the requirements:

$$\alpha_3 > 0, \quad \alpha_4 > 0. \quad (2.55)$$

There is a possibility that α_5 and/or α_6 may be negative. In such cases there is an additional discriminant condition which is obtained by forbidding real roots of the

⁷It seems worthwhile to remark, as briefly noted in section II above, that our potential is significantly simpler than the general ones discussed in these references. This follows because of the imposition of the technicolor inspired requirements of “strong” $SU(2)_L \times SU(2)_R$ symmetry as well as P and C conservation on the Higgs potential. To compare with these references we note that our $\alpha_3, \alpha_4, \alpha_6$ correspond to their $\lambda_1, \lambda_2, \lambda_3$ respectively. On the other hand they have two more quartic invariants while we have just one more. Our final $SU(2)_L \times SU(2)_R$ quartic invariant has the coefficient α_5 . Note that the square of $i[\Phi^\dagger \Psi - \Psi^\dagger \Phi]$ has the electroweak $SU(2)_L$ invariance but does not satisfy the larger “technicolor” invariance we are requiring. If we take linear combinations of our α_5 term with this disallowed piece we could recover both the usual λ_4 and λ_5 terms. This also demonstrates that the conventional λ_4 and λ_5 terms do not obey the $O(4)$ invariance being imposed in the present model. Our simplified potential results in the very much simplified mass formulas given in Eqs.(2.61) for the masses of the additional Higgs particles.

quadratic form obtained by dividing through by $(I_1)^2$. It has the form:

$$(\alpha_5 \cos^2 \theta + \alpha_6)^2 < 4\alpha_3\alpha_4, \quad (2.56)$$

for any θ . As examples,

$$(\alpha_5 + \alpha_6)^2 < 4\alpha_3\alpha_4, \quad \alpha_6^2 < 4\alpha_3\alpha_4. \quad (2.57)$$

Stronger information on the α coefficients arises, as to be discussed next, from calculating the particle masses and interactions by expanding the potential around the physical minimum $\langle \sigma \rangle \neq 0$, $\langle \eta \rangle = 0$. The latter corresponds to our assumed underlying parity invariance. A simple calculation verifies that $\langle \partial V / \partial \sigma \rangle = \langle \partial V / \partial \eta \rangle = 0$ for this minimum.

The α_1 and α_3 terms in Eq. (2.47) correspond to the usual single Higgs model. In the present case, parity invariance prevents the σ from mixing with the η so α_1 and α_3 are determined just as in the standard model. Then α_1 is negative and related to α_3 by the minimization equation:

$$\alpha_1 + 2\alpha_3 v^2 = 0, \quad (2.58)$$

where the vacuum value, v is given as

$$v = \langle \sigma \rangle \approx 246 \text{ GeV}. \quad (2.59)$$

The Higgs squared mass is obtained as

$$m_\sigma^2 = 8\alpha_3 v^2. \quad (2.60)$$

The potential also yields $m_\pi^2 = 0$ for all three ‘‘pions’’, which, in the unitary gauge get absorbed into massive gauge bosons. For the particles in the Ψ multiplet, the squared masses are obtained as,

$$m_\eta^2 = 2 [\alpha_2 + (\alpha_5 + \alpha_6)v^2],$$

$$m^2(a^0) = m^2(a^\pm) \equiv m_a^2 = 2 [\alpha_2 + \alpha_6 v^2]. \quad (2.61)$$

Notice that the three “a” particles are degenerate in mass. Furthermore there is no mixing between the two Higgs multiplets.

Defining a shifted Higgs field $\sigma = v + \tilde{\sigma}$, the interaction terms in the Lagrangian resulting from the Higgs potential are:

$$\begin{aligned} & -\alpha_3(\tilde{\sigma}^4 + 4v\tilde{\sigma}^3) - \alpha_4(\mathbf{a}^2 + \eta^2)^2 \\ & -\alpha_5\eta^2(2v\tilde{\sigma} + \tilde{\sigma}^2) - \alpha_6(\mathbf{a}^2 + \eta^2)(2v\tilde{\sigma} + \tilde{\sigma}^2). \end{aligned} \quad (2.62)$$

The interaction vertices for Feynman rules can be read off from this equation. For later convenience we identify the coupling constants for the $\sigma\eta\eta$ and $\sigma a^0 a^0$ vertices,

$$g_{\sigma\eta\eta} = 4v(\alpha_5 + \alpha_6), \quad g_{\sigma a^0 a^0} = 4v\alpha_6. \quad (2.63)$$

It may be noted from Eqs. (2.58) and (2.60) that specifying the Higgs mass, m_σ will fix the coefficients α_1 and α_3 . Furthermore specifying m_η , m_a and $g_{\sigma\eta\eta}$ will fix α_2 , α_5 and α_6 . Information about α_4 is related to the a- η scattering amplitude. We will not need α_4 in the present paper.

The allowed ranges of the α parameters are constrained by the requirement that the squared masses m_σ^2 , m_η^2 and m_a^2 be positive definite. This agrees with the requirement that $V(\sigma, \eta)$ have a minimum, rather than a maximum or saddle point at the point $(\sigma, \eta) = (v, 0)$. Specifically, we have:

$$\begin{aligned} A & \equiv \frac{\partial^2 V}{\partial \sigma^2}(v, 0) = 2\alpha_1 + 12v^2\alpha_3 = m_\sigma^2, \\ B & \equiv \frac{\partial^2 V}{\partial \sigma \partial \eta}(v, 0) = 0, \\ C & \equiv \frac{\partial^2 V}{\partial \eta^2}(v, 0) = 2\alpha_2 + 2v^2(\alpha_5 + \alpha_6) = m_\eta^2. \end{aligned} \quad (2.64)$$

The condition for no saddle point, $B^2 - AC < 0$ as well the condition for a minimum rather than a maximum, $A + C > 0$ are both clearly satisfied for positive definite squared masses.

No undetermined parameters are introduced here. It is necessary to first give conventions for the W_μ^0 - B_μ mixing matrix:

$$\begin{bmatrix} Z_\mu \\ A_\mu \end{bmatrix} = \begin{bmatrix} c & s \\ -s & c \end{bmatrix} \begin{bmatrix} W_\mu^0 \\ B_\mu \end{bmatrix},$$

where s and c are respectively the sine and cosine of the mixing angle. They are connected to the proton charge, e and the coupling constants in Eq. (2.52) by $g = -e/s$ and $g' = -e/c$.

2.3.3 First Model for a Hidden Higgs Scenario

Stimulated by precision calculations in the standard model giving the Higgs mass prediction, See page 128 of [7],

$$m_\sigma = 89_{-28}^{+38} GeV, \quad (2.65)$$

a number of groups have revived [52] an older idea [53] that the Higgs might be light and not yet detected because of a competitive decay mode to some hard to observe new particles. It would seem that a decay mode in the present model, $\sigma \rightarrow \eta\eta$ is a reasonable candidate for such a competing channel. As we observe above, the η occurs only in quadratic form in the Higgs potential and only together with a conceivably much heavier **a** particle in the gauge-Higgs part of the Lagrangian. Thus it could have escaped detection.

For the present purpose we need the formula for the predicted Higgs width for its decay into $\eta\eta$:

$$\Gamma(\sigma \rightarrow \eta\eta) = \frac{g_{\sigma\eta\eta}^2}{32\pi m_\sigma} \sqrt{1 - \frac{4m_\eta^2}{m_\sigma^2}}, \quad (2.66)$$

wherein $g_{\sigma\eta\eta}$ and m_η are given in Eqs. (2.63) and (2.61) respectively. It can be seen that these two quantities are determined by the parameters α_2 and $\alpha_5 + \alpha_6$. The

typical Higgs search involves the reaction:

$$Z \rightarrow Z^* + \sigma, \quad (2.67)$$

wherein the virtual Z^* decays into $\mu^+\mu^-$ and the Higgs decays primarily into $b\bar{b}$ jets.

The formula for $\Gamma(\sigma \rightarrow b\bar{b})$ is:

$$\Gamma(\sigma \rightarrow b\bar{b}) = \frac{3m_\sigma m_b^2}{8\pi v^2} \left(1 - \frac{4m_b^2}{m_\sigma^2}\right)^{3/2}, \quad (2.68)$$

where $m_b \approx 4.2$ GeV is a conventional estimate for the b quark mass. We need the ratio,

$$R = \frac{\Gamma(\sigma \rightarrow \eta\eta)}{\Gamma(\sigma \rightarrow b\bar{b})}. \quad (2.69)$$

Now if $P_{standard}$ gives the strength of the Higgs signal in the standard model scenario, the reduced strength due to the existence of the competitive $\eta\eta$ decay mode in the present scenario would be,

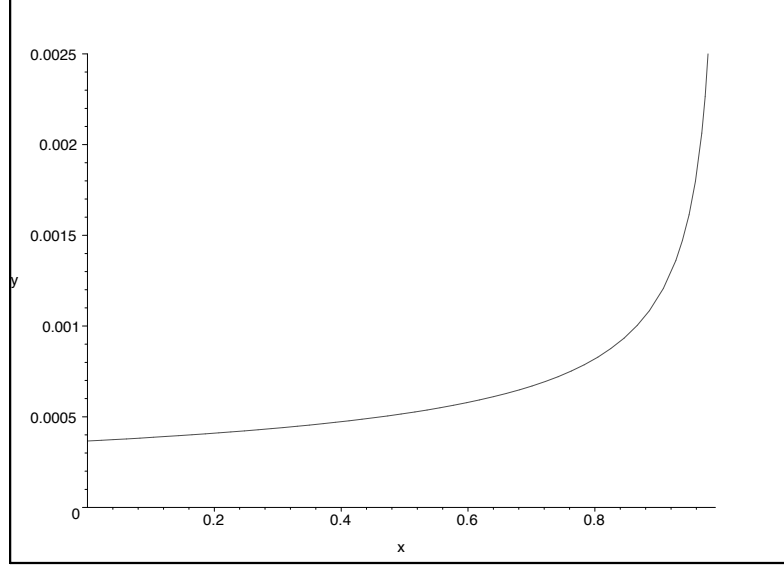
$$\begin{aligned} P_{new} &= \frac{\Gamma(\sigma \rightarrow b\bar{b})}{\Gamma(\sigma \rightarrow b\bar{b}) + \Gamma(\sigma \rightarrow \eta\eta)} P_{standard} \\ &= \frac{1}{1 + R} P_{standard}. \end{aligned} \quad (2.70)$$

It was noted [52] that a value, $R = 0.8$ would decrease the presently expected Higgs signal below the detection threshold. Using the numbers just given we have,

$$R = 2184y\sqrt{1-x}, \quad (2.71)$$

where $x=(2m_\eta/m_\sigma)^2$ and $y = (g_{\sigma\eta\eta}/v)^2$. A plot of y vs x for the value $R = 0.8$ is shown in Fig. 2.10. Any point on that curve is a solution for suppression of the $b\bar{b}$ Higgs signal.

Three typical points, together with the corresponding values of the Higgs potential parameters α_2 and $\alpha_5 + \alpha_6$ are given in Table 6.1.

Figure 2.10 y vs. x .

m_η (GeV)	$g_{\sigma\eta\eta}$ (GeV)	$\alpha_5 + \alpha_6$	α_2 (GeV ²)
14.1	4.8	4.91×10^{-3}	-198
31.5	5.6	5.69×10^{-3}	+151
42.2	8.4	8.51×10^{-3}	+376

Table 2.3 Values of m_η , $g_{\sigma\eta\eta}$ and Higgs potential parameters which give suitable suppression of the Higgs signal.

In the present scenario, with $m_a > m_\eta$, the η boson has “annihilation” modes but not decay modes. On the other hand the \mathbf{a} particles have leading decay modes of the forms,

$$a^0 \rightarrow Z + \eta, \quad a^+ \rightarrow W^+ + \eta, \quad (2.72)$$

wherein it has been assumed that the \mathbf{a} 's are sufficiently heavier than the massive gauge bosons. If the \mathbf{a} 's are lighter than the massive gauge bosons but still heavier than the η , one would expect important decays like,

$$a^0 \rightarrow \eta + \mu^+ + \mu^-, \quad a^+ \rightarrow \eta + \pi^+ \quad (139). \quad (2.73)$$

These two decays are mediated by virtual Z and W bosons respectively. The formula for the decay width of a heavy a^+ by the reaction in Eq. (2.72) is readily found to be:

$$\Gamma(a^+ \rightarrow W^+ + \eta) = \frac{k}{8\pi m_a^2} \mathcal{F}(a^+ \rightarrow W^+ + \eta), \quad (2.74)$$

where the momentum, k of each of the two daughter particles in the a^+ rest frame is:

$$k = \frac{1}{2m_a} \sqrt{[m_a^2 - (m_\eta + m_W)^2][m_a^2 - (m_\eta - m_W)^2]}, \quad (2.75)$$

and the squared amplitude summed over the final W^+ polarization states is:

$$\mathcal{F}(a^+ \rightarrow W^+ + \eta) = \left(\frac{e}{2s}\right)^2 \left[\frac{(m_\eta^2 - m_a^2)^2}{m_W^2} - m_a^2 - m_\eta^2 - 2m_a \sqrt{k^2 + m_\eta^2} \right]. \quad (2.76)$$

We may use the same formula for $\Gamma(a^0 \rightarrow Z + \eta)$ if we replace m_W by m_Z and the overall factor $(e/(2s))^2$ by $(e/(2sc))^2$. These \mathbf{a} widths are listed in Table 2.4 for a characteristic range of \mathbf{a} masses in cases where they are heavy enough to decay into the gauge boson modes. The η mass is taken to be 31.5 GeV, the central value in Table 6.1. It is seen that the widths are in the range 0.2 to 2 MeV for the \mathbf{a} masses shown. This may be compared to the width, 2.5 MeV, for the Higgs (sigma) to decay into two η 's according to Eq. (2.66) taking $m_\eta = 31.5$ GeV.

Also listed in Table 2.4 are the associated dimensionless coupling constants α_5 and α_6 in the Higgs potential. These are all less than unity, indicating that for the mass range under discussion, the new part of the Higgs sector is not very “strongly coupled”.

$m_{\mathbf{a}}$ (GeV)	$\Gamma(a^+ \rightarrow W^+\eta)$ (GeV)	$\Gamma(a^0 \rightarrow Z\eta)$ (GeV)	α_5	α_6
150	2.14×10^{-4}	1.52×10^{-4}	-0.178	0.235
200	8.70×10^{-4}	7.69×10^{-4}	-0.322	0.379
250	2.07×10^{-3}	1.94×10^{-3}	-0.508	0.565

Table 2.4 Widths of the \mathbf{a} bosons for various mass values and associated Higgs potential parameters.

It is amusing to remark that the quartic coupling constant α_5 is negative. The discussion at the end of section III implies that this is of no concern, since the squared masses of all the Higgs particles are positive. Note that the positive α_6 is larger than the magnitude of α_5 .

Since the η under study in the present scenario does not have any decay modes, it would appear to be another candidate for the “dark matter” required to understand galactic structures. Work in this direction will be presented elsewhere.

2.3.4 Second Hidden Higgs Model

It was stressed in [52] that Higgs search experiments⁸ which look for an appropriate Z (say by tagging $\mu^+\mu^-$ pairs) together with the *absence* of any other particle signals could eliminate the possibility of a light Higgs. They point out that the Higgs can therefore be shielded only if there is a “cascade” decay of the decay products (η ’s in

⁸A detailed discussion of the relevant experiments is given in [52].

the first model) to final states containing a recognizable particle. The η 's have no decays in our model, however.

We can shield a light Higgs in such an experiment if we assume that the three \mathbf{a} particles are lighter than half the Higgs mass and that the η is lighter still. For example, with a Higgs mass of 115 GeV, \mathbf{a} masses of 50 GeV could do the job. The \mathbf{a} 's would be heavy enough that they would not alter the well known Z width. (This mechanism is clearly suitable for shielding Higgs bosons which are roughly more massive than the Z). Then the decay modes

$$\sigma \rightarrow a^+ + a^-, \quad \sigma \rightarrow a^0 + a^0, \quad (2.77)$$

are possible. Furthermore, the Eqs. (2.73) show that the a 's decay into the inert η as well as the recognizable particles π^\pm or $\mu^+\mu^-$. It is still possible of course for there to be some $\sigma \rightarrow \eta + \eta$ in addition to these modes. To illustrate the present scenario we will assume for simplicity that the coupling constant, $g_{\sigma\eta\eta}$ has been tuned to be negligible. Then the relevant decay width is:

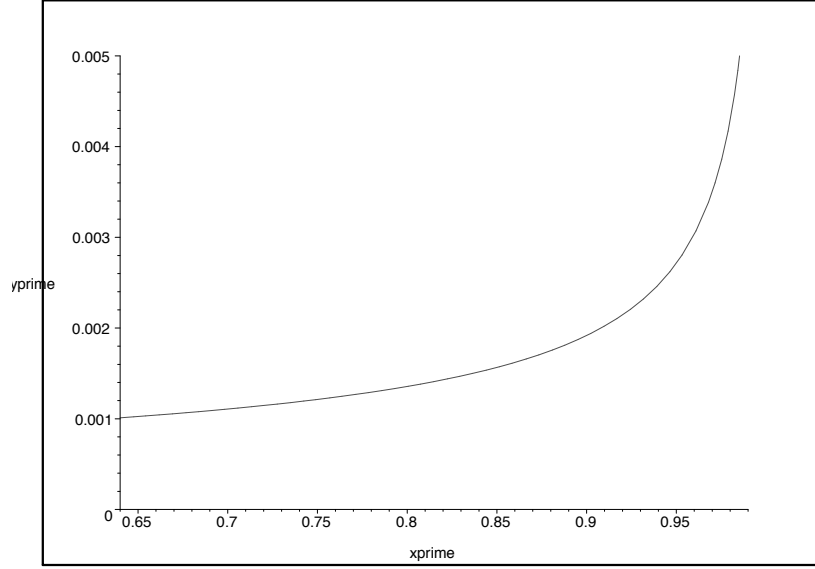
$$\begin{aligned} \Gamma(\sigma \rightarrow a^+ a^-) + \Gamma(\sigma \rightarrow a^0 a^0) = \\ 3\Gamma(\sigma \rightarrow a^0 a^0) = \frac{3g_{\sigma a^0 a^0}^2}{32\pi m_\sigma} \sqrt{1 - \frac{4m_a^2}{m_\sigma^2}}. \end{aligned} \quad (2.78)$$

Proceeding as before we define,

$$R' = \frac{3\Gamma(\sigma \rightarrow a^0 a^0)}{\Gamma(\sigma \rightarrow b\bar{b})} = 1319y'\sqrt{1 - x'^2}, \quad (2.79)$$

where $x' = (2m_a/m_\sigma)^2$ and $y' = 3(g_{\sigma a^0 a^0}/v)^2$. A plot of y' vs x' for the value $R' = 0.8$ is shown in Fig. 2.11. Any point on that curve is a solution for suppression of the $b\bar{b}$ Higgs signal. In contrast to Fig. 2.10, the x' variable is not displayed down to zero, indicating that the shielding is only operative for roughly $m_a > m_Z/2$.

Three typical points, together with the corresponding values of the Higgs potential parameters α_2 and α_6 are given in Table 2.5.

Figure 2.11 y' vs. x' .

m_a (GeV)	$g_{\sigma a^0 a^0}$ (GeV)	α_6	α_2 (GeV ²)
48.1	4.7	4.82×10^{-3}	576
51.4	5.2	5.32×10^{-3}	674
54.5	6.2	6.32×10^{-3}	723

Table 2.5 Values of m_a , $g_{\sigma a^0 a^0}$ and Higgs potential parameters which give suitable suppression of the Higgs signal. Here we take $m_\sigma = 115$ GeV.

One notices, as in the previous shielding model, that the dimensionless coupling constant α_6 is much less than one, so the Higgs bosons are not strongly coupled. If we want to tune the $\sigma \rightarrow \eta\eta$ contribution to be small, Eq. (2.63) indicates that α_5 should be taken negative and slightly less in magnitude than α_6 .

Effectively, the present “cascade” type shielding mechanism would have characteristic signals of a $\pi^+\pi^-$ pair together with two unobservable η 's or two $\mu^+\mu^-$ pairs together with two unobservable η 's.

Chapter 3

SU(3) Linear Sigma Models and Chiral Nonets

3.1 Brief Review of the Model

Historically, the nonet structure of elementary particle multiplets has suggested the spin 1/2 quark substructure and, with the help of the “slightly” broken flavor symmetry SU(3), has provided an enormous amount of information about the properties of the observed low lying hadronic states. For example, the lightest meson multiplets appear to be those of the pseudoscalars and vectors, consistent with s -wave quark-antiquark bound states. The next heaviest set of meson multiplets seems to be generally consistent with p -wave bound states, yielding a scalar nonet, a tensor nonet and two axial vector nonets.

This chiral point of view may be especially relevant for studying the light scalars since they are the “chiral partners” of the zero mass pseudoscalars. To implement this picture systematically one may introduce a $q\bar{q}$ chiral nonet containing 9 scalar and 9 pseudoscalar fields as well as a $qq\bar{q}\bar{q}$ nonet also containing 9 scalars and 9

pseudoscalars. Furthermore, the light quark mass terms should be added as well as suitable terms to mock up the $U(1)_A$ anomaly of QCD.

The model employs the 3×3 matrix chiral nonet fields,

$$M = S + i\phi, \quad M' = S' + i\phi'. \quad (3.1)$$

The matrices M and M' transform in the same way under chiral $SU(3)$ transformations but may be distinguished by their different $U(1)_A$ transformation properties. M describes the “bare” quark antiquark scalar and pseudoscalar nonet fields while M' describes “bare” scalar and pseudoscalar fields containing two quarks and two antiquarks. At the symmetry level in which we are working, it is unnecessary to further specify the four quark field configuration. The four quark field may, most generally, be imagined as some linear combination of a diquark-antidiquark and a “molecule” made of two quark-antiquark “atoms”.

The general Lagrangian density which defines our model is,

$$\mathcal{L} = -\frac{1}{2}\text{Tr}(\partial_\mu M \partial_\mu M^\dagger) - \frac{1}{2}\text{Tr}(\partial_\mu M' \partial_\mu M'^\dagger) - V_0(M, M') - V_{SB}, \quad (3.2)$$

where $V_0(M, M')$ stands for a function made from $SU(3)_L \times SU(3)_R$ (but not necessarily $U(1)_A$) invariants formed out of M and M' .

As discussed [17], the leading choice of terms corresponding to eight or fewer underlying quark plus antiquark lines at each effective vertex reads,

$$\begin{aligned} V_0 = & -c_2 \text{Tr}(MM^\dagger) + c_4^a \text{Tr}(MM^\dagger MM^\dagger) \\ & + d_2 \text{Tr}(M'M'^\dagger) + e_3^a (\epsilon_{abc} \epsilon^{def} M_d^a M_e^b M_f^c + h.c.) \\ & + c_3 \left[\gamma_1 \ln\left(\frac{\det M}{\det M^\dagger}\right) + (1 - \gamma_1) \ln\left(\frac{\text{Tr}(MM^\dagger)}{\text{Tr}(M'M'^\dagger)}\right) \right]^2. \end{aligned} \quad (3.3)$$

All the terms except the last two (which mock up the axial anomaly) have been chosen to also possess the $U(1)_A$ invariance. The symmetry breaking term which models the

QCD mass term takes the form,

$$V_{SB} = -2 \text{Tr}(A S), \quad (3.4)$$

where $A = \text{diag}(A_1, A_2, A_3)$ are proportional to the three light quark masses. The model allows for two-quark condensates, $\alpha_a = \langle S_a^a \rangle$ as well as four-quark condensates $\beta_a = \langle S'^a_a \rangle$. Here we assume¹ [54] isotopic spin symmetry so $A_1 = A_2$ and,

$$\alpha_1 = \alpha_2 \neq \alpha_3, \quad \beta_1 = \beta_2 \neq \beta_3. \quad (3.5)$$

We also need the “minimum” conditions,

$$\left\langle \frac{\partial V_0}{\partial S} \right\rangle + \left\langle \frac{\partial V_{SB}}{\partial S} \right\rangle = 0, \quad \left\langle \frac{\partial V_0}{\partial S'} \right\rangle = 0. \quad (3.6)$$

There are twelve parameters describing the Lagrangian and the vacuum. These include the six coupling constants given in Eq. (3.3), the two quark mass parameters, ($A_1 = A_2, A_3$) and the four vacuum parameters ($\alpha_1 = \alpha_2, \alpha_3, \beta_1 = \beta_2, \beta_3$). The four minimum equations reduce the number of needed input parameters to eight.

Five of these eight are supplied by the following masses together with the pion decay constant,

$$\begin{aligned} m[a_0(980)] &= 984.7 \pm 1.2 \text{ MeV}, \\ m[a_0(1450)] &= 1474 \pm 19 \text{ MeV}, \\ m[\pi(1300)] &= 1300 \pm 100 \text{ MeV}, \\ m_\pi &= 137 \text{ MeV}, \\ F_\pi &= 131 \text{ MeV}. \end{aligned} \quad (3.7)$$

Because $m[\pi(1300)]$ has such a large uncertainty, we will examine predictions depending on the choice of this mass within its experimental range. The sixth input will be

¹The isospin violation case for the single M linear sigma model was treated here.

taken as the light “quark mass ratio” A_3/A_1 , which will be varied over an appropriate range. The remaining two inputs will be taken from the masses of the four (mixing) isoscalar, pseudoscalar mesons. This mixing is characterized by a 4×4 matrix M_η^2 . A practically convenient choice is to consider $\text{Tr}M_\eta^2$ and $\det M_\eta^2$ as the inputs.

Given these inputs there are a very large number of predictions. At the level of the quadratic terms in the Lagrangian, we predict all the remaining masses and decay constants as well as the angles describing the mixing between each of (π, π') , (K, K') , (a_0, a'_0) , (κ, κ') multiplets and each of the 4×4 isosinglet mixing matrices (each formally described by six angles).

In the case of the $I = 0$ scalars there are four particles which mix with each other; the squared mass matrix then takes the form,

$$(X_0^2) = \begin{bmatrix} 4 e_3^a \beta_3 - 2 c_2 + 12 c_4^a \alpha_1^2 & 4 \sqrt{2} e_3^a \beta_1 & 4 e_3^a \alpha_3 & 4 \sqrt{2} e_3^a \alpha_1 \\ 4 \sqrt{2} e_3^a \beta_1 & -2 c_2 + 12 c_4^a \alpha_3^2 & 4 \sqrt{2} e_3^a \alpha_1 & 0 \\ 4 e_3^a \alpha_3 & 4 \sqrt{2} e_3^a \alpha_1 & 2 d_2 & 0 \\ 4 \sqrt{2} e_3^a \alpha_1 & 0 & 0 & 2 d_2 \end{bmatrix}. \quad (3.8)$$

For this matrix the basis states are consecutively,

$$\begin{aligned} f_a &= \frac{S_1^1 + S_2^2}{\sqrt{2}} & n\bar{n}, \\ f_b &= S_3^3 & s\bar{s}, \\ f_c &= \frac{S_1'^1 + S_2'^2}{\sqrt{2}} & ns\bar{n}\bar{s}, \\ f_d &= S_3'^3 & nn\bar{n}\bar{n}. \end{aligned} \quad (3.9)$$

The non-strange (n) and strange (s) quark content for each basis state has been listed at the end of each line above.

3.1.1 Chiral Nonet Mixing in $\pi\pi$ Scattering

We will work with the above Lagrangian (i.e. without introducing any new parameters) and investigate the effect of unitarization on the isosinglet, zero angular momentum partial wave $\pi\pi$ scattering amplitude computed at tree order.

We will treat the pion scattering amplitude unitarization by using the K -matrix method. As the model involves two nonets of scalars, there are altogether four isosinglet scalar mesons (two from each nonet) that contribute as poles in the pion scattering amplitude. Therefore the K -matrix unitarization has to deal with all four poles at the same time resulting in a more involved version of the conventional single-pole K -matrix unitarization.

The advantages of the K -matrix approach to unitarization are that it does not introduce any new parameters and that it forces exact unitarity. It is plausible since if one starts from a pure pole in the partial wave amplitude, one ends up with a pure Breit Wigner shape. A disadvantage is that it neglects, in the simple version we use, the effects of the opening of thresholds like the $K\bar{K}$ on the $\pi\pi$ amplitude. This is not expected to be too serious for our initial appraisal here.

The tree level $\pi\pi$ scattering amplitude is,

$$A(s, t, u) = -\frac{g}{2} + \sum_i \frac{g_i^2}{m_i^2 - s}, \quad (3.10)$$

where the four point coupling constant is related to the “bare” four-point couplings as,

$$\begin{aligned} g &= \left\langle \frac{\partial^4 V}{\partial\pi^+ \partial\pi^- \partial\pi^+ \partial\pi^-} \right\rangle, \\ &= \sum_{A,B,C,D} \left\langle \frac{\partial^4 V}{\partial(\phi_1^2)_A \partial(\phi_2^1)_B \partial(\phi_1^2)_C \partial(\phi_2^1)_D} \right\rangle \\ &\times (R_\pi)_{A1} (R_\pi)_{B1} (R_\pi)_{C1} (R_\pi)_{D1}, \end{aligned} \quad (3.11)$$

where the sum is over “bare” pions and $A, B, \dots = 1, 2$ with 1 denoting nonet M and

2 denoting nonet M' . R_π is the pion rotation matrix (given, for typical parameters in [20]).

The physical scalar-pseudoscalar-pseudoscalar couplings are related to the bare couplings,

$$g_i = \left\langle \frac{\partial^3 V}{\partial f_i \partial \pi^+ \partial \pi^-} \right\rangle = \sum_{M,A,B} \left\langle \frac{\partial^3 V}{\partial f_M \partial (\phi_1^2)_A \partial (\phi_2^1)_B} \right\rangle (L_0)_{Mi} (R_\pi)_{A1} (R_\pi)_{B1}, \quad (3.12)$$

where A and $B = 1, 2$ and $M = 1, 2, 3$ and 4 and respectively represent the four bases in Eq. (3.43). L_0 is the isosinglet scalar rotation matrix.

The only non-vanishing “bare” four-point and three-point couplings are,

$$\begin{aligned} \left\langle \frac{\partial^4 V}{\partial (\phi_1^2)_1 \partial (\phi_2^1)_1 \partial (\phi_1^2)_1 \partial (\phi_2^1)_1} \right\rangle &= 8 c_4^a, & (3.13) \\ \left\langle \frac{\partial^3 V}{\partial f_a \partial (\phi_1^2)_1 \partial (\phi_2^1)_1} \right\rangle &= 4 \sqrt{2} c_4^a \alpha_1, \\ \left\langle \frac{\partial^3 V}{\partial f_b \partial (\phi_1^2)_1 \partial (\phi_2^1)_2} \right\rangle &= \left\langle \frac{\partial^3 V}{\partial f_b \partial (\phi_1^2)_2 \partial (\phi_2^1)_1} \right\rangle, \\ &= \left\langle \frac{\partial^3 V}{\partial f_c \partial (\phi_1^2)_1 \partial (\phi_2^1)_1} \right\rangle = 4 e_3^a. & (3.14) \end{aligned}$$

Now we project Eq. (3.10) to the $I = J = 0$ partial wave amplitude. The K -matrix unitarization of this “Born” scattering amplitude T_0^{0B} defines the unitary partial wave amplitude,

$$T_0^0 = \frac{T_0^{0B}}{1 - i T_0^{0B}}, \quad (3.15)$$

wherein,

$$T_0^{0B} = T_\alpha + \sum_i \frac{T_\beta^i}{m_i^2 - s}, \quad (3.16)$$

with,

$$T_\alpha = \frac{1}{64\pi} \sqrt{1 - \frac{4m_\pi^2}{s}} \left[-5g_4 + \frac{1}{p_\pi^2} \sum_i g_i^2 \ln \left(1 + \frac{4p_\pi^2}{m_i^2} \right) \right], \quad (3.17)$$

$$T_\beta^i = \frac{3}{32\pi} \sqrt{1 - \frac{4m_\pi^2}{s}} g_i^2, \quad (3.18)$$

$$p_\pi = \frac{1}{2}\sqrt{s - 4m_\pi^2}. \quad (3.19)$$

3.1.2 Comparison with Experiment

For comparison with experiment it is convenient to focus on the real part of the partial wave scattering amplitude in Eq. (3.15). For typical values of parameters we find the behavior illustrated in Fig. (3.1). The zeros which occur can be understood as follows. First, they can result from a zero of T_0^{0B} . Such a zero occurs at threshold, for example. Secondly, a zero can also result from the poles in T_0^{0B} at $s = m_i^2$ in Eq. (3.16) corresponding to the “bare” masses.

We compare the predictions of our model for the scattering amplitude with the corresponding experimental data up to about 1.2 GeV in Fig 3.2 for two values of the SU(3) symmetry breaking parameter A_3/A_1 and three choices of the only roughly known “heavy pion” mass $m[\Pi(1300)]$. One sees that, without using any new parameters, the mixing mechanism of [20] predicts the scattering amplitude in reasonable qualitative agreement with the experimental data up to around 1 GeV. This provides some support for the validity of this mixing mechanism.

For interpretation of the physical resonances it is conventional to look at the pole positions in the complex plane of the analytically continued expression for T_0^0 . We examine these physical pole positions by solving for the complex roots of the denominator of the K -matrix unitarized amplitude Eq. (3.15),

$$\mathcal{D}(s) = 1 - iT_0^{0B} = 0, \quad (3.20)$$

with T_0^{0B} given by Eq. (3.16). We search for solutions, $s^{(j)} = s_r^{(j)} + is_i^{(j)} = m_j^2 - im_j\Gamma_j$ of this equation, where m_j and Γ_j are interpreted as the mass and decay width of the j^{th} physical resonance (which would hold for small Γ). A first natural attempt would

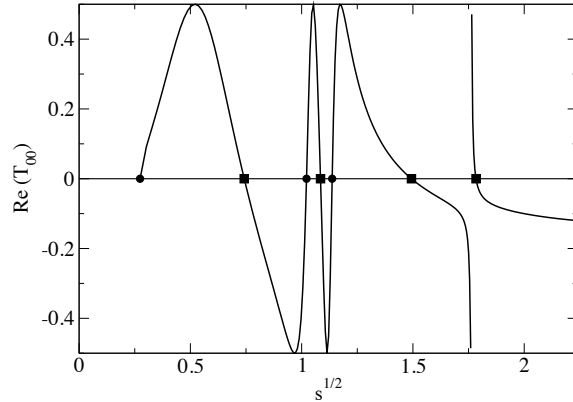


Figure 3.1 The real part of the unitarized $\pi\pi$ scattering amplitude for a typical choice of parameters. The four squares correspond to the poles in T_0^{0B} . The circles correspond to locations where $T_0^{0B} = 0$.

be to simultaneously solve the two equations,

$$\begin{aligned}\operatorname{Re}\mathcal{D}(s_r, s_i) &= 0, \\ \operatorname{Im}\mathcal{D}(s_r, s_i) &= 0.\end{aligned}\tag{3.21}$$

However, this approach turns out to be rather complicated to be implement. A more efficient numerical approach is to consider the single equation involving only positive quantities,

$$\mathcal{F}(s_r, s_i) = |\operatorname{Re}(\mathcal{D}(s_r, s_i))| + |\operatorname{Im}(\mathcal{D}(s_r, s_i))| = 0.\tag{3.22}$$

A search of parameter space leads to four solutions for the pole positions². As an example, for the choice of $A_3/A_1 = 30$ and $m[\Pi(1300)] = 1.215$ GeV, the function \mathcal{F} is plotted over the complex plane around the first pole. We see a clear local minimum at which the function is zero, hence pointing to a solution of Eq. (3.20). Similarly, other areas of the complex plane are searched and altogether four poles are found.

²We have double checked the results by developing an approximate analytical approach in which the amplitude is unitarized locally in the neighbourhood of each resonance.

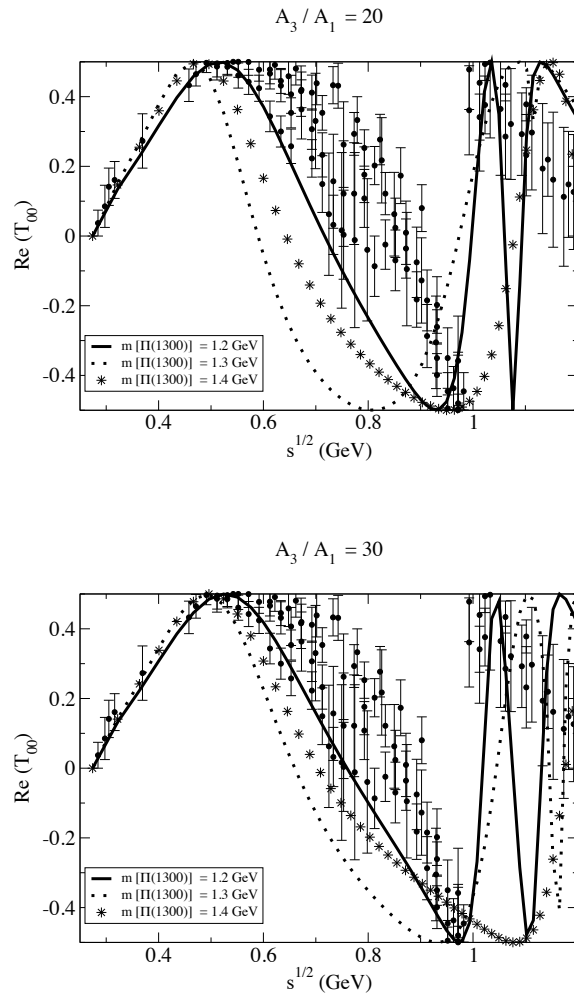


Figure 3.2 Real part of unitarized scattering amplitude for two values of A_3/A_1 and three choices of $m[\Pi(1300)]$.

The results are given in Table 3.1 for $m[\Pi(1300)] = 1.215$ GeV and two choices of $A_3/A_1 = 20$ and 30. For each choice we see that this model predicts a light and broad scalar meson below 1 GeV which is a clear indication of $f_0(600)$ or σ . We see that the characteristics of the second predicted state around 1 GeV are close to those expected for $f_0(980)$. The third and the fourth predicted states should correspond to two of $f_0(1370)$, $f_0(1500)$ and $f_0(1710)$.

We have performed the same analysis over the range of the parameter $m[\Pi(1300)] = 1.2 - 1.4$ GeV, and for two choices of $A_3/A_1 = 20$ and 30. The physical masses and the decay widths are given in Figs. 3.4 and 3.5, respectively. The effect of the unitarization can be seen in Fig. 3.4 where the physical masses are compared with the “bare” masses; the unitarization reduces the mass, particularly for the first and the third predicted states.

Pole	Mass (MeV)	Width (MeV)	Mass (MeV)	Width (MeV)
1	483	455	477	504
2	1012	154	1037	84
3	1082	35	1127	64
4	1663	2.1	1735	3.5

Table 3.1 The physical mass and decay width of the isosinglet scalar states, with $m[\Pi(1300)] = 1.215$ GeV and with $A_3/A_1 = 20$ (the first two columns) and with $A_3/A_1 = 30$ (the last two columns).

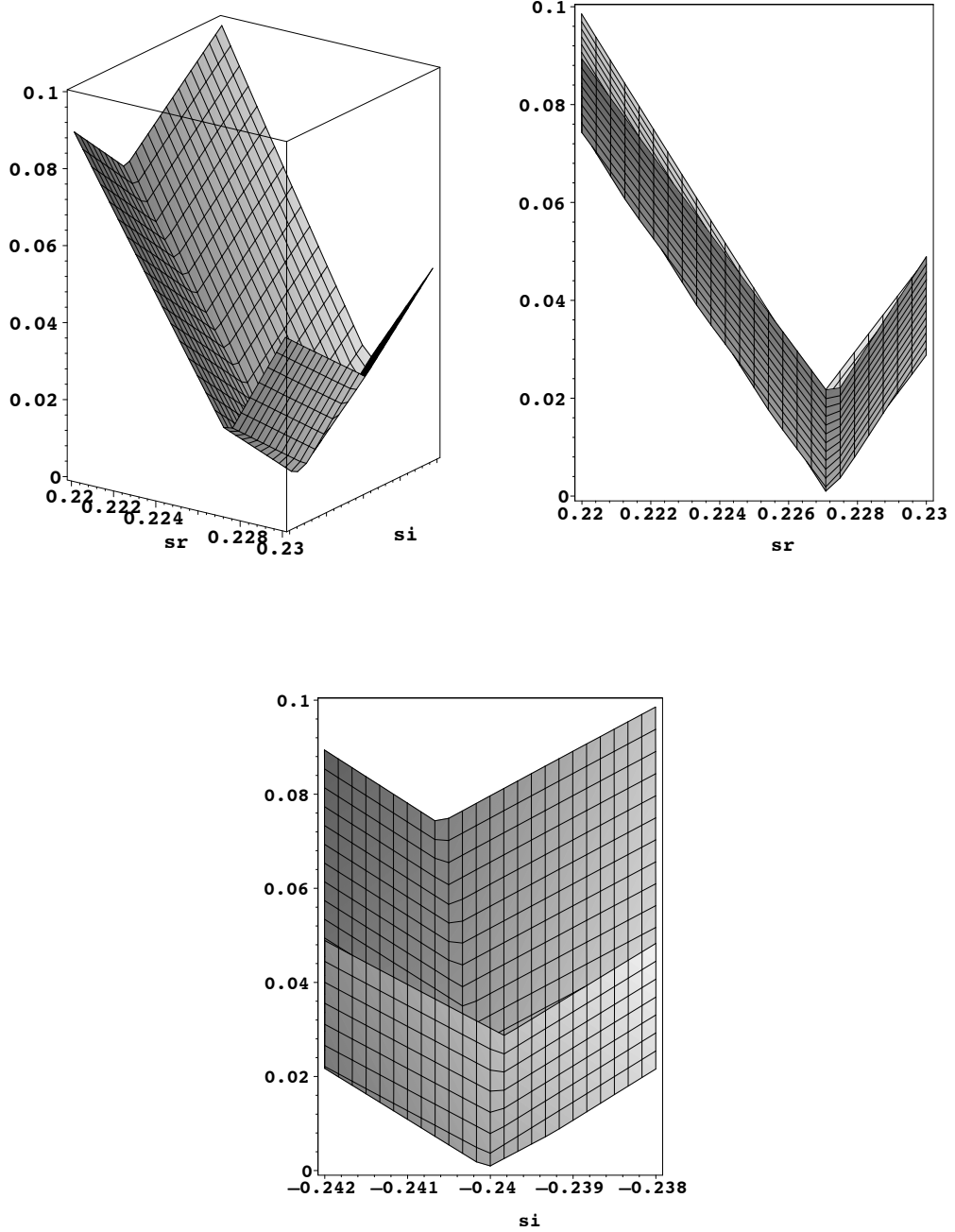


Figure 3.3 The local minimum of function $\mathcal{F}(s_R, s_I)$ defined in Eq. (3.22) at the position of the lightest isosinglet scalar pole in the complex s plane for $m[\Pi(1300)] = 1.215$ GeV and $A_3/A_1 = 30$. Top left is the plot of function $\mathcal{F}(s_R, s_I)$ vs s_R and s_I , followed by projection of this function onto \mathcal{F} - s_R and onto \mathcal{F} - s_I planes.

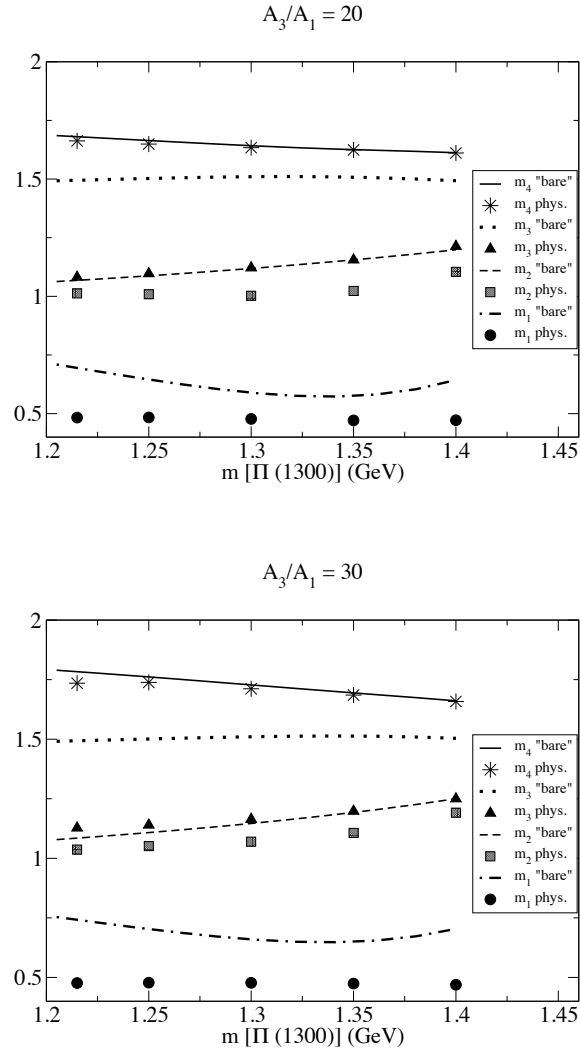


Figure 3.4 Predicted physical masses are compared with the “bare” masses for two values of A_3/A_1 over the experimental range of $m[\Pi(1300)]$.

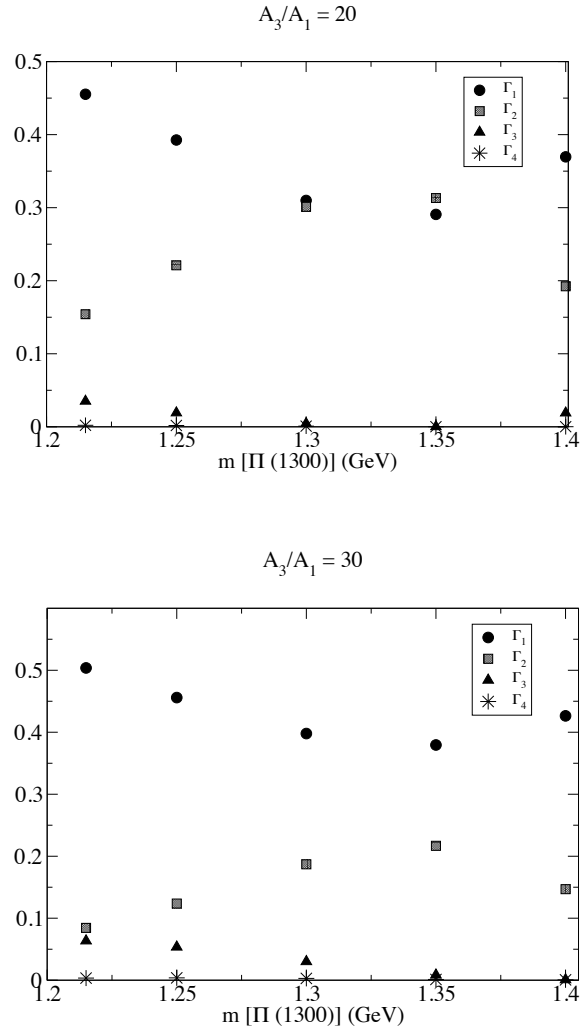


Figure 3.5 Predicted decay widths for two values of A_3/A_1 over the experimental range of $m[\Pi(1300)]$.

3.2 More on Two Chiral Nonets – Three Flavors are Special

Even though one can not write down the exact QCD wave functions of the low lying mesons it is easy to write down schematic descriptions of how quark fields may combine to give particles with specified transformation properties. The usual chiral nonet $M(x)$ realizing the $q\bar{q}$ structure is then written as:

$$M_a^{\dot{b}} = (q_{bA})^\dagger \gamma_4 \frac{1 + \gamma_5}{2} q_{aA}, \quad (3.23)$$

where a and A are respectively flavor and color indices. For clarity, on the left hand side the undotted index transforms under the $SU(3)_L$ while the dotted index transforms under the $SU(3)_R$.

One possibility for the $qq\bar{q}\bar{q}$ states is to make them as “molecules” from two quark-antiquark nonets. This leads to the following schematic form:

$$M_a^{(2)\dot{b}} = \epsilon_{acd} \epsilon^{\dot{b}\dot{e}\dot{f}} (M^\dagger)_{\dot{e}}^c (M^\dagger)_{\dot{f}}^d. \quad (3.24)$$

Note that the fields M and $M^{(2)}$ transform in the same way under chiral $SU(3)$ as well as under the discrete P and C symmetries, as required if they are to mix with each other according to the scheme shown above. As noted in the Appendix (A.3), the axial U(1) transformation properties of M and $M^{(2)}$ differ from each other and provide a measure of whether the state is of one quark-antiquark type, two quark-antiquark type etc. In the chiral Lagrangian there are terms which break the axial U(1) in a manner dictated by the QCD axial anomaly. In A.3 it is also pointed out that schematic fields $M^{(3)}$ and $M^{(4)}$ which have “diquark-antidiquark” forms instead of the “molecular” form can also be constructed. There has been some discussion in the literature about which type is favored [55]. In the present approach either is

allowable. In fact it was shown in [19] that the molecular form can be transformed using Fierz identities to a linear combination of the “diquark-antidiquark” forms. We thus assume that some unspecified linear combination of $M^{(2)}$, $M^{(3)}$ and $M^{(4)}$, denoted by M' , represents the $qq\bar{q}\bar{q}$ chiral nonet which mixes with M . As in the previous section, the decomposition into pseudoscalar and scalar fields is given by,

$$M = S + i\phi, \quad M' = S' + i\phi'. \quad (3.25)$$

There is no problem finding a chiral formulation for a $q\bar{q}$ 16-plet M_a^b . However we can not find a suitable schematic meson wave function with the same chiral transformation property constructed, for example, as a “molecule” out of two such states. The closest we can come for a two-part “molecule” is:

$$M_{ag}^{(2)b\dot{h}} = \epsilon_{agcd}\epsilon^{\dot{b}\dot{h}\dot{e}\dot{f}}(M^\dagger)_e^c(M^\dagger)_{\dot{f}}^{\dot{d}}. \quad (3.26)$$

However, instead of transforming under $SU(4)_L \times SU(4)_R$ as $(L, R) = (4, \bar{4})$ as desired, this object transforms as $(L, R) = (6, \bar{6})$, owing to the two sets of antisymmetric indices (ag and $b\dot{h}$) which appear. Hence, it should not mix in the chiral symmetry limit with the initial four flavor $q\bar{q}$ state (See Eq. (3.31)). Of course it would be possible to multiply the right hand side of Eq. (3.26) by a third field $(M^\dagger)_h^g$. That does give the correct transformation property to mix with the four flavor version of Eq. (3.31). However it corresponds to a three quark- three antiquark molecule. We assume that, especially after quark mass terms are added, an “elementary particle” state of such a form is unlikely to be bound.

The same problem emerges in the four flavor case when we alternatively construct composites of the diquark-antidiquark states given in Eqs. (A.20) and (A.22) of A.3. As above, this yields a composite state transforming like $(6, \bar{6})$ (rather than the desired $(4, \bar{4})$):

$$M_{gp}^{(3)\dot{f}\dot{q}} = (L^{gpE})^\dagger R^{\dot{f}\dot{q}E}, \quad (3.27)$$

where,

$$\begin{aligned} L^{gpE} &= \epsilon^{gpab} \epsilon^{EAB} q_{aA}^T C^{-1} \frac{1 + \gamma_5}{2} q_{bB}, \\ R^{\dot{f}\dot{q}E} &= \epsilon^{\dot{f}\dot{q}\dot{c}\dot{d}} \epsilon^{EAB} q_{\dot{c}A}^T C^{-1} \frac{1 - \gamma_5}{2} q_{\dot{d}B}. \end{aligned} \quad (3.28)$$

We could contract L^{gpE} with a left handed quark field and $R^{\dot{f}\dot{q}E}$ with a right handed quark field to obtain the desired overall transformation property at the expense of having a three quark- three antiquark state (which we are assuming to be unbound).

It is clear that essentially the same argument would hold for five or more quark flavors.

Going in the direction of fewer flavors, we now note that there is also no suitable schematic "molecular" wavefunction available in the 2-flavor case for mixing with the quark-antiquark state. The closest we can come here for a "molecule" has the form:

$$M^{(2)} = \epsilon_{cd} \epsilon^{\dot{e}\dot{f}} (M^\dagger)_{\dot{e}}^c (M^\dagger)_{\dot{f}}^d. \quad (3.29)$$

This is clearly unsatisfactory since it transforms like (1,1) under $SU(2)_L \times SU(2)_R$ rather than the (2,2) required for mixing according to our assumed model. Actually one must be a little more careful because it is well known that the object $M_a^{\dot{b}}$ is not irreducible under chiral transformations in the 2-flavor case. It may be interesting to show that the same result is obtained when this fact is taken into account. The irreducible representations are formed by making use of the fact that $\tau_2 M^* \tau_2$ transforms in the same way as M . Then we may consider the irreducible linear combinations:

$$\begin{aligned}\frac{1}{\sqrt{2}}(M + \tau_2 M^* \tau_2) &\equiv \sigma I + i\pi \cdot \tau \\ \frac{1}{\sqrt{2}}(M - \tau_2 M^* \tau_2) &\equiv i\eta I + \mathbf{a} \cdot \tau,\end{aligned}\tag{3.30}$$

where the usual $SU(2)$ chiral multiplet containing π and σ is recognized as well as the parity reversed one containing η and the isovector scalar particle \mathbf{a} . Since $SU(2)_L \times SU(2)_R$ is equivalent to the group $SO(4)$ we may consider the fields π and σ as making up an isotopic four vector, p_μ and the fields \mathbf{a} and η as comprising another four vector q_μ . A “molecule” state which could mix with, say p_μ would have to be another four vector made as a product of p_μ and q_μ . The combination $p_\mu q_\mu$ is a singlet, the combination $\epsilon_{\mu\nu\alpha\beta} p_\alpha q_\beta$ has six components and the symmetric traceless combination has nine components. This confirms that there is no allowed mixing with a possible molecule at the chiral level in the two flavor case.

One might wonder why, if mixing is possible in the three flavor case, it is not possible in the two flavor case, which is just a subset of the former. The answer is already contained in Eq. (3.24). If we want to find something that mixes with the quark-antiquark π^+ particle we should look at the (12) matrix element. On the right hand side, one sees that the “molecule” field which mixes contains an extra $s\bar{s}$ pair, which is simply not present in the two flavor model.

Thus we see that flavor $SU(3)$ has some interesting special features for schematically constructing bound states with well defined chiral transformation properties.

A possibility for the mixing of a quark antiquark state with a different state not of “molecular” (or more generally, two quark-two antiquark) type, would be to consider a so called radial excitation. For mixing with $M_a^{\dot{b}}$, such a state could be schematically written as $f(\square)M_a^{\dot{b}}$, where f is a function of the d’Alembertian. In this case, one would not expect the inverted multiplets which appear in the “molecular” picture.

3.3 Semi-Leptonic Decay Modes of the $D_s^+(1968)$

On the experimental side of the subject, information on the light scalars has often been extracted from study of $\pi\pi$ and other scattering processes. Another way is to search for scalar resonances explicitly in particle decay processes. Recently, the CLEO collaboration has reported [56] good evidence for the scalar $f_0(980)$ in the semi-leptonic decay of the $D_s^+(1968)$ meson. Since there is more phase space available, it may be possible to find other scalar iso-singlet states in this and similar semi-leptonic decays of heavy mesons. There are also isosinglet pseudoscalar states like the η and $\eta'(980)$ which can be studied and in fact have been already reported in the decays of the $D_s^+(1968)$.

As a possibly helpful adjunct to future work in this direction we will also make some theoretical estimates of the semi-leptonic decay widths of the $D_s^+(1968)$ into the four scalar isosinglet states and the four pseudoscalar isosinglet states which are predicted in the chiral model mentioned above.

First, we will discuss the hadronic “weak currents” which are needed for the calculation. These are mathematically given by the so-called Noether currents of the sigma model Lagrangian being employed. We work in the approximation where renormalization of these currents from the symmetry limit are neglected. This means that there are no arbitrary parameters available to us. Nevertheless there are some subtleties. To explain these we build up the model in three stages rather than just writing the final result immediately. These models give the usual “current algebra” results near the threshold of pion-pion scattering but also yield some additional interesting features away from threshold.

3.3.1 Chiral SU(3) Model – $K\ell 3$ Decay as a Simple Example

Starting from Eq. (3.31), the usual $q\bar{q}$ chiral nonet ($M = S + i\phi$) is schematically written with chiral SU(3) indices displayed as:

$$M_a^b = (q_{bA})^\dagger \gamma_4 \frac{1 + \gamma_5}{2} q_{aA}, \quad (3.31)$$

where a and A are respectively flavor and color indices.

Using matrix notation (e.g. $M_a^b \rightarrow M_{ab}$) the Noether vector and axial currents read,

$$\begin{aligned} V_\mu &= i\phi \overleftrightarrow{\partial}_\mu \phi + iS \overleftrightarrow{\partial}_\mu S, \\ A_\mu &= S \overleftrightarrow{\partial}_\mu \phi - \phi \overleftrightarrow{\partial}_\mu S, \end{aligned} \quad (3.32)$$

The axial symmetry breaking is measured by the vacuum value of S :

$$S = \tilde{S} + \langle S \rangle, \quad \langle S_a^b \rangle = \alpha_a \delta_a^b, \quad (3.33)$$

where the normalization is $\alpha_1 + \alpha_2 = F_\pi \approx 130.4$ MeV and $\alpha_1 + \alpha_3 = F_K \approx 156.1$ MeV. Note that the overall normalization constant for V_μ gives the correct value for the ordinary electromagnetic current. This determines the normalization for the weak currents in the $SU(3)_L \times SU(3)_R$ symmetry limit. For the vector currents this amounts to an implementation of the ‘‘conserved vector current hypothesis’’ introduced for beta decay many years ago [57]. Such an approximation is well known not to be as good for the axial current case, but may at least furnish an order of magnitude estimate. In detail, with the usual SU(3) tensor indices, the currents read:

$$\begin{aligned} V_{\mu a}^b &= i\phi_a^c \overleftrightarrow{\partial}_\mu \phi_c^b + i\tilde{S}_a^c \overleftrightarrow{\partial}_\mu \tilde{S}_c^b + i(\alpha_a - \alpha_b) \partial_\mu \tilde{S}_a^b, \\ A_{\mu a}^b &= \tilde{S}_a^c \overleftrightarrow{\partial}_\mu \phi_c^b - \phi_a^c \overleftrightarrow{\partial}_\mu \tilde{S}_c^b + (\alpha_a + \alpha_b) \partial_\mu \phi_a^b, \end{aligned} \quad (3.34)$$

For example, the relevant hadronic current needed to describe the semi-leptonic decay $K^+ \rightarrow \pi^0 + e^+ + \nu_e$ is

$$V_{\mu 1}^3 = \phi_1^c \overleftrightarrow{\partial}_\mu \phi_c^3 + i(\alpha_1 - \alpha_3) \partial_\mu \tilde{S}_1^3. \quad (3.35)$$

We consider the matrix element, between an initial K^+ state with 4-momentum k and a final π^0 state with four momentum p , of the strangeness changing vector current $V_{\mu 1}^3$,

$$\langle \pi^0(p) | V_{\mu 1}^3 | K^+(k) \rangle \sim f_+(t)(k+p)_\mu + f_-(t)(k-p)_\mu, \quad (3.36)$$

where $t = -(k-p)^2$.

The first term of Eq. (3.35) contributes at tree level to the f_+ form factor while the second term contributes to the f_- form factor. These two contributions are illustrated in Figs. 3.6a and 3.6b in which the W boson which is connected to the leptonic current acts at the points \times . Here we are evaluating this matrix element in the framework of the plain $SU(3)$ linear sigma model in which, furthermore, the vector and axial vector mesons have not been included.

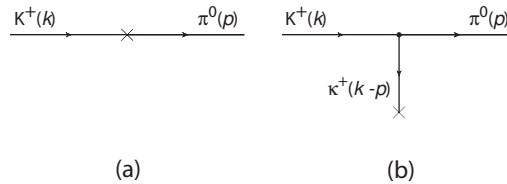


Figure 3.6 $K\ell 3$ decay hadronic current.

According to the usual Feynman rules,

$$\begin{aligned} f_+ &= -\frac{1}{\sqrt{2}}, \\ f_- &= -\frac{1}{\sqrt{2}} \left[\frac{\alpha_3 - \alpha_1}{\alpha_3 + \alpha_1} \right] \left[\frac{m_\kappa^2 - m_\pi^2}{m_\kappa^2 - t} \right], \end{aligned} \quad (3.37)$$

wherein m_κ denotes the mass of the strange scalar particle contained in this model. Furthermore, the explicit form of the $K\kappa\pi$ coupling constant in the model was used in the expression for f_- [11]. Notice that the first bracket in the equation for f_- evaluates to about 0.16 and that the physical κ mass is about 800 MeV in the plain SU(3) linear sigma model.

It is interesting that this decay allows one to learn something about the properties of the κ meson. For this purpose it is necessary to use the process where a final μ^+ is observed rather than a final e^+ . That is because the contribution of $f_-(t)$ to the decay width is proportional to the final lepton mass. Of course the effect of the $K^*(892)$, which contributes importantly to the $f_+(t)$ form factor should also be included to get increased accuracy.

3.3.2 SU(3) MM' Model

For this model we start from another chiral field ($M^{(2)} = S' + i\phi'$), introduced in Eq. (3.24), constructed out of two quarks and two anti-quarks as:

$$M_a^{(2)b} = \epsilon_{acd} \epsilon^{\dot{b}\dot{e}\dot{f}} (M^\dagger)_{\dot{e}}^c (M^\dagger)_{\dot{f}}^d. \quad (3.38)$$

Then the Noether currents involve the sum of pieces constructed from the unprimed fields and from the primed fields. The latter take the form,

$$\begin{aligned} V_{\mu a}^{rb} &= i\phi_a^{rc} \overleftrightarrow{\partial}_\mu \phi_c^{rb} + i\tilde{S}_a^{rc} \overleftrightarrow{\partial}_\mu \tilde{S}_c^{rb} + i(\beta_a - \beta_b) \partial_\mu \tilde{S}_a^{rb}, \\ A_{\mu a}^{rb} &= S_a^{rc} \overleftrightarrow{\partial}_\mu \phi_c^{rb} - \phi_a^{rc} \overleftrightarrow{\partial}_\mu \tilde{S}_c^{rb} + (\beta_a + \beta_b) \partial_\mu \phi_a^{rb}, \end{aligned} \quad (3.39)$$

wherein,

$$S' = \tilde{S}' + \langle S' \rangle, \quad \langle S'_a{}^b \rangle = \beta_a \delta_a^b. \quad (3.40)$$

The total currents are denoted as:

$$\begin{aligned}
V_{\mu a}^b(\text{total}) &= V_{\mu a}^b + V_{\mu a}^{b\prime}, \\
A_{\mu a}^b(\text{total}) &= A_{\mu a}^b + A_{\mu a}^{b\prime}.
\end{aligned} \tag{3.41}$$

In contrast to the chiral $SU(3)$ model above, all the primed and corresponding unprimed fields mix to give physical fields of definite mass. As a simple example, the transformation between the physical π^+ and π'^+ fields and the original fields (say ϕ^+ and ϕ'^+) is [15]:

$$\begin{bmatrix} \pi^+ \\ \pi'^+ \end{bmatrix} = R_\pi^{-1} \begin{bmatrix} \phi_1^2 \\ \phi_1^{\prime 2} \end{bmatrix} = \begin{bmatrix} \cos \theta_\pi & -\sin \theta_\pi \\ \sin \theta_\pi & \cos \theta_\pi \end{bmatrix} \begin{bmatrix} \phi_1^2 \\ \phi_1^{\prime 2} \end{bmatrix},$$

which also defines the transformation matrix, R_π .

The pion decay constant as well as (formally) the decay constant for the much heavier $\pi(1300)$ particle are defined by the part of the axial current linear in the fields:

$$\begin{aligned}
A_{\mu 1}^2(\text{total}) &= F_\pi \partial_\mu \pi^+ + F_{\pi'} \partial_\mu \pi'^+ + \dots, \\
F_\pi &= (\alpha_1 + \alpha_2) \cos \theta_\pi - (\beta_1 + \beta_2) \sin \theta_\pi, \\
F_{\pi'} &= (\alpha_1 + \alpha_2) \sin \theta_\pi + (\beta_1 + \beta_2) \cos \theta_\pi.
\end{aligned} \tag{3.42}$$

The angle θ_π depends on the detailed dynamics. [15]

In what follows it will be useful for us to specify the mixing matrix for the four isoscalar scalar mesons in this model. A basis for these states is given in terms of the four component vector $f = (f_a, f_b, f_c, f_d)$ where,

$$\begin{aligned}
f_a &= \frac{S_1^1 + S_2^2}{\sqrt{2}} \quad n\bar{n}, \\
f_b &= S_3^3 \quad s\bar{s}, \\
f_c &= \frac{S_1^{\prime 1} + S_2^{\prime 2}}{\sqrt{2}} \quad ns\bar{n}\bar{s}, \\
f_d &= S_3^{\prime 3} \quad nn\bar{n}\bar{n}.
\end{aligned} \tag{3.43}$$

In the above, the quark content is indicated on the right for convenience. Note that s stands for a strange quark while n stands for a non-strange quark. However these basis states are not mass eigenstates. Again, the detailed dynamics of the model is required to specify this. For typical values of the model's input parameters (see [20]) the mass eigenstates make up a four vector, $F = L_0^{-1}f$ with,

$$(L_o^{-1}) = \begin{bmatrix} 0.601 & 0.199 & 0.600 & 0.489 \\ -0.107 & 0.189 & 0.643 & -0.735 \\ 0.790 & -0.050 & -0.391 & -0.470 \\ 0.062 & -0.960 & 0.272 & -0.019 \end{bmatrix} \quad (3.44)$$

The physical states are identified, with nominal mass values, as

$$F = \begin{bmatrix} f_0(600) \\ f_0(980) \\ f_0(1370) \\ f_0(1800) \end{bmatrix} \quad (3.45)$$

It will also be interesting for us to give the typical result of the model for the mixing of the four isoscalar pseudoscalars. The analogous basis states are:

$$\begin{aligned} \eta_a &= \frac{\phi_1^1 + \phi_2^2}{\sqrt{2}} & n\bar{n}, \\ \eta_b &= \phi_3^3 & s\bar{s}, \\ \eta_c &= \frac{\phi_1^1 + \phi_2^2}{\sqrt{2}} & ns\bar{n}\bar{s}, \\ \eta_d &= \phi_3^3 & nn\bar{n}\bar{n}. \end{aligned} \quad (3.46)$$

For typical values of the model's input parameters (see [20]) the mass eigenstates make up a four component vector, $P = R_0^{-1}\eta$ with,

$$P = \begin{bmatrix} \eta(547) \\ \eta(958) \\ \eta(1295) \\ \eta(1760) \end{bmatrix} \quad (3.47)$$

(These identifications correspond to the favored scenario discussed in section V of [20]). The dynamically determined mixing matrix is then:

$$(R_o^{-1}) = \begin{bmatrix} -0.675 & 0.661 & -0.205 & 0.255 \\ 0.722 & 0.512 & -0.363 & 0.291 \\ -0.134 & -0.546 & -0.519 & 0.644 \\ 0.073 & 0.051 & 0.746 & 0.660 \end{bmatrix} \quad (3.48)$$

3.3.3 Hybrid MM' Model with a Heavy Flavor

As discussed in Sec. 3.2, the case of three flavors is special in the sense that it is the only one in which a two quark-two antiquark field has the correct chiral transformation property to mix (in the chiral limit) with M . In order to respect this property when a heavy meson is included in the Lagrangian, we should demand that “heavy” spin zero mesons be made of just one quark and one antiquark. In a linear sigma model the kinetic term would then be written as:

$$\mathcal{L} = -\frac{1}{2}\text{Tr}^4(\partial_\mu M \partial_\mu M^\dagger) - \frac{1}{2}\text{Tr}^3(\partial_\mu M' \partial_\mu M'^\dagger), \quad (3.49)$$

where the meaning of the superscript on the trace symbol is that the first term should be summed over the heavy quark index as well as the three light indices. This stands in contrast to the second term which is just summed over the three light quark indices pertaining to the two quark-two antiquark field M' . Since the Noether currents are sensitive only to these kinetic terms in the model, the vector and axial

vector currents with flavor indices 1 through 3 in this model are just the same as in Eq. (3.41) above. However if either or both flavor indices take on the value 4 (referring to the heavy flavor) the current will only have contributions from the field M . This should be clarified by the following example,

$$\begin{aligned} V_{\mu 4}^a(\text{total}) &= V_{\mu 4}^a = i\phi_4^c \overleftrightarrow{\partial}_\mu \phi_c^a + iS_4^c \overleftrightarrow{\partial}_\mu S_c^a, \\ A_{\mu 4}^a(\text{total}) &= A_{\mu 4}^a = S_4^c \overleftrightarrow{\partial}_\mu \phi_c^a - \phi_4^c \overleftrightarrow{\partial}_\mu S_c^a. \end{aligned} \quad (3.50)$$

Here the unspecified indices can run from 1 to 4. This equation is correct by construction but does not tell the whole story since the connection between the fields above and the physical states involves, as in the preceding cases, the details of the non-derivative (“potential”) terms of the effective Lagrangian.

3.3.4 $D_s^+(1968) \rightarrow f_0(980)e^+\nu_e$

The initial motivation for this work was the recent experimental discovery [56] of the semileptonic decay mode,

$$D_s^+(1968) \rightarrow f_0(980)e^+\nu_e, \quad (3.51)$$

in which the $f_0(980)$ was identified from its two pion decay mode.

A relevant generalization is to consider other scalar isosinglet candidates than the $f_0(980)$. For example the SU(3) $M - M'$ model contains four different isoscalar scalars, F_i . In addition, there are four different isoscalar pseudoscalars in that model, P_i . Here we shall calculate the predictions of that model for all eight of these decays in the simplest approximation. This should provide some useful orientation. In fact there are no parameters which have not already been determined in the previous treatment [20] of the model.

The usual weak interaction Lagrangian is,

$$\mathcal{L} = \frac{g}{2\sqrt{2}}(J_\mu^- W_\mu^+ + J_\mu^+ W_\mu^-), \quad (3.52)$$

wherein,

$$\begin{aligned} J_\mu^- &= i\bar{U}\gamma_\mu(1 + \gamma_5)VD + i\bar{\nu}_e\gamma_\mu(1 + \gamma_5)e, \\ J_\mu^+ &= i\bar{D}\gamma_\mu(1 + \gamma_5)V^\dagger U + i\bar{e}\gamma_\mu(1 + \gamma_5)\nu_e. \end{aligned} \quad (3.53)$$

Here the column vectors of the quark fields take the form:

$$U = \begin{bmatrix} u \\ c \\ t \end{bmatrix}, \quad D = \begin{bmatrix} d \\ s \\ b \end{bmatrix}, \quad (3.54)$$

and the CKM matrix, V is explicitly,

$$V = \begin{bmatrix} V_{ud} & V_{us} & V_{ub} \\ V_{cd} & V_{cs} & V_{cb} \\ V_{td} & V_{ts} & V_{tb} \end{bmatrix}. \quad (3.55)$$

A picture describing the relevant D_s decays is given in Fig. (3.7).

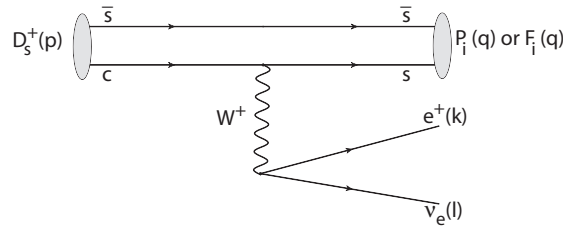


Figure 3.7 D_s decay.

The corresponding semi-leptonic decay amplitudes are thus,

$$\text{amp}(D_s^+(p)) \rightarrow \left\{ \begin{array}{c} P_i(q) \\ F_i(q) \end{array} \right\} + e^+(k) + \nu_e(l) = -i \frac{G_F}{\sqrt{2}} V_{cs} \left\{ \begin{array}{c} \langle P_i(q) | V_{\mu 4}^3(\text{total}) | D_s^+(p) \rangle \\ \langle F_i(q) | A_{\mu 4}^3(\text{total}) | D_s^+(p) \rangle \end{array} \right\} \times \bar{u}(\mathbf{l}) \gamma_\mu (1 + \gamma_5) v(\mathbf{k}), \quad (3.56)$$

where the spinor $v(\mathbf{k})$ represents the outgoing e^+ and $\bar{u}(\mathbf{l})$ represents the outgoing ν_e . The relevant hadronic operators can be rewritten in terms of the mass eigenstate scalar isosinglets and the pseudoscalar isosinglets using Eqs. (3.45) and (3.47) as:

$$\begin{aligned} V_{\mu 4}^3(\text{total}) &= i D_s^+ \overleftrightarrow{\partial}_\mu \phi_3^3 + \dots \\ &= i D_s^+ \sum_j (R_0)_{2j} \overleftrightarrow{\partial}_\mu P_j + \dots \end{aligned} \quad (3.57)$$

$$\begin{aligned} A_{\mu 4}^3(\text{total}) &= -D_s^+ \overleftrightarrow{\partial}_\mu S_3^3 + \dots \\ &= -D_s^+ \sum_j (L_0)_{2j} \overleftrightarrow{\partial}_\mu F_j + \dots \end{aligned} \quad (3.58)$$

The transposed matrices L_0 and R_0 are given in Eqs. (3.44) and (3.48) respectively, based on a typical numerical solution for the model parameters [20]. Next the amplitudes are given by,

$$\text{amp}(D_s^+(p)) \rightarrow \left\{ \begin{array}{c} P_i(q) \\ F_i(q) \end{array} \right\} + e^+(k) + \nu_e(l) = \frac{G_F}{\sqrt{2}} V_{cs} \left\{ \begin{array}{c} (R_0)_{2i} \\ -i(L_0)_{2i} \end{array} \right\} (p_\mu + q_\mu) \bar{u}(\mathbf{l}) \gamma_\mu (1 + \gamma_5) v(\mathbf{k}), \quad (3.59)$$

The squared amplitudes, summed over the emitted lepton's spins, are then,

$$G_F^2 |V_{cs}|^2 \frac{1}{m_e^2} \left\{ \begin{array}{c} ((R_0)_{2i})^2 \\ ((L_0)_{2i})^2 \end{array} \right\} [2k \cdot (p+q)l \cdot (p+q) - l \cdot k(p+q)^2], \quad (3.60)$$

wherein m_e has been set to zero except for the overall $1/m_e^2$ factor.

This yields the unintegrated decay width,

$$\frac{d\Gamma}{d|\mathbf{q}|} = \frac{G_F^2 |V_{cs}|^2}{12\pi^3} \left\{ \begin{array}{l} ((R_0)_{2i})^2 \\ ((L_0)_{2i})^2 \end{array} \right\} m(D_s) \frac{|\mathbf{q}|^4}{q_0}. \quad (3.61)$$

For integrating this expression we need,

$$|q_{max}| = \frac{m^2(D_s) - m_i^2}{2m(D_s)}, \quad (3.62)$$

where m_i is the mass of the isosinglet meson F_i or P_i and also the indefinite integral formula, where $x = |\mathbf{q}|$,

$$\int \frac{x^4 dx}{\sqrt{x^2 + m_i^2}} = \frac{x^3}{4} \sqrt{x^2 + m_i^2} - \frac{3}{8} m_i^2 x \sqrt{x^2 + m_i^2} + \frac{3}{8} m_i^4 \ln(x + \sqrt{x^2 + m_i^2}). \quad (3.63)$$

Table 3.2 summarizes the calculations of the predicted widths, for D_s^+ decays into the four pseudoscalar singlet mesons ($\eta_1 = \eta(547)$, $\eta_2 = \eta(982)$, $\eta_3 = \eta(1225)$, $\eta_4 = \eta(1794)$). Notice that the listed masses, m_i are the ‘‘predicted’’ ones in the present model) and leptons.

m_i (MeV)	$(R_0)_{2i}$	$(q_{max})_i$ (MeV)	Γ_i (MeV)
553	0.661	906.20	4.14×10^{-11}
982	0.512	739.00	7.16×10^{-12}
1225	-0.546	602.74	2.57×10^{-12}
1794	0.051	166.31	2.65×10^{-17}

Table 3.2 pseudoscalars.

Table 3.3, with the same conventions, summarizes the calculations of the predicted

widths for D_s^+ decays into the four scalar singlet mesons ($(f_1, f_2 \dots) = (\sigma, f_0(980), \dots)$) and leptons.

m_i (MeV)	$(L_0)_{2i}$	$(q_{max})_i$ (MeV)	Γ_i (MeV)
477	0.199	933.23	4.56×10^{-12}
1037	0.189	710.79	7.80×10^{-13}
1127	-0.050	661.30	3.62×10^{-14}
1735	-0.960	219.21	3.85×10^{-14}

Table 3.3 scalars.

Experimental data exist for only three of these eight decay modes.

$$\begin{aligned}
 \Gamma(D_s^+ \rightarrow \eta e^+ \nu_e) &= (3.5 \pm 0.6) \times 10^{-11} \text{ MeV} \\
 \Gamma(D_s^+ \rightarrow \eta' e^+ \nu_e) &= (1.29 \pm 0.30) \times 10^{-11} \text{ MeV} \\
 \Gamma(D_s^+ \rightarrow f_0 e^+ \nu_e) &= (2.6 \pm 0.4) \times 10^{-12} \text{ MeV}
 \end{aligned} \tag{3.64}$$

It is encouraging that even though our calculation utilized the simplest model for the current and no arbitrary parameters were introduced, the prediction for the lightest hadronic mode, $\Gamma(D_s^+ \rightarrow \eta e^+ \nu_e)$ agrees with the measured value. In the case of the decay $D_s^+ \rightarrow \eta e^+ \nu_e$ the predicted width is about 30% less than the measured value. For the mode $D_s^+ \rightarrow f_0(980) e^+ \nu_e$ our predicted value is about one third the measured value. Conceivably, considering the large predicted width into the very broad sigma state centered at 477 MeV, some of the higher mass sigma events might have been counted as $f_0(980)$ events, which would improve the agreement. It would be very interesting to obtain experimental information about the energy regions relevant to the other five predicted isosinglet modes.

Furthermore, these width predictions are based on Eqs. (3.44) and (3.48) corresponding to particular choices for the quark mass ratio A_3/A_1 and the precise mass of the very broad $\Pi(1300)$ resonance. Varying these within the allowable ranges gives rise to the allowed range of predictions displayed in Figs. (3.8) and (3.9). One can see that raising $m[\Pi(1300)]$ and/or lowering A_3/A_1 yields better agreement for the predicted semi-leptonic decay width of the $f_0(980)$. Clearly, the simple model here provides reasonable estimates for the semileptonic decay widths of the $D_s^+(1968)$.

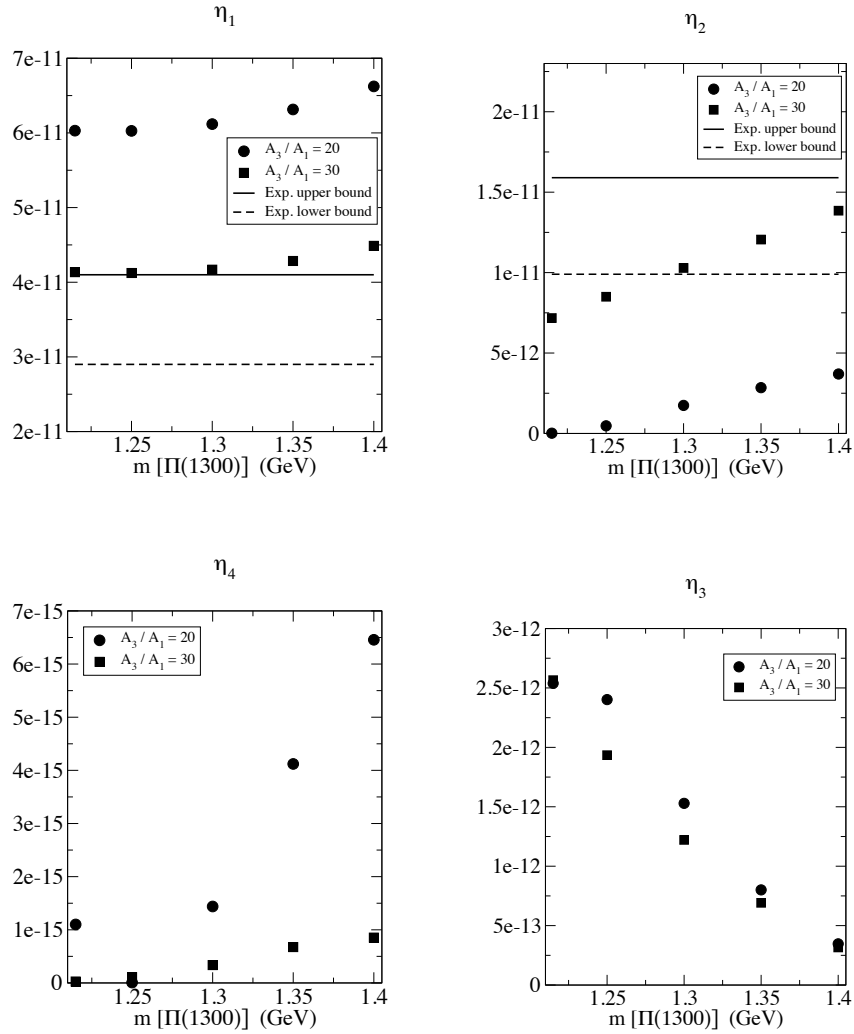


Figure 3.8 Starting from the upper left and proceeding clockwise: The dependences of the pseudoscalar partial widths on the current quark mass ratio A_3/A_1 and on the value of the $\Pi(1300)$ mass.

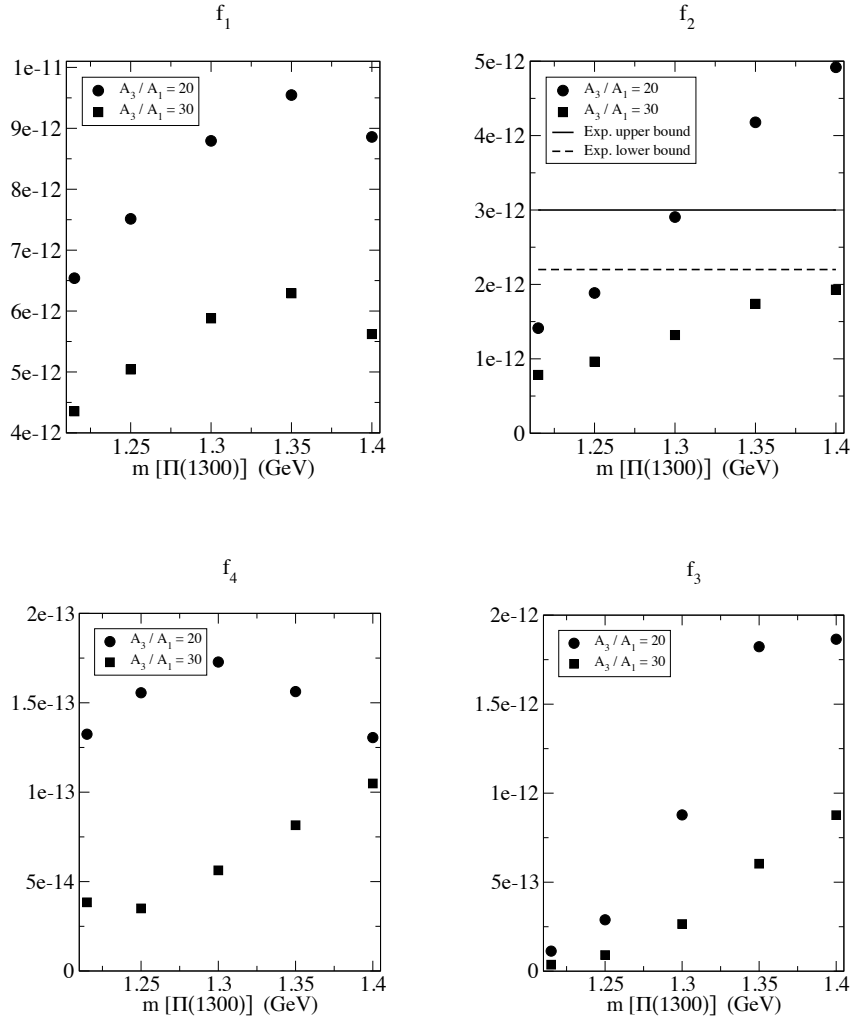


Figure 3.9 Starting from the upper left and proceeding clockwise: The dependences of the scalar partial widths on the current quark mass ratio A_3/A_1 and on the value of the $\Pi(1300)$ mass.

Chapter 4

Conclusions for Linear Sigma Models

We studied different aspects of linear sigma model in this part of the thesis. We realized that the use of the simplest linear sigma model at tree level does not give just one number (a scattering length) but gives an infinite series of numbers which can be conveniently compared with the series resulting from chiral perturbation theory. Another amusing feature is that this approach provides a specific model for the expansion parameter of this series; namely $m_\pi^2/(m_B^2 - m_\pi^2)$. Of course, in comparison with chiral perturbation theory, there is an obvious difference in that the latter approach includes the effect of loop integrals. The loop integrals enforce that chiral perturbation theory carried to all orders should result in fully unitarized scattering amplitudes. In the present approach it is possible to obtain exactly unitary partial wave amplitudes without introducing any new parameters by means of the K -matrix technique.

It is well known that to accurately model low energy pion physics it is necessary to take the ρ meson into account in addition to the σ . So the next step is to investigate

the pion scattering amplitude computed from a linear sigma model in which the vector meson as well as an axial vector meson (for chiral symmetry) are included. To begin the study of the scattering amplitude in the resonant s -wave channel we fit the near threshold NA48/2 data [39] up to about 370 MeV using the tree amplitude. A good fit was obtained by choosing the bare sigma mass, m_σ to be about 420 MeV. A similarly good fit in the sigma model without spin 1 fields needed m_σ to be about 620 MeV instead (See Fig. 2.3). Once a value of m_σ is chosen, the amplitude is also predicted at higher energies. It was pointed out (see Fig. 2.4 that those values of m_σ resulted in “global” pictures of the s -wave scattering which was considerably distorted. Much better “global” pictures emerge from choices of bare sigma mass, m_σ about 850 MeV. However such a value for m_σ results in, as seen in Fig. 2.7, some loss of precision for the region just near threshold. From the standpoint of learning about the sigma, the higher bare sigma mass is evidently the more suitable one.

It seems that the light sigma and the $f_0(980)$ are, not surprisingly, the main features of the $I = 0$, s -wave pion-pion scattering amplitude in this energy range. Adding the rho meson changes somewhat the parameters of the sigma needed for fitting. Comparing the “global” fits to the resonant s -wave pion pion scattering amplitude up to about 800 MeV, it is seen that the linear sigma model without the spin 1 particles actually gives a better fit than the one with the spin 1 particles included. This seems to be due to the higher polynomial terms induced by the Yang Mills interaction.

The key equation obtained is Eq. (2.23) or equivalently, Eq. (2.37). If the minus sign in this equation is chosen, it was shown that there is no consistent solution of parameters when inputs are taken from the possible application to QCD of this model. On the other hand, the minus sign choice allows a solution with $m_\rho > m_A$, which is plausibly related to a “minimal walking technicolor” application of the effective

Lagrangian. If the plus sign choice is made in this equation, it was shown that the QCD application of the model is allowed though a “walking technicolor” application, while possible, seems to correspond to an extremely large rho boson width. There is also a special case in this equation when the square root vanishes so the sign choice is irrelevant. In that situation, the Weinberg and KSRF relations are both satisfied in the unphysical limit where $B = 0$.

Of course, in the application to the minimal walking technicolor model [43], the present piece would have to be embedded in a larger framework with an initial $SU(4)$ symmetry. One might similarly expect that the behaviors of the sigma (=Higgs) and the technicolor spin 1 bosons would be similar to those seen here [58].

We also noted that a technicolor theory underlying the standard electroweak model is likely to result in a Higgs potential which possesses standard “strong” interaction symmetries like chiral $SU(2)$, parity and charge conjugation. This is obvious for the single Higgs doublet model. Imposing the same requirement for a two doublet model results in an interesting picture, which is rather constrained compared to a general two doublet model. In particular the second doublet doesn’t mix with the first one although it interacts with it. This leads to at least one possible dark matter candidate.

A number of very interesting Higgs scenarios can be constructed. The most conservative one would make the second doublet heavier than the first. We considered an opposite picture with lighter second doublet members. This provides extra decay modes for the usual Higgs boson and enables us to construct models which might hide the usual Higgs from being observed in certain experiments. These models involve all, but one, of the parameters in our Higgs potential. Information about the remaining one, α_4 might be found by considering the connection with dark matter observations.

We used a chiral $SU(3)$ model [20] containing not only the usual pseudoscalar and scalar nonets describing quark-antiquark bound states but also pseudoscalar and

scalar nonets describing states with the same quantum numbers but constructed out of two quarks and two antiquarks in a general way. In this model the physical particles correspond to mixtures of these two types. We studied the predictions of the real (mass) and imaginary (width) parts of the pion scattering amplitude poles representing the isoscalar scalar singlets. The model has four scalars so the process is technically complicated. No new parameters were introduced here, either for the model itself or to treat the scattering.

The fact that the comparison with the experimental scalar candidates is reasonable is in itself a non trivial conclusion. Also the fact that the simple single channel K -matrix unitarization (using no new parameters) seems to work may be useful to point out. Presumably the results would be improved if the effect of the $K\bar{K}$ channel were to be included. Mixing with a possible glueball state is another relevant effect. The worst prediction seems to be the too low mass value for pole 3. We note from Fig. 3.4 that there is a relatively large difference between the “bare” mass and the pole mass in this case. The inclusion of the $K\bar{K}$ threshold effects may improve this feature.

It may also be interesting to compare the predictions of pole 1 and pole 2 with those calculated in a similar manner using the single M SU(3) sigma model [11]. The agreement is quite good. However, in that model, the result was calculated using the most general form of the interaction potential involving the field matrix M ; an attempt to just use the “renormalizable” terms did not give as good a result. In the present case it was not necessary to introduce any additional terms in the Lagrangian to get good results for the $\pi\pi$ scattering.

The above model was supplemented by invariant terms which model the axial U(1) anomaly as well as the usual terms which model the quark masses. Before it was broken, the $U(1)_A$ quantum number distinguished the “two quark-two antiquark” mesons from the “quark-antiquark” mesons. The starting point for the mixing was

that a schematic two quark-two antiquark product state could be constructed with the same $SU(3)_L \times SU(3)_R$ transformation property as the original "quark-antiquark" state. Of course this is just a "kinematic" statement and does not presume to say that the dynamical binding has been established or that large quark masses do not change this picture. We have shown that this kinematical feature in the chiral limit does not hold for $SU(n)_L \times SU(n)_R$ when n is different from three. In the case of $n = 4$, it was seen that three quark- three antiquark states could have the same transformation property but we assumed that the 6-object bound state and other higher ones (needed for still larger n) would be unlikely to be bound as an "elementary particle".

We constructed a kind of hybrid model with 4 flavors to for studying semi-leptonic decays of charmed mesons into scalar plus leptons. There we have also noted a possible experimental test of the kinematical criterion for the doubling of scalar and pseudoscalar states in the charm sector. We saw that the partial widths for semi-leptonic decays of the $D_s^+(1968)$ into isoscalar scalar singlets and pseudoscalar singlets plus leptons could be well estimated in a simple model where the hadronic current was taken to be the Noether current associated with a minimal linear sigma model.

The agreement between experiment and theory was better for the decays into the η and η' than for the decay into the $f_0(980)$. The former involve the hadronic vector current, which is "protected" according to the conserved vector current hypothesis, while the latter involves the "unprotected" axial vector current. Clearly it would be interesting to try this technique for other semi-leptonic decays of charmed mesons and also for bottom mesons. We considered the case when the charged lepton was e^+ rather than the cases of μ^+ or τ^+ . In those two cases an additional form factor as in the calculation of the $K\ell 3$ decay should be taken into account.

Information about the scalars, involving however more work for disentangling the effects of the strong interaction, can also be obtained from the non-leptonic decay

modes of the charm and bottom mesons. The study of the decay like $B_c^+ \rightarrow \text{scalar} + e^+ + \nu_e$ might be useful for learning about mixing between a $c\bar{c}$ scalar and the lighter three flavor scalars. A straightforward, but not necessarily short, improvement of this calculation would be to include both vector and axial vector mesons in the starting Lagrangian from which the currents are calculated.

Part II

S_3 Symmetry for Neutrino Masses and Mixing

Chapter 5

Introduction to S_3 Symmetry

5.1 S_3 Symmetry

At present, the particle physics community is planning, as a follow-up to the enormously important experiments of the last decade [59] - [66], an extensive program with the goal of more accurately understanding the neutrino masses and mixings. There is really no accepted theory for an a priori prediction of these quantities. Hence it seems worthwhile to investigate in detail various theoretical models to develop plausible scenarios which might be tested.

The standard model interaction term for β decay or $\pi^- \rightarrow e^- \bar{\nu}_e$ includes the leptonic piece:

$$\mathcal{L} = \frac{ig}{\sqrt{2}} W_\mu^- \bar{e}_L \gamma_\mu \nu_e + h.c., \quad (5.1)$$

The object ν_e is now known to be a linear combination of neutrino mass eigenstates, $\hat{\rho}_i$:

$$\nu_e = \sum K_{ei} \hat{\rho}_i \quad (5.2)$$

where, in a basis with the charged leptons diagonal, the full lepton mixing matrix

is written as:

$$K = \begin{pmatrix} K_{e1} & K_{e2} & K_{e3} \\ K_{\mu1} & K_{\mu2} & K_{\mu3} \\ K_{\tau1} & K_{\tau2} & K_{\tau3} \end{pmatrix} \quad (5.3)$$

As has been discussed by many authors [67] - [81] the results of neutrino oscillation experiments are (neglecting possible phases to be discussed later) roughly consistent with the “tribimaximal mixing” matrix:

$$K_{TBM} = \begin{pmatrix} \frac{-2}{\sqrt{6}} & \frac{1}{\sqrt{3}} & 0 \\ \frac{1}{\sqrt{6}} & \frac{1}{\sqrt{3}} & \frac{1}{\sqrt{2}} \\ \frac{1}{\sqrt{6}} & \frac{1}{\sqrt{3}} & \frac{-1}{\sqrt{2}} \end{pmatrix} \equiv R. \quad (5.4)$$

Many different approaches have been used to explain the form of K . A “natural”, and often investigated one uses the parallel three generation structure of the fundamental fermion families as a starting point. An underlying discrete symmetry S_3 , the permutation group on three objects, is then assumed. [82]- [89] The permutation matrices S are,

$$\begin{aligned} S^{(1)} &= \begin{bmatrix} 1 & 0 & 0 \\ 0 & 1 & 0 \\ 0 & 0 & 1 \end{bmatrix}, & S^{(12)} &= \begin{bmatrix} 0 & 1 & 0 \\ 1 & 0 & 0 \\ 0 & 0 & 1 \end{bmatrix}, & S^{(13)} &= \begin{bmatrix} 0 & 0 & 1 \\ 0 & 1 & 0 \\ 1 & 0 & 0 \end{bmatrix}, \\ S^{(23)} &= \begin{bmatrix} 1 & 0 & 0 \\ 0 & 0 & 1 \\ 0 & 1 & 0 \end{bmatrix}, & S^{(123)} &= \begin{bmatrix} 0 & 0 & 1 \\ 1 & 0 & 0 \\ 0 & 1 & 0 \end{bmatrix}, & S^{(132)} &= \begin{bmatrix} 0 & 1 & 0 \\ 0 & 0 & 1 \\ 1 & 0 & 0 \end{bmatrix} \end{aligned} \quad (5.5)$$

This defining representation is not irreducible. The 3-dimensional space breaks up into irreducible 2-dimensional and 1-dimensional spaces. One may note that the tribimaximal matrix, K_{TBM} is an example of the transformation which relates the given basis to the irreducible one. This fact provides our motivation for investigating the

S_3 symmetry, even though many other interesting approaches exist. The symmetry requirement reads,

$$[S, M_\nu] = 0, \quad (5.6)$$

where S stands for any of the six matrices in Eq. (5.5) and M_ν is the neutrino mass matrix.

By explicitly evaluating the commutators one obtains the solution:

$$M_\nu = \alpha \begin{bmatrix} 1 & 0 & 0 \\ 0 & 1 & 0 \\ 0 & 0 & 1 \end{bmatrix} + \beta \begin{bmatrix} 1 & 1 & 1 \\ 1 & 1 & 1 \\ 1 & 1 & 1 \end{bmatrix} \equiv \alpha \mathbf{1} + \beta d. \quad (5.7)$$

α and β are, in general, complex numbers for the case of Majorana neutrinos while d is usually called the “democratic” matrix.

5.2 Need for Perturbation

It is easy to verify that this M_ν may be brought to diagonal (but not necessarily real) form by the real orthogonal matrix, $R = K_{TBM}$ defined above:

$$R^T(\alpha \mathbf{1} + \beta d)R = \begin{bmatrix} \alpha & 0 & 0 \\ 0 & \alpha + 3\beta & 0 \\ 0 & 0 & \alpha \end{bmatrix}. \quad (5.8)$$

R may be written in terms of the eigenvectors of M_ν as:

$$R = \begin{bmatrix} \vec{r}_1 & \vec{r}_2 & \vec{r}_3 \end{bmatrix}, \quad (5.9)$$

For example, \vec{r}_1 is the first column of the tribimaximal matrix, Eq. (5.4). Physically one can assign different masses to the mass eigenstate \vec{r}_2 in the 1-dimensional basis and to the (doubly degenerate) eigenstates \vec{r}_1 and \vec{r}_3 in the 2-dimensional basis. At

first glance this sounds ideal since it is well known that the three neutrino masses are grouped into two almost degenerate ones (“solar neutrinos”) and one singlet, with different values. However, since we are demanding that R be taken as the tribimaximal form, the physical identification requires \vec{r}_1 and \vec{r}_2 to be the “solar” neutrino eigenstates rather than the degenerate ones \vec{r}_1 and \vec{r}_3 . This had been considered a serious objection to the present approach since often a scenario is pictured in which the mass eigenvalue for \vec{r}_3 is considerably larger than the roughly degenerate masses associated with \vec{r}_1 and \vec{r}_2 . A way out was suggested in [67] where it was noted that, for values of $m_1 + m_2 + m_3$ larger than around 0.3 eV, the neutrino spectrum would actually be approximately degenerate. This may be seen in detail by consulting the chart in Table 1 of [67] wherein the neutrino masses are tabulated as a function of an assumed value of the third neutrino mass, m_3 . Actually it is seen that there is also a region around $m_3 \approx 0.04$ eV and $m_1 + m_2 + m_3 \approx 0.18$ eV where an assumed initial degeneracy may be reasonable. To make physical sense out of such a scenario, it was suggested that the neutrino mass matrix be written as,

$$M_\nu = M_\nu^{(0)} + M_\nu^{(1)} + M_\nu^{(2)}, \quad (5.10)$$

where $M_\nu^{(0)}$ has the full S_3 invariance and has degenerate (at least approximately) eigenvalues. Furthermore, the smaller $M_\nu^{(1)}$ is invariant under a particular S_2 subgroup of S_3 and breaks the degeneracy. Finally, $M_\nu^{(2)}$ is invariant under a different S_2 subgroup of S_3 and is assumed to be smaller still. The strengths are summarized as:

$$M_\nu^{(0)} > M_\nu^{(1)} > M_\nu^{(2)}. \quad (5.11)$$

This is inspired by the pre-QCD flavor perturbation theory of the strong interaction which works quite well. In that case the initially unknown strong interaction Hamiltonian is expanded as

$$H = H^{(0)} + H^{(1)} + H^{(2)}. \quad (5.12)$$

Here $H^{(0)}$ is the dominant $SU(3)$ flavor invariant piece, $H^{(1)}$ is the smaller Gell-Mann Okubo perturbation [90] which transforms as the eighth component of a flavor octet representation and breaks the symmetry to $SU(2)$ and $H^{(2)}$, which transforms as a different component of the octet representation and breaks the symmetry further to the hypercharge $U(1)$, is smaller still.

There is a possible immediate objection to the assumption that the neutrino mass eigenvalues be degenerate in the initial S_3 invariant approximation; after all Eq. (5.8) shows that there are two different eigenvalues α and $\alpha + 3\beta$. This was overcome by recognizing that these are both complex numbers and that they could both have the same magnitude but different directions. Having the same magnitude guarantees that all three physical masses will be the same. This introduces a physical phase ψ corresponding to the angle between α and $\alpha + 3\beta$.

In the strong interaction case, the initial $SU(3)$ invariance was found to be reasonably well obeyed. It is thus natural to ask what predictions may exist in the initial S_3 invariant approximation in our neutrino model. It was found [67] that the leptonic factor for neutrinoless double beta decay, m_{ee} could be predicted in this limit to be,

$$|m_{ee}| = \frac{m}{3} \sqrt{5 + 4\cos\psi}, \quad (5.13)$$

where m is the degenerate neutrino mass and ψ is the Majorana type phase mentioned above. This led to the inequality

$$m > |m_{ee}| \geq m/3. \quad (5.14)$$

The next chapter is based on our work where we will consider the effect of the perturbations $M_\nu^{(1)}$ [91] and $M_\nu^{(2)}$ [92]. Many authors [93] - [95] have suggested that a μ - τ symmetry ((23) symmetry in the present language) is associated with tribimaximal mixing in the neutrino sector. Thus it is a natural S_2 symmetry choice for $M_\nu^{(1)}$ and $M_\nu^{(2)}$. Recently, Chen and Wolfenstein [68] applied this type of perturbation to our

present model with the additional assumption that the Majorana phase ψ takes the value π . This corresponds to CP conservation. Their result for $|m_{ee}|$ is in agreement with the lower limit in Eq. (5.14). Here we will investigate the first perturbed case without assuming that special value of ψ .

Before going on to this we will present an amusing argument to show that the (23) perturbation is naturally associated with the tribimaximal form (modulo the majorana type phase ψ) rather than a tribimaximal form multiplied by a rotation in the two dimensional degenerate subspace (which is physically irrelevant at the S_3 invariant level). This is based on the fact that degenerate perturbation theory must be employed, which leads to a stability condition. Further we will show that other S_2 perturbations are mathematically consistent but do not lead to the desired tribimaximal form.

Chapter 6

Perturbation Analysis

6.1 Effects of Different Perturbations

In the present framework there are three different possible perturbations, each characterized by the S_2 subgroup which remains invariant. Let us first consider the favored perturbation which leaves invariant the S_2 subgroup, consisting of $S^{(1)}$ and $S^{(23)}$. Apart from a piece which may be reabsorbed in Eq. (5.7), such a perturbation has the form,

$$\Delta = \begin{pmatrix} 0 & 0 & 0 \\ 0 & t & u \\ 0 & u & t \end{pmatrix} \quad (6.1)$$

where t and u are parameters. It is convenient to adopt the language of ordinary quantum mechanics perturbation theory. We should then work in a basis like Eq. (5.8) where M_ν in Eq. (5.7) is diagonal. However, because of the double degeneracy between the eigenvectors \vec{r}_1 and \vec{r}_3 in Eq. (5.4), the matrix R is not the unique one which diagonalizes M_ν . We should really use the more general matrix $RX(\xi)$ where

$X(\xi)$ is given by:

$$X(\xi) = \begin{pmatrix} \cos\xi & 0 & -\sin\xi \\ 0 & 1 & 0 \\ \sin\xi & 0 & \cos\xi \end{pmatrix}. \quad (6.2)$$

In this basis Δ has the form:

$$X^T R^T \Delta R X = \begin{pmatrix} \frac{c^2(t+u)}{3} + s^2(t-u) & \frac{\sqrt{2}}{3}c(t+u) & \frac{2sc}{3}(t-2u) \\ \frac{\sqrt{2}}{3}c(t+u) & \frac{2}{3}(t+u) & -\frac{\sqrt{2}}{3}s(t+u) \\ \frac{2sc}{3}(t-2u) & -\frac{\sqrt{2}}{3}s(t+u) & \frac{s^2(t+u)}{3} + c^2(t-u) \end{pmatrix}. \quad (6.3)$$

Here, $c = \cos\xi$ and $s = \sin\xi$. Note that, before adding a perturbation, the S_3 symmetry predicts the lepton mixing matrix to be $RX(\xi)$ rather than the desired tribimaximal form, R .

In perturbation theory, the first correction to the m^{th} eigenvector involves the ratio $\frac{\langle n|H^{(1)}|m\rangle}{E_m - E_n}$. For degenerate perturbation theory it is of course necessary that the numerator vanishes for those states with $E_n = E_m$. Here we simply require for the (13) matrix element:

$$(X(\xi)^T K_{TBM}^T \Delta K_{TBM} X(\xi))_{13} = 0. \quad (6.4)$$

This yields in general, $\sin(2\xi) = 0$. The solution with $\xi = 0$ is the desired tribimaximal form. The solution with $\xi = \pi$ just changes the signs of the first and third columns. However, the solutions with $\xi = \pi/2$ and $\xi = 3\pi/2$ interchange the first and third columns, which does not agree with experiment. Thus, apart from a discrete ambiguity, the tribimaximal form is uniquely chosen when a smooth connection with the (23)-type perturbation is required. Of course, the smooth connection corresponds to choosing the correct initial states for the perturbation treatment.

It is easy to see that perturbations which leave the other two S_2 subgroups invariant, do not lead to mixing matrices of the desired tribimaximal form. The perturba-

tion which commutes with $S^{(12)}$ is:

$$\Delta' = \begin{pmatrix} t' & u' & 0 \\ u' & t' & 0 \\ 0 & 0 & 0 \end{pmatrix}. \quad (6.5)$$

Similarly, the perturbation which commutes with $S^{(13)}$ has the form:

$$\Delta'' = \begin{pmatrix} t'' & 0 & u'' \\ 0 & 0 & 0 \\ u'' & 0 & t'' \end{pmatrix}. \quad (6.6)$$

The stability condition for obtaining the tribimaximal mixing for the Δ' perturbation would require the matrix element $(K_{TBM}^T \Delta' K_{TBM})_{13}$ to vanish; instead it takes the value $\frac{\sqrt{3}}{6}(t' - 2u')$. Similarly, the stability condition for the Δ'' perturbation does not work since the matrix element $(K_{TBM}^T \Delta'' K_{TBM})_{13}$ takes the generally non-zero value $\frac{\sqrt{3}}{6}(-t'' + 2u'')$.

While we have seen that the stability condition for (23) invariant perturbations enforces the experimentally plausible tribimaximal mixing, the underlying S_3 symmetry should allow characteristic stable mixing matrices to emerge for either the (12) invariant or (13) invariant perturbations. What are their forms? In the case of a (12) perturbation, the stability condition associated with degenerate perturbation theory reads:

$$(K^T \Delta' K)_{13} = 0. \quad (6.7)$$

Here the characteristic mixing matrix emerges as $K = K_{TBM} X(\xi)$ for a suitable value of ξ . The solution is easily seen to have the form:

$$K_{TBM} X\left(\frac{\pi}{6}\right) = \begin{pmatrix} \frac{1}{\sqrt{3}} & \frac{1}{\sqrt{2}} & \frac{1}{\sqrt{6}} \\ \frac{1}{\sqrt{3}} & \frac{-1}{\sqrt{2}} & \frac{1}{\sqrt{6}} \\ \frac{1}{\sqrt{3}} & 0 & \frac{-2}{\sqrt{6}} \end{pmatrix}. \quad (6.8)$$

In the case of a (13) invariant perturbation, the stability condition associated with degenerate perturbation theory reads:

$$(K^T \Delta'' K)_{13} = 0. \quad (6.9)$$

Here the characteristic stable mixing matrix turns out to be:

$$K_{TBM} X\left(\frac{\pi}{3}\right) = \begin{pmatrix} \frac{-1}{\sqrt{6}} & \frac{1}{\sqrt{3}} & \frac{1}{\sqrt{2}} \\ \frac{2}{\sqrt{6}} & \frac{1}{\sqrt{3}} & 0 \\ \frac{-1}{\sqrt{6}} & \frac{1}{\sqrt{3}} & \frac{-1}{\sqrt{2}} \end{pmatrix}. \quad (6.10)$$

The situation is summarized in Table 6.1. Mathematically, any of the three perturbations will result in a stable mixing matrix. However, only the (23) perturbation gives the experimentally allowed tribimaximal form. For example, we see that the zero value of K_{13} , in good present agreement with experiment, only holds for the Δ [(23)-type] perturbation.

Perturbation	Mixing matrix
Δ	K_{TBM}
Δ'	$K_{TBM} X\left(\frac{\pi}{6}\right)$
Δ''	$K_{TBM} X\left(\frac{\pi}{3}\right)$

Table 6.1 Characteristic, stable mixing matrices for each S_2 invariant perturbation.

6.2 Zeroth Order Setup

In order to go further we adopt convenient conventions for the, in general, complex parameters α and β defined in Eq. (5.7). The goal is to adjust a phase, ψ in order that the zeroth order spectrum has three exactly degenerate neutrinos. As shown in

Fig. 6.1, we take the 2-vector 3β to be real positive. Then the 2-vector α lies in the third quadrant as:

$$\alpha = -i|\alpha|e^{-i\psi/2}, \quad (6.11)$$

where the physical phase ψ lies in the range:

$$0 < \psi \leq \pi. \quad (6.12)$$

Finally $|\alpha|$ is related to β by,

$$|\alpha| = \frac{3\beta}{2\sin(\psi/2)}. \quad (6.13)$$

In the limiting case $\psi = \pi$, α takes the real value,

$$\alpha = -\frac{3\beta}{2} \quad (\psi = \pi). \quad (6.14)$$

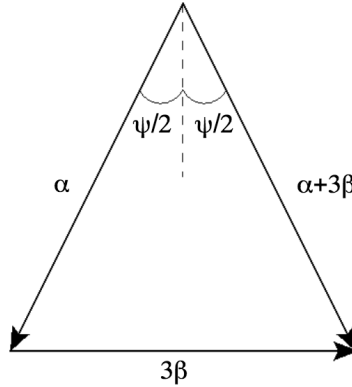


Figure 6.1 Isosceles triangle with angle ψ between the equal length 2-vectors α and $\alpha + 3\beta$.

6.3 Analysis of the First Perturbation

For simplicity we will consider the parameters t and u in Eq. (6.1) to be real rather than complex. The entire neutrino mass matrix to first order is $M_\nu = \alpha \mathbf{1} + \beta d + \Delta$. Since we are working in a basis where the zeroth order piece is diagonalized by the tribimaximal matrix, R , we must diagonalize the matrix:

$$R^T(\alpha \mathbf{1} + \beta d + \Delta)R = \alpha \mathbf{1} + \begin{pmatrix} \frac{t+u}{3} & \frac{\sqrt{2}}{3}(t+u) & 0 \\ \frac{\sqrt{2}}{3}(t+u) & 3\beta + \frac{2}{3}(t+u) & 0 \\ 0 & 0 & t-u \end{pmatrix}. \quad (6.15)$$

Diagonalizing the upper left 2×2 sub-matrix yields the three, in general, complex eigenvalues:

$$\begin{aligned} \alpha + \frac{3}{2}(\beta + T)(1 - \sqrt{1 - \frac{4\beta T}{3(\beta + T)^2}}) &\approx \alpha + T, \\ \alpha + \frac{3}{2}(\beta + T)(1 + \sqrt{1 + \frac{4\beta T}{3(\beta + T)^2}}) &\approx \alpha + 3\beta + 2T, \\ \alpha + t - u, & \end{aligned} \quad (6.16)$$

where we introduced the abbreviation, $T = (t + u)/3$. The indicated approximations to the exact eigenvalues correspond to working to first order in the parameters t and u . Remember that according to our original setup, t and u are supposed to be small compared to $|\alpha|$ and β . Since Fig. 6.1 shows that generally $|\alpha| > 3\beta/2$, it is sufficient that $|t|$ and $|u|$ be small compared to β .

In this approximation the corresponding eigenvectors are the columns of,

$$R_1 \approx \begin{pmatrix} 1 & \frac{\sqrt{2}}{9\beta}(t+u) & 0 \\ -\frac{\sqrt{2}}{9\beta}(t+u) & 1 & 0 \\ 0 & 0 & 1 \end{pmatrix}. \quad (6.17)$$

The entire diagonalization may be presented as,

$$K^T(\alpha\mathbf{1} + \beta d + \Delta)K = \begin{pmatrix} m_1 & 0 & 0 \\ 0 & m_2 & 0 \\ 0 & 0 & m_3 \end{pmatrix}. \quad (6.18)$$

Here m_1 , m_2 and m_3 are the three (positive) neutrino masses and

$$K = RR_1P \quad (6.19)$$

is the full neutrino mixing matrix (in a basis where the charged leptons are diagonal).

The neutrino masses, to order $(t, u)/\beta$, are seen to be:

$$\begin{aligned} m_1 &\approx \frac{3\beta}{2} \csc\left(\frac{\psi}{2}\right) \left[1 - \frac{2}{9\beta}(t+u)\sin^2\left(\frac{\psi}{2}\right) \right], \\ m_2 &\approx \frac{3\beta}{2} \csc\left(\frac{\psi}{2}\right) \left[1 + \frac{4}{9\beta}(t+u)\sin^2\left(\frac{\psi}{2}\right) \right], \\ m_3 &\approx \frac{3\beta}{2} \csc\left(\frac{\psi}{2}\right) \left[1 - \frac{6}{9\beta}(t-u)\sin^2\left(\frac{\psi}{2}\right) \right]. \end{aligned} \quad (6.20)$$

These mass parameters were made real, positive by the introduction of the phase matrix:

$$P = \begin{pmatrix} e^{-i\tau} & 0 & 0 \\ 0 & e^{-i\sigma} & 0 \\ 0 & 0 & e^{-i\rho} \end{pmatrix}, \quad (6.21)$$

where,

$$\begin{aligned} \tau &\approx \frac{\pi}{2} + \frac{1}{2} \tan^{-1} \left[\frac{\cot(\psi/2)}{1 - \frac{2(t+u)}{9\beta}} \right] \\ \sigma &\approx \pi - \frac{1}{2} \tan^{-1} \left[\frac{\cot(\psi/2)}{1 + \frac{4(t+u)}{9\beta}} \right] \\ \rho &\approx \frac{\pi}{2} + \frac{1}{2} \tan^{-1} \left[\frac{\cot(\psi/2)}{1 - \frac{2(t-u)}{3\beta}} \right]. \end{aligned} \quad (6.22)$$

To compare with experiment, we have important information from neutrino oscillation experiments [59]- [66]. It is known that [96]

$$\begin{aligned} A &\equiv m_2^2 - m_1^2 = (8 \pm 0.3) \times 10^{-5} \text{eV}^2, \\ B &\equiv |m_3^2 - m_2^2| = (2.5 \pm 0.5) \times 10^{-3} \text{eV}^2. \end{aligned} \quad (6.23)$$

Also, constraints on cosmological structure formation yield [97] a rough bound,

$$m_1 + m_2 + m_3 < 0.7 \text{eV}. \quad (6.24)$$

The two allowed spectrum types are:

$$\begin{aligned} \text{Type1} : \quad & m_3 > m_2 > m_1, \\ \text{Type2} : \quad & m_2 > m_1 > m_3. \end{aligned} \quad (6.25)$$

Now, from Eq. (6.20) we see to leading order:

$$\begin{aligned} m_2^2 - m_1^2 &= 3\beta(t + u), \\ m_3^2 - m_2^2 &= \beta(-5t + u). \end{aligned} \quad (6.26)$$

The quantities βt and βu may thus be obtained for a type 1 spectrum as:

$$\begin{aligned} \beta t &= A/18 - B/6 \approx -4.13 \times 10^{-4} \text{eV}^2, \\ \beta u &= 5A/18 + B/6 \approx 4.39 \times 10^{-4} \text{eV}^2, \end{aligned} \quad (6.27)$$

where the central experimental values were used. In the type 2 spectrum case, we should change $B \rightarrow -B$ in the above to find,

$$\begin{aligned} \beta t &= A/18 + B/6 \approx 4.21 \times 10^{-4} \text{eV}^2, \\ \beta u &= 5A/18 - B/6 \approx -3.94 \times 10^{-4} \text{eV}^2 \end{aligned} \quad (6.28)$$

Thus the, assumed real, S_3 violation parameters βt and βu are now known for each spectrum type. Information about the quantity β may in principle be obtained from the perturbed lepton mixing matrix given in Eq. (6.19):

$$K \approx \begin{pmatrix} \frac{-2}{\sqrt{6}} - \frac{\sqrt{2}(t+u)}{9\beta\sqrt{3}} & \frac{1}{\sqrt{3}} - \frac{2(t+u)}{9\beta\sqrt{3}} & 0 \\ \frac{1}{\sqrt{6}} - \frac{\sqrt{2}(t+u)}{9\beta\sqrt{3}} & \frac{1}{\sqrt{3}} + \frac{(t+u)}{9\beta\sqrt{3}} & \frac{1}{\sqrt{2}} \\ \frac{1}{\sqrt{6}} - \frac{\sqrt{2}(t+u)}{9\beta\sqrt{3}} & \frac{1}{\sqrt{3}} + \frac{(t+u)}{9\beta\sqrt{3}} & \frac{-1}{\sqrt{2}} \end{pmatrix} P. \quad (6.29)$$

With a usual parameterization (See, for example, Eq. (10) of [98])¹ the matrix with zero (13) element takes the form,

$$K = \begin{pmatrix} c_{12} & s_{12} & 0 \\ -s_{12}c_{23} & c_{12}c_{23} & s_{23} \\ s_{12}s_{23} & -c_{12}s_{23} & c_{23} \end{pmatrix} P, \quad (6.30)$$

where c_{12} is short for $\cos\theta_{12}$ for example. This amounts to the predictions,

$$\begin{aligned} c_{12} &= -\frac{2}{\sqrt{6}} - \frac{\sqrt{2}(\beta t + \beta u)}{9\sqrt{3}\beta^2}, \\ c_{23} &= -\frac{1}{\sqrt{2}}, \\ s_{13} &= 0. \end{aligned} \quad (6.31)$$

Notice that, when the perturbation is absent, this agrees with the tribimaximal form used here if both θ_{12} and θ_{23} lie in the second quadrant. The results of a recent study ([99], [100]) of neutrino oscillation experiments are:

$$\begin{aligned} (s_{23})^2 &= 0.50_{-0.06}^{+0.07}, \\ (s_{12})^2 &= 0.304_{-0.016}^{+0.022}. \end{aligned} \quad (6.32)$$

One immediately notices that the prediction, $(s_{23})^2 = 1/2$ is unchanged from its tribimaximal value by the perturbation and agrees with the new analysis. On the

¹This reference also discusses a more symmetrical parameterization which may be convenient for treating neutrinoless double beta decay in general

other hand the tribimaximal prediction, $(s_{12})^2 = 1/3$ is slightly changed from its tribimaximal value and actually lies slightly above the upper experimental error bar. This is probably not a serious disagreement but it might be instructive to try to fix it using the predicted perturbation in the present model:

$$(s_{12})^2 = \frac{1}{3} - \frac{4}{27} \frac{\beta t + \beta u}{\beta^2}. \quad (6.33)$$

For either the type 1 or type 2 assumed spectrum, the perturbation is seen to be in the correct direction to lower the value of s_{12}^2 , as desired. However, because of the large cancellation between βt and βu , this effect is extremely small for a reasonable value of β^2 ; even with β as small as 0.05 eV, $(s_{12})^2$ is only lowered to 0.332.

It is also interesting to discuss the absolute masses of the neutrinos rather than just the differences of their squares. Since the differences are known, let us focus on one of them, say m_3 :

$$m_3 \approx \frac{3\beta}{2} \csc\left(\frac{\psi}{2}\right) - \frac{\beta t - \beta u}{\beta} \sin\left(\frac{\psi}{2}\right). \quad (6.34)$$

Notice that the first term on the right hand side is, using Eq. (6.13), simply the zeroth order degenerate mass, $|\alpha|$ while the second term represents the correction. Also note that (see Fig. 6.1) the point $\psi = 0$ is not allowed. Considering ψ as a parameter (related to the strength of neutrinoless double beta decay), this equation represents a quadratic formula giving β in terms of the absolute mass m_3 for any assumed ψ . In Fig. 6.2, adopting the criterion that $|t|/\beta$ and $|u|/\beta$ be less than 1/5 for perturbative behavior, we display the perturbative region in the $m_3 - \psi$ plane. In contrast to the case of m_3 , m_1 and m_2 are seen to have small corrections since they of course depend on $\beta(t + u)$ rather than $\beta(t - u)$.

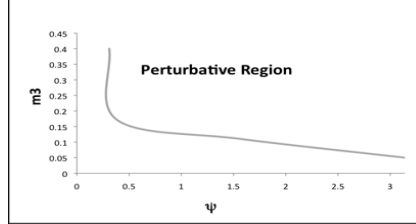


Figure 6.2 Sketch of perturbative region in the m_3 - ψ plane. It is about the same for both type 1 and type 2 neutrino spectra. Note that ψ is measured in radians and m_3 is measured in eV.

6.3.1 Neutrinoless Double Beta Decay

The characteristic physical novelty of a theory with Majorana type neutrinos is the prediction of a small, but non-zero, rate for the neutrinoless double beta decay of a nucleus: $(A, Z) \rightarrow (A, Z + 2) + 2e^-$. The appropriate leptonic factor describing the amplitude for this process is,

$$|m_{ee}| = |m_1(K_{11})^2 + m_2(K_{12})^2 + m_3(K_{13})^2|. \quad (6.35)$$

Substituting in the neutrino masses to order $(t, u)/\beta$ from Eq. (6.20) as well as Eq. (6.21) yields:

$$|m_{ee}| \approx \frac{3\beta}{2\sin(\frac{\psi}{2})} \left| \frac{2}{3} + \frac{4(t+u)}{27\beta} \cos^2\left(\frac{\psi}{2}\right) + \left[\frac{1}{3} - \frac{4(t+u)}{27\beta} \cos^2\left(\frac{\psi}{2}\right) \right] e^{2i(\tau-\sigma)} \right|. \quad (6.36)$$

The needed intermediate quantity $\cos[2(\tau - \sigma)]$ may be easily obtained from Eqs. (6.22) by construction of a suitable right triangles to be:

$$\cos[2(\tau - \sigma)] \approx \cos\psi - \frac{(t + u)\sin\psi}{9\beta}.$$

We then find, correct to first order in $(t, u)/\beta$,

$$|m_{ee}| = \frac{\beta}{2\sin(\psi/2)} \sqrt{5 + 4\cos\psi}, \quad (6.37)$$

which is just the zeroth order result. The experimental bound on $|m_{ee}|$ is given [101] as,

$$|m_{ee}| < (0.35 - 1.30)\text{eV}, \quad (6.38)$$

which is small enough so that there is hope the possibility of a Majorana neutrino might be settled in the near future. Since the correction to $|m_{ee}|$ has been seen to be zero in this model we can take over the zeroth order inequality in Eq. (5.14). This means that the existence of the Majorana phase, ψ can alter the amplitude for neutrinoless double beta decay by a factor of three for given (approximately degenerate) neutrino masses.

6.4 Adding the Second Perturbation and s_{13} Mixing Parameter

Here we will choose for the second order perturbation, the matrix:

$$\Delta' = \begin{pmatrix} t' & u' & 0 \\ u' & t' & 0 \\ 0 & 0 & 0 \end{pmatrix}. \quad (6.39)$$

For simplicity we again consider the parameters, t' and u' to be real.

Note that this second order perturbation preserves the S_2 subgroup which involves the 1-2 interchange. One might wonder about also including a perturbation, Δ'' which preserves the 1-3 S_2 subgroup. However, that is not expected to give anything new since this combination already has the same number of parameters as the most general symmetric matrix, M_ν .

In the present case the zeroth order term has the discrete group S_3 invariance and two different S_2 subgroups are left invariant by the two perturbations.

To include the 2^{nd} -order perturbation, Eq. (6.39), we must diagonalize,

$$\begin{aligned} H &= R_1^T R^T (\alpha I + \beta d + \Delta + \Delta') R R_1 \\ &\equiv H^0 + H' \end{aligned} \quad (6.40)$$

where, after some computation and neglect of still higher order terms, we obtain:

$$H' = R_1^T R^T \Delta' R R_1 \approx \begin{pmatrix} \frac{5}{6}t' - \frac{2}{3}u' & -\frac{1}{3\sqrt{2}}(t' + u') & \frac{1}{2\sqrt{3}}(t' - 2u') \\ -\frac{1}{3\sqrt{2}}(t' + u') & \frac{2}{3}(t' + u') & \frac{1}{\sqrt{6}}(t' + u') \\ \frac{1}{2\sqrt{3}}(t' - 2u') & \frac{1}{\sqrt{6}}(t' + u') & \frac{1}{2}t' \end{pmatrix}. \quad (6.41)$$

We introduced the notation H^0 (Everything in Eq. (6.40) except for Δ') and H' to indicate that, rather than making an explicit diagonalization we will regard, the result to first order as a “zeroth order Hamiltonian”, the given second order term, Eq. (6.39) as a “first order perturbation” and use ordinary quantum mechanics perturbation theory to proceed. In that approach one has of course the corrections to the energies as:

$$E'_n = \langle \psi_n | H' | \psi_n \rangle, \quad (6.42)$$

while the corrections to the eigenvectors are,

$$\psi_m^{(1)} = \sum_{n \neq m} \frac{\langle \psi_n | H' | \psi_m \rangle}{E_m - E_n} \psi_n. \quad (6.43)$$

A more general perturbation approach, which gives the same results, is discussed in the Appendix (B.1). The lepton mixing matrix up to and including second order then reads:

$$K = RR_1R_2P = (\psi_1, \psi_2, \psi_3)P, \quad (6.44)$$

where the ψ_i are the columns of RR_1R_2 and furthermore P is the phase matrix needed for the neutrino masses to be real positive; explicitly,

$$\begin{aligned} \psi_1 &= \frac{1}{\sqrt{6}} \begin{pmatrix} -2 - 2\frac{t+u}{9\beta} + 2\frac{t'+u'}{\beta} \\ 1 - 2\frac{t+u}{9\beta} - 3\frac{t'-2u'}{t-2u} + \frac{t'+u'}{9\beta} \\ 1 - 2\frac{t+u}{9\beta} + 3\frac{t'-2u'}{t-2u} + \frac{t'+u'}{9\beta} \end{pmatrix}, \\ \psi_2 &= \frac{1}{\sqrt{3}} \begin{pmatrix} 1 - 2\frac{t+u}{9\beta} + \frac{t'+u'}{9\beta} \\ 1 + \frac{t+u}{9\beta} - \frac{t'+u'}{18\beta} + \frac{t'+u'}{6} \\ 1 + \frac{t+u}{9\beta} - \frac{t'+u'}{18\beta} - \frac{t'+u'}{6} \end{pmatrix}, \\ \psi_3 &= \frac{1}{\sqrt{2}} \begin{pmatrix} -\frac{1}{2}\frac{t'-2u'}{t-2u} - \frac{t'+u'}{9\beta} \\ 1 + \frac{1}{4}\frac{t'-2u'}{t-2u} - \frac{t'+u'}{9\beta} \\ -1 + \frac{1}{4}\frac{t'-2u'}{t-2u} - \frac{t'+u'}{9\beta} \end{pmatrix}, \end{aligned} \quad (6.45)$$

and the phase matrix has the form,

$$P = \begin{pmatrix} e^{-i\tau} & 0 & 0 \\ 0 & e^{-i\sigma} & 0 \\ 0 & 0 & e^{-i\rho} \end{pmatrix}, \quad (6.46)$$

wherein,

$$\begin{aligned}
\tau &\approx \frac{\pi}{2} + \frac{1}{2} \tan^{-1} \left[\frac{\cot(\psi/2)}{1 - \frac{2(t+u)}{9\beta} - \frac{5t'}{9\beta} - \frac{4u'}{9\beta}} \right] \\
\sigma &\approx \pi - \frac{1}{2} \tan^{-1} \left[\frac{\cot(\psi/2)}{1 + \frac{4(t+u)}{9\beta} + \frac{4(t'+u')}{9\beta}} \right] \\
\rho &\approx \frac{\pi}{2} + \frac{1}{2} \tan^{-1} \left[\frac{\cot(\psi/2)}{1 - \frac{2(t+u)}{3\beta} - \frac{t'}{3\beta}} \right].
\end{aligned} \tag{6.47}$$

Note that we are free to subtract $(\tau + \sigma + \rho)/3$ from each of these three entries. Then the sum of the modified three entries will vanish in accordance with the requirement that there be only two independent Majorana phases. The real positive neutrino masses to second order are then:

$$\begin{aligned}
m_1 &\approx \frac{3}{2} \beta \csc \frac{\psi}{2} \left[1 - \frac{2}{9\beta} (t + u + \frac{5}{2}t' - 2u') \sin^2 \frac{\psi}{2} \right], \\
m_2 &\approx \frac{3}{2} \beta \csc \frac{\psi}{2} \left[1 + \frac{4}{9\beta} (t + u + t' + u') \sin^2 \frac{\psi}{2} \right], \\
m_3 &\approx \frac{3}{2} \beta \csc \frac{\psi}{2} \left[1 - \frac{2}{3\beta} (t - u + \frac{1}{2}t') \sin^2 \frac{\psi}{2} \right].
\end{aligned} \tag{6.48}$$

Notice that the zeroth order masses have the characteristic strength, β while the first order masses are suppressed by $(t, u)/\beta$ and the second order masses are suppressed by $(t', u')/\beta$.

Also notice that the absolute values of the neutrino masses depend on the Majorana phase, ψ . However, the lepton number conserving neutrino oscillations can not depend on a Majorana phase² [102]. As a check of this we see that the phase ψ cancels out when one considers the mass *differences*,

²One needs the presently unobserved neutrino antineutrino oscillations or other lepton number violating processes to see the Majorana phases,

$$\begin{aligned}
A &\equiv m_2^2 - m_1^2 \approx 3\beta(t + u) + \frac{9}{2}\beta t', \\
B &\equiv m_3^2 - m_2^2 \approx \beta(-5t + u) - \beta\left(\frac{7}{2}t' + 2u'\right), \\
C &\equiv m_3^2 - m_1^2 \approx 2\beta(-t + 2u) + \beta(t' - 2u').
\end{aligned} \tag{6.49}$$

Of course, A , B and C are not independent. There are two, presently unresolved, experimental possibilities:

$$\begin{aligned}
\textit{Type1} : & \quad m_3 > m_2 > m_1, \\
\textit{Type2} : & \quad m_2 > m_1 > m_3.
\end{aligned} \tag{6.50}$$

The corresponding relations are:

$$\begin{aligned}
\textit{Type1} : & \quad |C| = |B| + A, \\
\textit{Type2} : & \quad |C| = |B| - A.
\end{aligned} \tag{6.51}$$

These relations were obtained by using the known positive sign of A and that only the two possibilities $m_3^2 > m_2^2 > m_1^2$ and $m_2^2 > m_1^2 > m_3^2$ are allowed. In the literature some works specify A and $|B|$ while others specify A and $|C|$.

The following best fit values for the perturbation parameters βt and βu were given in the first order treatment:

$$\begin{aligned}
\beta t &\approx -4.13 \times 10^{-4} \text{eV}^2, \\
\beta u &\approx 4.39 \times 10^{-4} \text{eV}^2, \quad \textit{Type1}
\end{aligned} \tag{6.52}$$

$$\begin{aligned}\beta t &\approx 4.21 \times 10^{-4} \text{eV}^2, \\ \beta u &\approx -3.94 \times 10^{-4} \text{eV}^2 \quad \textit{Type2}.\end{aligned}\tag{6.53}$$

6.4.1 Elements of the Mixing Matrix

We employ the following parameterization [98] of the leptonic mixing matrix, K :

$$K = \begin{pmatrix} c_{12}c_{13} & s_{12}c_{13} & s_{13}e^{-i\gamma} \\ -s_{12}c_{23} - c_{12}s_{13}s_{23}e^{i\gamma} & c_{12}c_{23} - s_{12}s_{13}s_{23}e^{i\gamma} & c_{13}s_{23} \\ s_{12}s_{23} - c_{12}s_{13}c_{23}e^{i\gamma} & -c_{12}s_{23} - s_{12}s_{13}c_{23}e^{i\gamma} & c_{13}c_{23} \end{pmatrix} P, \tag{6.54}$$

where c_{12} is short for $\cos\theta_{12}$ for example. P is the diagonal matrix of Majorana type phases given in Eqs. (6.46) and (6.47) for the present model. For simplicity we are presently neglecting the conventional CP violation and thus setting $\gamma = 0$. To specify s_{12} , s_{13} and s_{23} , it is clearly sufficient to compare the (1-2), (1-3) and (2-3) matrix elements of K in Eq. (6.54) with those calculated in Eq. (6.45). This yields:

$$\begin{aligned}s_{12}c_{13} &= \frac{1}{\sqrt{3}} - \frac{2}{\sqrt{3}} \frac{t+u}{9\beta} + \frac{1}{\sqrt{3}} \frac{t'+u'}{9\beta}, \\ s_{13} &= -\frac{1}{2\sqrt{2}} \frac{t'-2u'}{t-2u} - \frac{1}{\sqrt{2}} \frac{t'+u'}{9\beta}, \\ s_{23}c_{13} &= \frac{1}{\sqrt{2}} + \frac{1}{4\sqrt{2}} \frac{t'-2u'}{t-2u} - \frac{1}{\sqrt{2}} \frac{t'+u'}{9\beta}.\end{aligned}\tag{6.55}$$

For an initial orientation we see that at zeroth order, s_{13} vanishes and also K has the tribimaximal form. When the first order perturbation characterized by t and u is added, neither s_{13} nor s_{23} change. However s_{12} is somewhat modified as discussed previously. When the second order perturbation characterized by t' and u' is added, s_{13} finally becomes non-zero while both s_{12} and s_{23} suffer further corrections.

But something unusual is happening; there are terms for s_{13} and s_{23} which behave like t'/t and are manifestly of first order in strength. These arise from the energy difference denominator in Eq. (6.43). Since we had to use degenerate perturbation theory at first order this denominator is proportional to the first order “energy” corrections rather than the zeroth order energies. Keeping terms of actual first order in strength we find the interesting relation:

$$s_{13} \approx -2\delta s_{23}, \quad (6.56)$$

where δs_{23} denotes the deviation of s_{23} from its tribimaximal value. Also the good approximation $c_{13} = 1$ was made.

Already, Fogli et. al. [99] and Schwetz et. al. [100] have pointed out that detailed analysis of existing neutrino oscillation experiments gives some hint for non zero s_{13} . Thus it seems interesting to see what predictions emerge from Eq. (6.56).

Expanding s_{23} around its “tribimaximal value” as $s_{23} = [s_{23}]_{TBM} + \delta s_{23}$, one gets:

$$(s_{23})^2 \approx \frac{1}{2} + \sqrt{2}\delta s_{23}. \quad (6.57)$$

Comparing with the results of a global analysis of the oscillation data given in Table A1 of [100] one then identifies, for respectively 1σ , 2σ and 3σ errors:

$$|\delta s_{23}| = 0.05, \quad 0.08, \quad 0.11. \quad (6.58)$$

Note that the three cases are associated with the experimental data relating to the 2-3 type neutrino oscillations. Using Eq. (6.56) then leads to the corresponding predictions,

$$|s_{13}| < 0.025, \quad 0.040, \quad 0.055. \quad (6.59)$$

It is amusing to note that these values range from about 1/4 to 1/2 of the “best fit” value $|s_{13}| = 0.11$, which is also presented in the first column of Table A1 in [100].

Of course, our estimates provide a test of the present theoretical model for neutrino parameters and have no connection with experimental data on $|s_{13}|$.

As discussed above, the theoretical estimate for $|s_{13}|$, is of characteristic first order strength, appearing as a ratio of a second order quantity divided by a first order quantity. Using Eq. (6.55) for s_{13} and neglecting the term of second order strength we can get an estimate of the relative second to first order effects:

$$\left| \frac{t' - 2u'}{t - 2u} \right| \approx 2\sqrt{2}|s_{13}| \approx 0.071, \quad 0.11, \quad 0.16, \quad (6.60)$$

wherein Eq. (6.59) was used. Evidently the second order effects seem to be suppressed by about 1/10 compared to the first order effects. On the other hand, as seen in Eq. (6.49), the quantities t' and u' enter in the true second order corrections for the neutrino mass differences. Thus those corrections are likely to be small – on the order of 10% of the first order mass splittings.

Chapter 7

Conclusions for S_3 Symmetry for Neutrino Masses and Mixing

In some ways the problem of “flavor” in the Standard Model is reminiscent of that in Strong Interaction physics before the quark model. At that time it was realized that, as a precursor to detailed dynamics, group theory might give important clues. Then the strong interactions were postulated to be $SU(3)$ flavor invariant with a weaker piece having just the the $SU(2)$ isospin (times hypercharge) invariance. In addition it was known that there was a still weaker isospin breaking (possibly QED) which by itself preserved a different $SU(2)$ invariance (so-called U-spin).

In the second part of the thesis, an analogy for neutrinos of this kind is studied in a perturbative framework using discrete group S_3 . At the S_3 invariant level the neutrino mixing matrix is actually arbitrary up to a rotation in a 2-dimensional subspace. This problem can be settled (since degenerate perturbation theory is involved) by specifying the transformation property of the perturbation to be added. Although there is widespread agreement that the first perturbation should preserve the S_2 subgroup which interchanges the second and third neutrinos, we presented for

completeness and interest, the mixing matrices for the other two possibilities also.

We carried out the perturbation analysis for any choice of a Majorana-type phase, ψ which plays an important role in this model. If ψ is considered fixed there are three parameters in the model (In [68] ψ was considered fixed at the value π). These three parameters can be taken as βt , βu and β defined above. The quantities βt and βu were found in terms of the neutrino squared mass differences for each choice of neutrino spectrum type, i.e. normal or inverted hierarchy. The value of β depends on the presently unknown absolute value of any neutrino mass. The magnitudes of βt and βu are similar (though not exactly equal) but differ in sign. Thus the perturbation corrections which involve $(\beta t + \beta u)$ are very small. Clearly (see the first of Eqs. (6.26)) this is due to the small solar neutrino mass difference. This situation occurs for the correction to the mixing parameter $\sin^2\theta_{12}$ in addition to m_1 and m_2 , the masses of the first two neutrinos. The perturbation dependence on $(\beta t - \beta u)$ is not suppressed however. This occurs for the mass, m_3 of the third neutrino. This result was used to make a sketch of the region in the ψ - m_3 plane for which the perturbation approach given seems numerically reasonable.

The explicit role of the Higgs sector, which is believed to be at the heart of the matter, was not discussed. However, this as well as some further technical details were discussed in [67]. For further treatment of this aspect is to investigate the weakest perturbation, the analog of the U-spin preserving perturbation in the strong interaction to get non-zero θ_{13} . For this purpose we designated the second order parameters as t' and u' . The first order corrections to the neutrino masses were suppressed by $(t, u)/\beta$ compared to zeroth order. For the mixing angles, the first order corrections had a previously obtained piece proportional to $(t, u)/\beta$ as well as a new piece proportional to $(t', u')/(t, u)$. The latter term arose because we used degenerate perturbation theory and is clearly important for s_{13} to be non-zero and

correlated to corrections of s_{23} .

We have numerically neglected, for both masses and mixing angles terms proportional to $(t', u')/\beta$. At first order, we considered $(t, u)/\beta$ to be about $1/5$. We found a characteristic strength of s_{13} to correspond to $(t', u')/(t, u)$ about $1/10$. Both of these magnitudes are roughly similar.

Note that Eqs. (6.49) for the neutrino mass differences and Eqs. (6.55) for the mixing angles do contain pieces of actual second order strength. These should be interesting to study in the future when more precise data becomes available.

The first order corrected formula for the neutrinoless double beta decay formula does not get any corrections at second order and hence still holds.

Appendix A

Part I Appendix

A.1 Lagrangian in Terms of Component Fields

The spin zero meson kinetic terms are:

$$\begin{aligned} -\frac{1}{2}\text{Tr}(D_\mu M D_\mu M^\dagger) &= -\frac{1}{2}\partial_\mu \boldsymbol{\pi} \cdot \partial_\mu \boldsymbol{\pi} - \frac{1}{2}\partial_\mu \sigma \partial_\mu \sigma + \frac{g}{\sqrt{2}} \mathbf{A}_\mu \cdot (\sigma \overleftrightarrow{\partial}_\mu \boldsymbol{\pi}) \\ &- \frac{g}{2\sqrt{2}} \epsilon_{abc} V_{\mu a} (\pi_b \overleftrightarrow{\partial}_\mu \pi_c) + g^2 \left[-\frac{\sigma^2}{4} \mathbf{A}_\mu \cdot \mathbf{A}_\mu \right. \\ &+ \frac{1}{2} \epsilon_{abc} \sigma \pi_a V_{\mu b} A_{\mu c} + \frac{1}{4} (\boldsymbol{\pi} \cdot \mathbf{V}_\mu)^2 - \frac{1}{4} (\boldsymbol{\pi} \cdot \boldsymbol{\pi}) (\mathbf{V}_\mu \cdot \mathbf{V}_\mu) \\ &\left. - \frac{1}{4} (\boldsymbol{\pi} \cdot \mathbf{A}_\mu)^2 \right]. \end{aligned} \tag{A.1}$$

The Yang-Mills terms are:

$$\begin{aligned}
-\frac{1}{2}\text{Tr}(F_{\mu\nu}^r F_{\mu\nu}^r + F_{\mu\nu}^l F_{\mu\nu}^l) &= -\frac{1}{4}[(\partial_\mu V_{\nu a} - \partial_\nu V_{\mu a})^2 + (\partial_\mu A_{\nu a} - \partial_\nu A_{\mu a})^2] \\
&- \frac{g}{2\sqrt{2}}\epsilon_{abc}[(\partial_\mu V_{\nu c} - \partial_\nu V_{\mu c})(V_{\mu a} V_{\nu b} + A_{\mu a} A_{\nu b}) \\
&- (\partial_\mu A_{\nu c} - \partial_\nu A_{\mu c})(V_{\mu a} A_{\nu b} + A_{\mu a} V_{\nu b})] \\
&- \frac{g^2}{8}[(\mathbf{V}_\mu \cdot \mathbf{V}_\mu)^2 - (\mathbf{V}_\mu \cdot \mathbf{V}_\nu)^2 + (\mathbf{A}_\mu \cdot \mathbf{A}_\mu)^2 \\
&- (\mathbf{A}_\mu \cdot \mathbf{A}_\nu)^2 + 2(\mathbf{V}_\mu \cdot \mathbf{V}_\mu)(\mathbf{A}_\nu \cdot \mathbf{A}_\nu) \\
&- 2(\mathbf{V}_\mu \cdot \mathbf{V}_\nu)(\mathbf{A}_\mu \cdot \mathbf{A}_\nu) + 4(\mathbf{V}_\mu \cdot \mathbf{A}_\mu)(\mathbf{V}_\nu \cdot \mathbf{A}_\nu) \\
&- 2(\mathbf{V}_\mu \cdot \mathbf{A}_\nu)(\mathbf{V}_\mu \cdot \mathbf{A}_\nu)]. \tag{A.2}
\end{aligned}$$

Finally, the spin one meson mass terms are:

$$\begin{aligned}
-m_0^2\text{Tr}(l_\mu l_\mu + r_\mu r_\mu) &= -\frac{1}{2}m_0^2(\mathbf{V}_\mu \cdot \mathbf{V}_\mu + \mathbf{A}_\mu \cdot \mathbf{A}_\mu), \\
-C\text{Tr}(l_\mu^2 M M^\dagger + r_\mu^2 M^\dagger M) &= -\frac{C}{4}(\mathbf{V}_\mu \cdot \mathbf{V}_\mu + \mathbf{A}_\mu \cdot \mathbf{A}_\mu)(\sigma^2 + \boldsymbol{\pi} \cdot \boldsymbol{\pi}), \\
B\text{Tr}(M r_\mu M^\dagger l_\mu) &= B[\frac{1}{8}\sigma^2(\mathbf{V}_\mu \cdot \mathbf{V}_\mu - \mathbf{A}_\mu \cdot \mathbf{A}_\mu) - \frac{1}{2}\epsilon_{abc}\sigma\pi_a V_{\mu b} A_{\mu c} \\
&+ \frac{1}{4}(\boldsymbol{\pi} \cdot \mathbf{V}_\mu)^2 - \frac{1}{8}(\boldsymbol{\pi} \cdot \boldsymbol{\pi})(\mathbf{V}_\mu \cdot \mathbf{V}_\mu) - \frac{1}{4}(\boldsymbol{\pi} \cdot \mathbf{A}_\mu)^2 \\
&+ \frac{1}{8}(\boldsymbol{\pi} \cdot \boldsymbol{\pi})(\mathbf{A}_\mu \cdot \mathbf{A}_\mu)]. \tag{A.3}
\end{aligned}$$

A.2 Pion-pion Scattering Amplitude

At tree level, the conventional Mandelstam scattering amplitude, $A(s, t, u)$ has the following contributions:

1) Zero derivative contact term:

$$\begin{aligned}
&-\tilde{g}_{\sigma\pi\pi}w^2/v, \\
\tilde{g}_{\sigma\pi\pi} &\equiv \frac{w^2}{v}(m_\sigma^2 - \frac{\tilde{m}_\pi^2}{w^2}). \tag{A.4}
\end{aligned}$$

Note that Eqs. (2.13) and (2.15) were used in obtaining this result.

2) Two derivative contact term:

$$\left(\frac{g^2}{2} + B - C\right)b^2w^2s - Bb^2\tilde{m}_\pi^2w^2 + 2b^2C\tilde{m}_\pi^2w^2. \quad (\text{A.5})$$

Note that the factor b^2 is due to the presence of a physical pion field in the original axial vector meson field, A_μ , as described in the first of Eqs. (2.15). Thus, b^2 labels the two derivative interaction terms.

3) Four derivative contact term:

$$-\frac{g^2}{2}b^4(2s^2 - t^2 - u^2 - 12\tilde{m}_\pi^2s + 16\tilde{m}_\pi^4) \quad (\text{A.6})$$

Note, as above, that the b^4 factor indicates these terms arise from the quartic Yang-Mills interaction of the axial vector gauge field.

4) Sigma pole in the s -channel:

$$\frac{1}{m_\sigma^2 - s}[-\tilde{g}_{\sigma\pi\pi} + \sqrt{2}\tilde{m}_\pi^2gbw - 2G(\tilde{m}_\pi^2 - \frac{s}{2})]^2, \quad (\text{A.7})$$

where,

$$G = -\frac{vg^2b^2}{2} - \frac{vBb^2}{4} + \frac{2gbw}{\sqrt{2}} - \frac{C}{2}b^2v. \quad (\text{A.8})$$

5) Rho poles in the t and u channels:

$$\frac{s-u}{m_\rho^2 - t}[-G_1 + \frac{gb^2}{2\sqrt{2}}t]^2 + \frac{s-t}{m_\rho^2 - u}[-G_1 + \frac{gb^2}{2\sqrt{2}}u]^2, \quad (\text{A.9})$$

where,

$$G_1 = \frac{g}{\sqrt{2}}\left(1 - \frac{Bv^2}{2m_0^2}\right). \quad (\text{A.10})$$

The full amplitude $A(s, t, u)$ is, of course, the sum of all five pieces just written.

Here, we will be interested in the $I = 0, 2$ projections:

$$\begin{aligned} T^0 &= 3A(s, t, u) + A(t, u, s) + A(u, s, t), \\ T^2 &= A(t, u, s) + A(u, s, t), \end{aligned} \quad (\text{A.11})$$

where the Mandelstam variables are $s = 4(p_\pi^2 + \tilde{m}_\pi^2)$, $t = -2p_\pi^2(1 - \cos\theta)$, $u = -2p_\pi^2(1 + \cos\theta)$, p_π being the spatial momentum of the pion in the center of mass frame.

The angular momentum l partial wave elastic scattering amplitude for isospin I is then defined as,

$$T_l^I = \frac{1}{64\pi} \sqrt{1 - \frac{4\tilde{m}_\pi^2}{s}} \int_{-1}^1 d\cos\theta P_l(\cos\theta) T^I(s, t, u). \quad (\text{A.12})$$

Using the above formula, we get:

$$\begin{aligned} T_0^0 &= \frac{1}{64\pi} \sqrt{1 - \frac{4\tilde{m}_\pi^2}{s}} \left[10 \left(\frac{m_\sigma^2 - \tilde{m}_\pi^2/w^2}{v^2} w^4 + (2C - B)b^2 w^2 \tilde{m}_\pi^2 \right) + \frac{6}{m_\sigma^2 - s} [-\tilde{g}_{\sigma\pi\pi} \right. \\ &+ \sqrt{2}\tilde{m}_\pi^2 g b w - 2G(\tilde{m}_\pi^2 - \frac{s}{2})]^2 + 4(G_1^2 R_1 + G_1 \frac{g b^2}{\sqrt{2}} R_2 + \frac{g^2 b^4}{8} R_3) - \frac{3g^2 b^4}{8} (4s^2 - \frac{64p_\pi^4}{3} \\ &- 24\tilde{m}_\pi^2 s + 32\tilde{m}_\pi^4) - \frac{g^2 b^4}{4} (-2s^2 + \frac{32p_\pi^4}{3} + 48\tilde{m}_\pi^2 s + 32\tilde{m}_\pi^4) + 6b^2 w^2 (\frac{g^2}{2} + B - C)s \\ &\left. + 2b^2 w^2 (\frac{g^2}{2} + B - C)(-4p_\pi^2) \right] \quad (\text{A.13}) \end{aligned}$$

where

$$\begin{aligned} C_1 &= -\tilde{g}_{\sigma\pi\pi} + \sqrt{2}\tilde{m}_\pi^2 g b w - 2G\tilde{m}_\pi^2, \\ S_1 &= \frac{1}{2p_\pi^2} \ln\left(\frac{m_\sigma^2 + 4p_\pi^2}{m_\sigma^2}\right), \quad S_2 = m_\sigma^2 S_1 - 2, \quad S_3 = 4p_\pi^2 + m_\sigma^2 S_2, \\ R_1 &= \frac{1}{2p_\pi^2} \ln\left(\frac{m_\rho^2 + 4p_\pi^2}{m_\rho^2}\right)(s + m_\rho^2 + 4p_\pi^2) - 2, \quad R_2 = m_\rho^2 R_1 - 4p_\pi^2 - 2s, \\ R_3 &= m_\rho^2 R_2 + \frac{16p_\pi^4}{3} + 4p_\pi^2 s. \quad (\text{A.14}) \end{aligned}$$

Similarly for the $I = 2$ case:

$$\begin{aligned} T_0^2 &= \frac{1}{64\pi} \sqrt{1 - \frac{4\tilde{m}_\pi^2}{s}} \left[4 \left(\frac{m_\sigma^2 - \tilde{m}_\pi^2/w^2}{v^2} w^4 + (2C - B)b^2 w^2 \tilde{m}_\pi^2 \right) \right. \\ &- 4(C_1^2 S_1 + 2C_1 G S_2 + G^2 S_3) + 4(G_1^2 R_1 + 2G_1 g b R_2 + g b^2 R_3) \\ &- \frac{g^2 b^4}{4} (-2s^2 + \frac{32p_\pi^4}{3} + 48\tilde{m}_\pi^2 s + 32m_\pi^4) \\ &\left. + 2b^2 w^2 (\frac{g^2}{2} + B - C)(-4p_\pi^2) \right] \quad (\text{A.15}) \end{aligned}$$

A.3 Notation and Further Details

Here we briefly discuss some notational and technical details. The γ matrices and the charge conjugation matrix have the form:

$$\gamma_i = \begin{bmatrix} 0 & -i\sigma_i \\ i\sigma_i & 0 \end{bmatrix}, \quad \gamma_4 = \begin{bmatrix} 0 & 1 \\ 1 & 0 \end{bmatrix}, \quad \gamma_5 = \begin{bmatrix} 1 & 0 \\ 0 & -1 \end{bmatrix}, \quad C = \begin{bmatrix} -\sigma_2 & 0 \\ 0 & \sigma_2 \end{bmatrix} \quad (\text{A.16})$$

Our convention for matrix notation is $M_a^b \rightarrow M_{ab}$. Then M transforms under chiral $\text{SU}(3)_L \times \text{SU}(3)_R$, charge conjugation C and parity P as

$$\begin{aligned} M &\rightarrow U_L M U_R^\dagger \\ C : \quad M &\rightarrow M^T, \quad P : \quad M(\mathbf{x}) \rightarrow M^\dagger(-\mathbf{x}). \end{aligned} \quad (\text{A.17})$$

Here U_L and U_R are unitary, unimodular matrices associated with the transformations on the left handed ($q_L = \frac{1}{2}(1 + \gamma_5)q$) and right handed ($q_R = \frac{1}{2}(1 - \gamma_5)q$) quark projections. For the $U(1)_A$ transformation one has:

$$M \rightarrow e^{2i\nu} M. \quad (\text{A.18})$$

Next consider nonets with “four quark”, $qq\bar{q}\bar{q}$ structures. An alternate possibility to the one given in Eq. (3.24) is that such states may be bound states of a diquark and an anti-diquark. There are two choices if the diquark is required to belong to a $\bar{3}$ representation of flavor $\text{SU}(3)$. In the first case it belongs to a $\bar{3}$ of color and is a spin singlet with the structure,

$$\begin{aligned} L^{gE} &= \epsilon^{gab} \epsilon^{EAB} q_{aA}^T C^{-1} \frac{1 + \gamma_5}{2} q_{bB}, \\ R^{gE} &= \epsilon^{\dot{g}\dot{a}\dot{b}} \epsilon^{EAB} q_{\dot{a}A}^T C^{-1} \frac{1 - \gamma_5}{2} q_{\dot{b}B}. \end{aligned} \quad (\text{A.19})$$

Then the matrix M has the form:

$$M_g^{(3)f} = (L^{gA})^\dagger R^{fA}. \quad (\text{A.20})$$

In a second alternate possibility, the diquark belongs to a 6 representation of color and has spin 1. It has the schematic chiral realization:

$$\begin{aligned} L_{\mu\nu,AB}^g &= L_{\mu\nu,BA}^g = \epsilon^{gab} q_{aA}^T C^{-1} \sigma_{\mu\nu} \frac{1 + \gamma_5}{2} q_{bB}, \\ R_{\mu\nu,AB}^{\dot{g}} &= R_{\mu\nu,BA}^{\dot{g}} = \epsilon^{\dot{g}ab} q_{\dot{a}A}^T C^{-1} \sigma_{\mu\nu} \frac{1 - \gamma_5}{2} q_{bB}, \end{aligned} \quad (\text{A.21})$$

where $\sigma_{\mu\nu} = \frac{1}{2i} [\gamma_\mu, \gamma_\nu]$. The corresponding M matrix has the form

$$M_g^{(4)f} = (L_{\mu\nu,AB}^g)^\dagger R_{\mu\nu,AB}^f, \quad (\text{A.22})$$

where the dagger operation includes a factor $(-1)^{\delta_{\mu 4} + \delta_{\nu 4}}$. The nonets $M^{(2)}$, $M^{(3)}$ and $M^{(4)}$ transform like M under all of $SU(3)_L \times SU(3)_R$, C , P . Under $U(1)_A$ all three transform with the phase $e^{-4i\nu}$, e.g.:

$$M^{(2)} \rightarrow e^{-4i\nu} M^{(2)}. \quad (\text{A.23})$$

It is seen that the $U(1)_A$ transformation distinguishes the “four quark” from the “two quark” states. In the full chiral Lagrangian treatment of the model under discussion there are explicit terms which model the breaking of this symmetry and hence cause the mixing.

Appendix B

Part II Appendix

B.1 Alternative perturbation method

We present here an alternative approach which leads to results in perturbation theory order by order. This can be applied to the case at hand or more generally when the mass matrix is invariant at zeroth order under a finite group G_0 and then we add perturbations of decreasing importance in the small parameter x such that for example the n^{th} perturbation is of order x^n and is invariant under a smaller group G_n . The mass matrix can then be written as an expansion in x ,

$$M(x) = M_0 + xM_1 + x^2M_2 + \dots \quad (\text{B.1})$$

where M_0 is invariant under G_0 , M_1 under G_1 and so on.

The eigenvalues (diagonal) and eigenvector matrices can also be expanded as,

$$\begin{aligned} M_d(x) &= M_{d0} + xM_{d1} + x^2M_{d2} + \dots \\ R(x) &= R_0 + xR_1 + x^2R_2 + \dots \end{aligned} \quad (\text{B.2})$$

where,

$$R^T(x)M(x)R(x) = M_d(x) \quad (\text{B.3})$$

is the eigenvalue equation.

If we differentiate Eq. (B.3) once we obtain:

$$R^{T'} M R + R^T M' R + R^T M R' = M'_d \quad (\text{B.4})$$

which can be written as:

$$[M_d, R^T R'] + R^T M' R = M'_d \quad (\text{B.5})$$

Here we used the orthonormality condition for the eigenvector matrix:

$$R^{T'} R + R^T R' = 0 \quad (\text{B.6})$$

Note that the matrix $R^{T'} R$ which appears in what follows is antisymmetric (in each order of perturbation theory) and in consequence all of its derivatives will be antisymmetric.

The second derivative and third derivative equations will read:

$$\begin{aligned} [M'_d, R^T R'] + [M_d, (R^T R)'] + [R^T M' R, R^T R'] + R^T M'' R &= M''_d, \\ [M'_d, R^T R'] + 2[M'_d, (R^T R)'] + [M_d, (R^T R)'] + [[R^T M' R, R^T R'], R^T R'] \\ + 2[R^T M'' R, R^T R'] + [R^T M' R, (R^T R)'] + R^T M''' R &= M'''_d \end{aligned} \quad (\text{B.7})$$

All commutators of diagonal matrices give zero on diagonal and in consequence the mass eigenvalues are obtained from the rest of the terms.

It is clear that by setting $x = 0$ one can associate the first derivative with the first order perturbation theory, second with second order and so on. The mass eigenvalues and the matrix $R^T R'$ can be extracted in each order from equations like Eq. (B.5) and Eq. (B.7).

Then one should use the orthonormality condition to obtain the eigenvector matrix according to:

$$R^T(x) R'(x) = R_0^T R_1 + x(R_1^T R_1 + 2R_0^T R_2) + \dots \quad (\text{B.8})$$

Using this method and $G_0 = S_3$, $G_1 = S_{23}$ and $G_2 = S_{12}$ one retrieves the eigenvalues and eigenvectors in each order of perturbation theory. The results agree with those presented in the main text.

Bibliography

- [1] D. J. Gross and F. Wilczek, Phys. Rev. Lett. **30**, 26 1343 (1973); H. D. Politzer Phys. Rev. Lett. **30**, 1346 (1973).
- [2] Hideki Yukawa Prog. Theor. Phys. Suppl. **1** (1955) 1.
- [3] M. Gell-Mann and M. Levy, Nuovo Cimento **16**, 705 (1960).
- [4] Y. Nambu and G. Jona-Lasinio, Phys. Rev. **122**, 345 (1961); 124, 246 (1961).
- [5] S. L. Adler and R. F. Dashen, Current Algebras and Application to Particle Physics (W. A. Benjamin, New York, 1968).
- [6] S. Weinberg, Phys. Rev. Lett. **19**, 1264 (1967); A. Salam, Elementary Particle Theory, edited by N. Svartholm (Almquist and Wiksells, Stockholm, 1969), p. 367.
- [7] K. Nakamura *et al.* (Particle Data Group) 2010 J. Phys. G: Nucl. Part. Phys. **37** 075021.
- [8] M. Napsuciale and S. Rodriguez, Phys. Rev. D **70**, 094043 (2004); F. Giacosa, Th. Gutsche, V. E. Lyubovitskij and A. Faessler, Phys. Lett. B **622**, 277 (2005); J. Vijande, A. Valcarce, F. Fernandez and B. Silvestre-Brac, Phys. Rev. D **72**, 034025 (2005); S. Narison, Phys. Rev. D **73**,

- 114024 (2006); L. Maiani, F. Piccinini, A. D. Polosa and V. Riquer, Eur. Phys. J. C **50**, 609 (2007); J. R. Pelaez, Phys. Rev. Lett. **92**, 102001 (2004); J. R. Pelaez and G. Rios, Phys. Rev. Lett. **97**, 242002 (2006); F. Giacosa, Phys. Rev. D **75**, 054007 (2007).
- [9] R. L. Jaffe, Phys. Rev. D **15**, 267 (1977). J. D. Weinstein and N. Isgur, Phys. Rev. Lett. **48**, 659 (1982).
- [10] D. Black, A. H. Fariborz and J. Schechter, Phys. Rev. D **61** 074001 (2000).
- [11] D. Black, A. H. Fariborz, S. Moussa, S. Nasri and J. Schechter, Phys. Rev. D **64**, 014031 (2001).
- [12] T. Teshima, I. Kitamura and N. Morisita, J. Phys. G **28**, 1391 (2002); *ibid* **30**, 663 (2004); F. Close and N. Tornqvist, *ibid.* **28**, R249 (2002); A. H. Fariborz, Int. J. Mod. Phys. A **19**, 2095 (2004); 5417 (2004); Phys. Rev. D **74**, 054030 (2006).
- [13] G. 't Hooft, G. Isidori, L. Maiani, A.D. Polosa and V. Riquer, Phys. Lett. B **662**, 424 (2008).
- [14] N. Yamamoto, M. Tachibana, T. Hatsuda and G. Baym, Phys. Rev. D **76**, 074001 (2007) and A. A. Andrianov and D. Espriu, Phys. Lett. B **663**, 450 (2008).
- [15] A.H. Fariborz, R. Jora and J. Schechter, Phys. Rev. D **72**, 034001 (2005).
- [16] A. H. Fariborz, R. Jora, and J. Schechter, Phys. Rev. D **76**, 114001 (2007).

- [17] A. H. Fariborz, R. Jora and J. Schechter, Phys. Rev. D **76**, 014011 (2007).
- [18] A. H. Fariborz, R. Jora and J. Schechter, Phys. Rev. D **77**, 034006 (2008).
- [19] A. H. Fariborz, R. Jora and J. Schechter, Phys. Rev. D **77**, 094004 (2008).
- [20] A. H. Fariborz, R. Jora and J. Schechter, Phys. Rev. D **79**, 074014 (2009).
- [21] D. Black, A. H. Fariborz, R. Jora, N. W. Park, J. Schechter and M. N. Shahid, Mod. Phys. Lett. A **24**, 2285 (2009).
- [22] A. H. Fariborz, N. W. Park, J. Schechter and M. N. Shahid, Phys. Rev. D **80**, 113001 (2009).
- [23] R. Jora, S. Moussa, S. Nasri, J. Schechter and M. N. Shahid, Int. J. Mod. Phys. A **23**, 5159 (2008).
- [24] R. Jora, A. H. Fariborz, J. Schechter and M. N. Shahid, Phys. Rev. D **84**, 113004 (2011).
- [25] R. Jora, A. H. Fariborz, J. Schechter and M. N. Shahid, Phys. Rev. D **83**, 034018 (2011).
- [26] R. Jora, A. H. Fariborz, J. Schechter and M. N. Shahid, Phys. Rev. D **84**, 094024 (2011).
- [27] G. Ecker, J. Gasser, A. Pich and E. de Rafael, Nucl. Phys **B321**, 311(1999).

- [28] J. A. Oller and E. Oset, Nucl. Phys. **A620**, 438 (1997).
- [29] H. Leutwyler, arXiv:hep-ph/0608218.
- [30] J. F. Donoghue, E. Golowich and B. R. Holstein, “Dynamics of the Standard Model”, Cambridge University Press, 1992.
- [31] G.’t Hooft, Nucl. Phys. **B72**, 461 (1974).
- [32] E. Witten, Nucl. Phys. **B160**, 57 (1979).
- [33] S. Weinberg, Phys. Rev. Lett. **17**, 616 (1966).
- [34] J. Gasser and H. Leutwyler, Phys. Lett. B **125**, 325 (1983).
- [35] G. Colangelo, J. Gasser and H. Leutwyler, Phys. Lett. B **488**, 261 (2000).
- [36] S. Pislak *et al.*, Phys. Rev.D **67**, 072004 (2003).
- [37] S. Gasiorowicz and D. A. Geffen, Rev. Mod. Phys. **41**, 531 (1969).
- [38] M. D. Scadron, F. Kleefeld and G. Rupp, arXiv:hep-ph/0601196; N. N. Achasov and G. N. Shestakov, Pis’ma Zh. Eksp. Teor. Fiz. **88**, 345 (2008); [JETP Lett. **88**, 295 (2008)]; S. Struber and D. H. Rischke, Phys. Rev. D **77**, 085004 (2008); D. Parganlija, F. Giacosa and D. H. Rischke, Proc. Sci., CONFINEMENT8(2008) 070 [arXiv:0812.2183].
- [39] J. R. Batley *et al.* (NA48/2 Collaboration), Eur. Phys. J. C **52**, 875 (2007). See also R. Kaminski, J. R. Pelaez and F. J. Yndurian, Phys. Rev. D **77**, 054015 (2008).
- [40] R. Kaminski, R. Garcia-Martin, P. Gryniewicz and J. R. Pelaez, Nucl. Phys. B, Proc. Suppl. **186**, 318 (2009). See also N. N. Achasov and G. N. Shestakov, Phys. Rev. Lett. **99**, 072001 (2007).

- [41] K. Kawarabayashi and M. Suzuki, Phys. Rev. Lett. **16**, 255 (1966); Ri-azuddin and Fayazuddin, Phys. Rev. **147**, 1071 (1966).
- [42] S. Weinberg, Phys. Rev. Lett. **18**, 507 (1967); T. Das, V. Mathur and S. Okubo, Phys. Rev. Lett. **18**, 761 (1967).
- [43] Important early papers on walking technicolor include B. Holdom, Phys. Rev. D **24**, 1441 (1981); V. A. Miransky and K. Yamawaki, Phys. Rev. D **55**, 5051 (1997); **56**, 3768 (E) (1997); T. Appelquist, D. Karabali, and L. C. R. Wijewardhana, Phys. Rev. Lett. **57**, 957 (1986); K. Lane, arXiv:hep-ph/0202265; C. T. Hill and E. H. Simmons, Phys. Rep. **381**, 235 (2003); **390**, 553 (2004); T. Appelquist, N. D. Christensen, M. Piai, and R. Shrock, Phys. Rev. D **70**, 093010 (2004). A detailed review of the minimal walking technicolor model is given in R. Foadi, M. T. Frandsen, T. A. Ryttov, and F. Sannino, Phys. Rev. D **76**, 055005 (2007). See also F. Sannino, arXiv:0804.0182. An historical review of the subject is given by K. Yamawaki, in the Proceedings of the International Symposium *pnA50*, Nagoya [Prog. Theor. Phys. Suppl. 167, 127 (2007)].
- [44] G. F. Giudice, C. Grojean, A. Pomarol and R. Rattazzi, JHEP **0706** 045 (2007)[arXiv:hep-ph/0703164] and B. Grinstein and M. Trott, Phys. Rev. D **76**, 073002 (2007)[arXiv:0704.1505].
- [45] A. Salomone, J. Schechter and T. Tudron, Phys. Rev. D **24**, 492 (1981).
- [46] L. Randall, arXiv:0711.4360[hep-ph] and S. Mantry, M. Trott and M.B. Wise, Phys. Rev. D **77**, 013006 (2008)[arXiv:0709.1505].
- [47] E. Ma, arXiv:0802.2917[hep-ph] and N. G. Deshpande and E. Ma, Phys. Rev. D **18**, 2574 (1978).

- [48] J.-M. Gerard and M. Herquet, Phys. Rev. Letts. **98**, 251802 (2007), arXiv:hep/0703051.
- [49] L. Lopez Honorez, E. Nezri, J. F. Oliver and M. H. G. Tytgat, JCAP **0702**, 028 (2007), arXiv:hep-ph/0612275; R. Barbieri, L. J. Hall and V. S. Rychkov, Phys. Rev. D **74**, 015007 (2006)[arXiv:hep-ph/0603188] and M. Cirelli, N. Fornengo and A. Strumia, arXiv:hep-ph/0512090.
- [50] S. Nie and M. Sher, Phys. Lett. **B449**, 89 (1999), arXiv:hep-ph/9811234 and I. F. Ginzburg and K. A. Kanishev, Phys. Rev. D **76**, 095013 (2007), arXiv:0704.3664[hep-ph].
- [51] Particle data group, J. Phys.G: Nucl. Part. Phys. **33**, 1 (2006).
- [52] S. Chang, R. Dermisek, J. F. Gunion and N. Weiner, arXiv:0801.4554 [hep-ph].
- [53] J. F. Gunion and H. E. Haber, Nucl. Phys. B **272**, 1 (1986); L.-F. Li, Y. Liu and L. Wolfenstein, Phys. Lett. B **159**, 45 (1985).
- [54] J. Schechter and Y. Ueda, Phys. Rev. D **4**, 733 (1971).
- [55] Y. S. Kalashnikova, A. E. Kudryavtsev, A. V. Nefediev, C. Hanhart and J. Haidenbauer, Eur. Phys. J. A**24**, 437 (2005).
- [56] K. M. Ecklund *et al.* (CLEO Collaboration), Phys. Rev. D **80**,052009 (2009).
- [57] S. S. Gerstein and Y. B. Zeldovich, Soviet Phys. JETEP **2**,576 (1956); R. P. Feynman and M. Gell-Mann, Phys. Rev. **109**,193 (1958).
- [58] See also R. Foadi, M. Jarvinen and F. Sannino, arXiv:0811.3718[hep-ph].

- [59] S. Fukuda *et al.* (Super Kamiokande Collaboration), Phys. Lett. B **539**, 179 (2002).
- [60] K. Eguchi *et al.* (KamLAND collaboration), Phys. Rev. Lett. **90**, 021802 (2003).
- [61] Q. R. Ahmad *et al.* (SNO collaboration), nucl-ex/0309004.
- [62] M. H. Ahn *et al.* (K2K collaboration), Phys. Rev. Lett. **90**, 041801 (2003).
- [63] W. Hampel *et al.* (GALLEX Collaboration), Phys. Lett. B **447**, 127 (1999).
- [64] J. N. Abdurashitov *et al.* (SAGE Collaboration), Phys. Rev. C **60**, 055801 (1999).
- [65] M. Apollonio *et al.* (CHOOZ Collaboration), Eur. Phys. J. C **27**, 331 (2003).
- [66] MINOS Collaboration, Phys. Rev. D **73**, 072002 (2006).
- [67] R. Jora, S. Nasri and J. Schechter, Int. J. Mod. Phys. A, **21**, 5875 (2006).
- [68] C.-Y. Chen and L. Wolfenstein, Phys. Rev. D **77**, 093009 (2008).
- [69] H. Fritzsch and Z.-Z.Xing, Phys. Lett. B **440**, 313 (1988).
- [70] P. F. Harrison, D. H. Perkins and W. G. Scott, Phys. Lett. **B530**,79 (2002).
- [71] Z.-Z.Xing, Phys. Lett. B **533**, 85 (2002).
- [72] X. G. He and A. Zee, Phys. Lett. B **560**, 87 (2003).

- [73] P. F. Harrison and W. G. Scott, *Phys. Lett. B* **557**, 76 (2003).
- [74] C. I. Low and R. R. Volkas, *Phys. Rev. D* **68**, 033007 (2003).
- [75] A. Zee, *Phys. Rev. D* **68**, 093002 (2003).
- [76] J. D. Bjorken, P. F. Harrison and W. G. Scott, *Phys. Rev. D* **74**, 073012 (2006).
- [77] R. N. Mohapatra, S. Nasri and H. B. Yu, *Phys. Lett. B* **639**, 318 (2006).
- [78] S. F. King, *Nucl. Phys. B* **576**, 85 (2000); S. F. King and N. N. Singh, *Nucl. Phys. B* **591**, 3 (2000).
- [79] M. Hirsch, A. Velanova del Morel, J. W. F. Valle and E. Ma, *Phys. Rev. D* **72**, (091301) (2005).
- [80] E. Ma, *Phys. Rev. D* **70** 031901 (2004).
- [81] N. Haba, A. Watanabe, and K. Yoshioka, *Phys. Rev. Lett.* **97**, 041601 (2006).
- [82] L. Wolfenstein, *Phys. Rev. D* **18**, 958 (1978).
- [83] S. Pakvasa and H. Sugawara, *Phys. Lett. B* **73**, 61 (1978); **82**, 105 (1979); E. Derman and H. S. Tsao, *Phys. Rev. D* **20**, 1207 (1979) and Y. Yamana, H. Sugawara and S. Pakvasa *Phys. Rev. D* **25**, 1895 (1982).
- [84] S.-L. Chen, M. Frigerio and E. Ma, *Phys. Rev. D* **70**, 073008 (2004); **70**, 079905(E) (2004).
- [85] M. Fukugita, M. Tanimoto and T. Yanagida, *Phys. Rev. D* **57**, 4429 (1998).

- [86] Z-z. Xing, D. Yang and S. Zhou, Phys. Lett. B **690**, 304 (2010).
- [87] D. A. Dicus, S-F. Ge and W. W. Repko, Phys. Rev. D **82**, 033005 (2010).
- [88] A. Montdragon, M. Montdragon and E. Peinado, J.Phys. **A41**, 304035 (2008); see also arXiv:0805.3507.
- [89] E. Ma and G. Rajasekaran, Phys. Rev. D **64**, 113012 (2001).
- [90] M. Gell-Mann, Phys. Rev. **125**, 1067 (1962); S. Okubo, Prog. Theor. Phys. **27**, 949 (1962); **28**, 24 (1962).
- [91] R. Jora, J. Schechter and M. N. Shahid, Phys. Rev. D **80**, 093007 (2009); Erratum: Phys. Rev. D **80**, 093007 (2009).
- [92] R. Jora, J. Schechter and M. N. Shahid, Phys. Rev. D **82**, 053006 (2010).
- [93] T. Fukuyama and H. Nishiura, arXiv:hep-ph/9702253; R. N. Mohapatra and S. Nussinov, Phys. Rev. D **60**, 013002 (1999); E. Ma and M. Raidal, Phys. Rev. Lett. **87**, 011802 (2001); C. S. Lam, Phys. Lett. B **507**, 214 (2001); T. Kitabayashi and M. Yasue, Phys.Rev. D **67** 015006 (2003); W. Grimus and L. Lavoura, Phys. Lett. B **572**, 189 (2003); J. Phys. G **30**, 73 (2004); Y. Koide, Phys.Rev. **D69**, 093001 (2004); Y. H. Ahn, Sin Kyu Kang, C. S. Kim, Jake Lee, Phys. Rev. D **73**, 093005 (2006); A. Ghosal, arXiv:hep-ph/0304090; W. Grimus and L. Lavoura, Phys. Lett. B **572**, 189 (2003); W. Grimus and L. Lavoura, J. Phys. G **30**, 73 (2004).
- [94] W. Grimus, A. S.Joshipura, S. Kaneko, L. Lavoura, H. Sawanaka, M. Tanimoto, Nucl. Phys. B **713**, 151 (2005); R. N. Mohapatra, J. High Energy Phys. 10 (2004) 027; A. de Gouvea, Phys.Rev. D **69**, 093007 (2004); R. N. Mohapatra and W. Rodejohann, Phys. Rev. D **72**, 053001

- (2005); T. Kitabayashi and M. Yasue, Phys. Lett. B **621**, 133 (2005); R. N. Mohapatra and S. Nasri, Phys. Rev. D **71**, 033001 (2005); R. N. Mohapatra, S. Nasri and H. B. Yu, Phys. Lett. B **615**, 231 (2005).
- [95] K. Matsuda and H. Nishiura, Phys. Rev. D **73**, 013008 (2006); A. Joshipura, Eur. Phys. J. C **53**, 77 (2007); R. N. Mohapatra, S. Nasri and H. B. Yu, Phys. Lett. B **636**, 114 (2006).
- [96] C. Amsler *et al.*, Phys. Lett. B **667**, 1 (2008).
- [97] D. N. Spergel *et al.*, Astrophys. J. Suppl. Ser. **148**: 175 (2003); S. Hannestad, J. Cosmol. Astropart. Phys. 05 (2003) 004.
- [98] S. S. Masood, S. Nasri and J. Schechter, Phys. Rev. D **71**, 093005 (2005).
- [99] G. L. Fogli, E. Lisi, A. Marrone, A. Palazzo and A. M. Rotunno, in *Proceedings of XIII International Workshop on Neutrino Telescopes, Venice* (2009), arXiv:0905.3549.
- [100] T. Schwetz, M. Tortola and J. W. F. Valle New J. Phys. **10**, 113011 (2008)..
- [101] H. V. Klapdor-Kleingrothaus *et al.*, Eur. Phys. J. A **12**, 147 (2001); C. Aalseth *et al.*, arXiv:hep-ph/0412300.
- [102] J. Schechter and J. W. F. Valle, Phys. Rev. **D23**, 1666 (1981).

Curriculum Vitae

NAME OF AUTHOR: Muhammad Naeem Shahid

PLACE OF BIRTH: Rawalpindi, Pakistan.

DATE OF BIRTH: April 21, 1978.

UNDERGRADUATE SCHOOL ATTENDED: Quaid-i-Azam University, Pakistan.

GRADUATE SCHOOL ATTENDED: Quaid-i-Azam University, Pakistan.

DEGREES AWARDED:

M.Sc., Physics, 2002.

M.Phil., Physics, 2005.

AWARDS:

Teaching Assistant, Syracuse University, 2007-2012.

Research Assistant, Syracuse University, 2007-2012.

PROFESSIONAL EXPERIENCE:

Poster presentation in DPF meeting 2011 at Brown University.